Role of Ion Channels and Exchangers in the Regulation of Dendritic Cells

Bedeutung von Ionenkanälen und -austauschern bei der Regulation von Dendritischen Zellen

DISSERTATION

der Fakultät für Chemie und Pharmazie
der Eberhard Karls Universität Tübingen

zur Erlangung des Grades eines Doktors
der Naturwissenschaften

2010

vorgelegt von

Nicole Heise geb. Matzner

Tag der mündlichen Prüfung: 20.04.2010

Dekan: Prof. Dr. Lars Wesemann

1. Berichterstatter: Prof. Dr. Michael Duszenko
2. Berichterstatter: Prof. Dr. med. Florian Lang

Table of Contents

List of Figures

List of Tables

Abbreviations

$[Ca^{2+}]_i$	intracellular calcium concentration
$1,25(OH)_2D_3$	1,25-dihydroxyvitamin D_3
1α-hydroxylase	$25(OH)_2D_3$-1α-hydroxylase
APC	antigen presenting cell
BCR	B cell receptor
BMDCs	bone marrow-derived DCs
CaMK	calmodulin kinase
CaMKK	calmodulin kinase kinase
Ca_v channel	voltage-gated Ca^{2+} channel
CRAC	Ca^{2+} release-activated Ca^{2+} channel
CTLs	cytotoxic T lymphocytes
DAG	diacylglycerol
DBP	vitamin D-binding protein
DBZ	3',4'-dichlorobenzamyl
DCs	dendritic cells
EAE	experimental autoimmune encephalomyelitis
EGTA	ethylene glycol tetraacetic acid
ELISA	enzyme-linked immunosorbent assay
ER	endoplasmic reticulum
FACS	fluorescence activated cell sorter
FBS	foetal bovine serum
Foxp3	forkhead box P3
GCRs	glucocorticoid receptors
GILZ	glucocorticoid-induced leucine zipper
GM-CSF	granulocyte-macrophage colony-stimulating factor
GNBP1	Gram-negative binding protein 1
I_{CRAC}	Ca^{2+} release-activated Ca^{2+} currents
IDO	indolamine-2,3-dioxygenase
IFN	interferon
IgE	immunoglobulin E
IKK	IκB-kinase
IL	interleukin
IL-1R	interleukin-1 receptor
IP_3	inositol-(1,4,5)-trisphosphate

IP$_3$R	inositol-(1,4,5)-trisphosphate receptor
IRAK	IL-1R-associated kinase
ITAM	immunoreceptor tyrosine-based activation motif
IκB	inhibitory molecule κB
Kv channel	voltage-gated K$^+$ channel
LCs	Langerhans cells
LPS	lipopolysaccharide
LRR	leucine-rich repeat
LTA	lipoteichoic acid (LTA)
MDP	muramyl dipeptide (MDP)
MgTx	margatoxin
MHC	major histocompatibility complex
MyDN	N-terminal death domain
NBS-LRR	nucleotide-binding site and leucine-rich repeat
NCKX	K$^+$-dependent Na$^+$/Ca^{2+} exchangers
NCX	K$^+$-independent Na$^+$/Ca^{2+} exchangers
NEAA	non-essential amino acids
NFAT	nuclear factor of activated T cells
NK cells	natural killer cells
NMDG	N-methyl-D-glucamine
NF-κB	nuclear factor κB
P/S	penicillin/streptomycin
PAMPs	pathogen-associated molecular patterns
PBS	phosphate buffered saline
PCR	polymerase chain reaction
PGN	peptidoglycan
PGRPs	PGN recognition proteins
PLC	phospholipase C
PM	perhexiline maleate
PMA	phorbol-12-myristate-13-acetate
PMCA	plasma membrane Ca^{2+}-ATPases
PRRs	pattern recognition receptors
PtdIns(4,5)P$_2$	phosphatidylinositol-(4,5)-bis-phosphate
RFU	relative fluorescence units
RT	room temperature
RT-PCR	reverse transcription polymerase chain reaction
SCID	severe combined immunodeficiency

SDS-PAGE	sodium dodecyl sulfate polyacrylamide gel electrophoresis
SERCA	sarco/endoplasmic reticulum Ca^{2+}-ATPases
SOCE	store-operated Ca^{2+} entry
SOCs	store-operated channels
STIM1	stromal interaction molecule 1
TCR	T cell receptor
TEA	tetraethylammonium
Th	helper T lymphocytes
TIR	Toll/IL-1 receptor-like domain
TLR	Toll-like receptor
TNF	tumor necrosis factor
Tregs	regulatory T lymphocytes
TRIF	TIR-domain-containing adapter-incucing interferon-β
TRP	transient receptor potential
TRPC	canonical transient receptor potential
TRPM	transient receptor potential melastatin
TRPV	transient receptor potential vanilloid
VDR	vitamin D receptor

1   Introduction

1.1   Dendritic cells in innate and adaptive immunity

Immune responses are mediated by a variety of cell types and soluble factors that are generally assigned to the innate or the adaptive immune system, although there is a broad overlap area of both parts of the immune system. Adaptive immunity serves to detect and identify "non-self" particles via cell surface receptors such as T cell receptor (TCR) and B cell receptor (BCR) on T and B lymphocytes, respectively. Receptor engagement results in clonal lymphocyte expansion to respond to a wide range of potential antigens [1,2]. The innate immune system, in contrast, represents the bodys' first barrier against pathogens [3]. Besides cellular components, it also includes the complement system and acute phase proteins, and serves to limit infection in the early hours after exposure to pathogens [1]. The innate immune system is phylogenetically conserved and senses pathogens via pattern recognition receptors such as Nod-like receptors [4], C-type lectin receptors [5], and Toll-like receptors (TLRs) [2]. TLRs are expressed on leukocytes (e.g. mast cells, natural killer (NK) cells, eosinophils and basophils) and phagocytes (e.g. dendritic cells (DCs), macrophages and neutrophils) and recognize specific microbial patterns that are common to many pathogens. TLR engagement results in the activation of both innate and adaptive immune responses [1,2].

Dendritic cells (DCs) are immune cells that originate from myeloid and plasmacytoid progenitor cells in the bone marrow. They belong to the innate immune system, but are also main players in the induction of adaptive immunity. DCs are resident in different tissues like epidermis, intestine or blood vessel walls. Upon tissue damage, DC precursors circulating in the blood are also attracted and enter the respective tissues as immature DCs (Figure 1). They can incorporate pathogens directly by receptor-mediated endocytosis, macropinocytosis or phagocytosis (of apoptotic and necrotic cells, viruses, bacteria, intracellular parasites such as *Leishmania*), which leads to cytokine production and further activation of eosinophils, macrophages and natural killer cells. DCs can also encounter pathogens indirectly through pathogen effects on stromal cells [6,7]. Following antigen capture and processing, activated DCs migrate to lymph nodes via lymph and blood, where they arrive as mature DCs and present antigenic fragments along with MHC class I and II molecules on their cell surface [6,8,9]. Furthermore, self and microbial glycolipids are presented in context with CD1 molecules to effector T lymphocytes [7,10,11]. This allows the selection of rare circulating antigen-specific lymphocytes. In this stage, DCs are termed

antigen-presenting cells (APCs). Antigen presentation by DCs subsequently leads to activation of naïve T lymphocytes, which migrate to the site of infection and eliminate microbes and/or microbe-infected cells. Helper T lymphocytes (Th) further activate eosinophils, macrophages and NK cells. Cytotoxic T lymphocytes (CTLs) serve to lyse infected cells. B lymphocytes become activated by interaction with T lymphocytes and DCs and migrate into various areas, where they mature into plasma cells that produce antibodies that neutralize the initial pathogen [6-9].
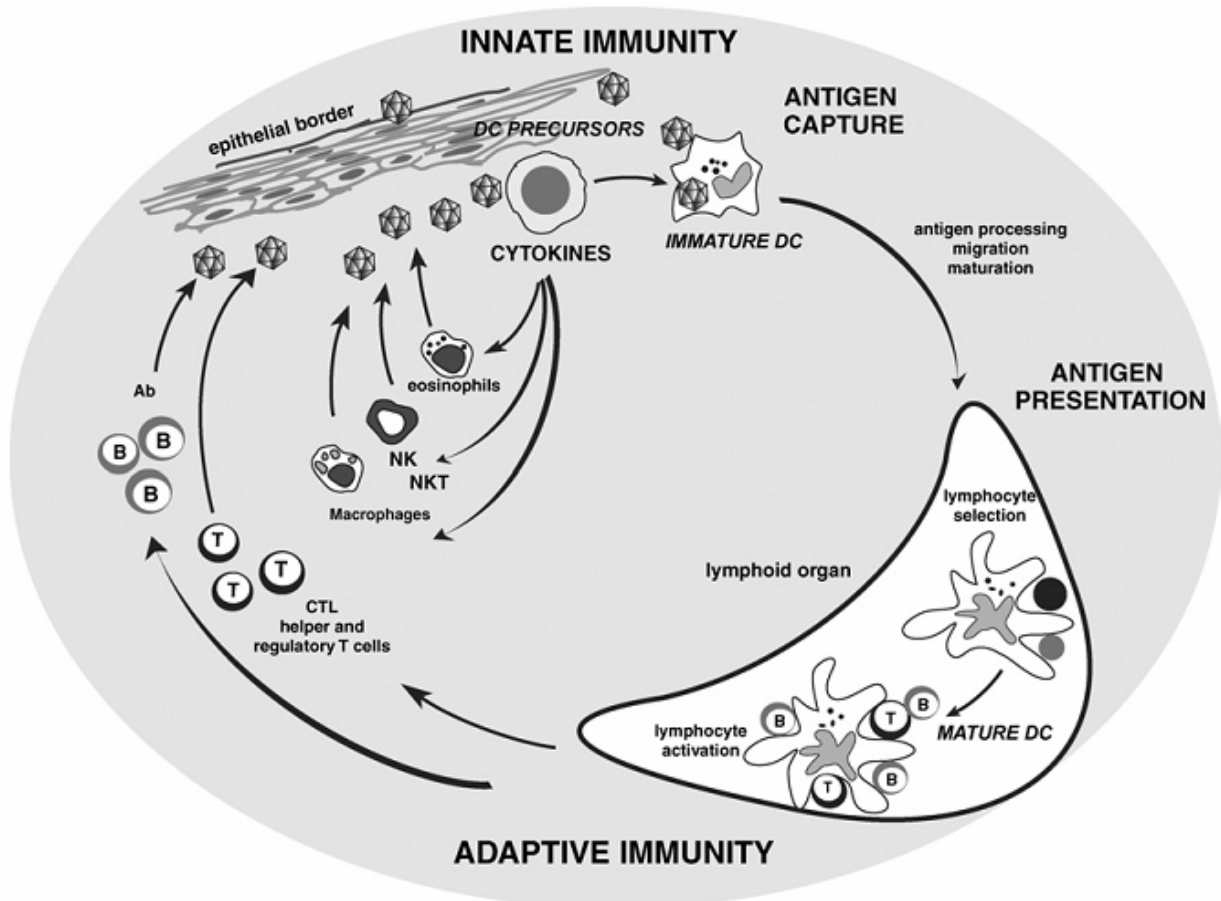
Figure 1. The life cycle of dendritic cells (DCs)
B – B-cell, CTL – cytotoxic T-cell, DC – dendritic cell, MF – macrophages, NK – natural killer cells, NKT – natural killer T-cells, T – T-cell. Taken from [7].

Effector Th lymphocytes derive from naïve CD4$^+$ T lymphocytes in response to antigenic stimulation, and their differentiation into various subsets depends on interaction with APCs and is further directed by costimulatory molecules and the production of polarizing cytokines. The Th1 subset is primarily involved in recognition of intracellular pathogens, and is characterized by a cytokine profile including interleukin (IL) -2, IL-3, interferon gamma (IFNγ) and tumor-necrosis-factor (TNF) β, thereby supporting cellular immunity against bacterial and

viral infections [3,12]. In addition, IL-12 is secreted by DCs in response to TLR activation, and induces Th1 polarization. IFNγ-producing cells such as activated NK cells induce DCs to produce IL-12 and further promote Th1 polarization [3]. In contrast to Th1 cells, the Th2 subset is directed against extracellular pathogens and supports humoral immunity by producing cytokines such as IL-4, IL-5, IL-6, IL-10, IL-13, and IL-25 [3,12]. The Th2-polarizing cytokine IL-4 is further provided by IL-4-secreting cells such as mast cells [3]. In 2005, another Th subset was discovered [13], termed Th17 cells, according to their secretion of IL-17; but these cells also produce IL-21 and IL-22. Th17 cells show strong proinflammatory effects, and are involved in fighting Gram-negative bacteria, fungi, and some protozoa [12]. Their development is promoted by cytokines such as IL-1, IL-6, and IL-23. In contrast, the development of Th17 is inhibited by IL-4 and IFNγ [12-14]. In addition to the Th lineages, CD4$^+$ effector T lymphocytes can further evolve into the lineage of regulatory T lymphocytes (Tregs), which has immunomodulatory functions. Tregs are important regulators of immunological self tolerance and can occur either naturally or induced. Naturally arising CD25$^+$CD4$^+$ Tregs are characterized by expression of forkhead box P3 (Foxp3), which is a key regulator of their development and function, since dysfunction or deficiency of Foxp3 is sufficient to overcome self tolerance [12,15,16]. Activation of Tregs is initiated by low amounts of antigen presented by immature DCs [16].

1.2 Pattern recognition via TLRs

The expression of TLRs by DCs is a key feature enabling them to respond to many extracellular signals. TLRs belong to the family of pattern recognition receptors (PRRs) and respond to a wide range of conserved structures within microbes, called pathogen-associated molecular patterns (PAMPs) [17,18]. Their involvement in innate immune responses was first described in *Drosophila* in 1988 [19]. The mammalian homologue was identified some years later. TLRs are type I transmembrane proteins consisting of a leucine-rich repeat (LRR) extracellular domain and a cytoplasmic domain homologuous to the human interleukin-1 receptor (IL-1R) cytoplasmic domain. While the extracellular portion is necessary for recognition of different agonists, the cytoplasmic domain connects the receptor to the intracellular signaling machinery [20,21].

Table 1. Toll like receptors and their ligands

Modified after [2,22].

	ligands	*originated from*
TLR1	Tri-acyl lipopeptides	*bacteria, mycobacteria*
	Lipoprotein	*Borellia burgdorferi*
TLR2	Lipoprotein/ lipopeptides	*variety of pathogens*
	Peptidoglycan (PGN)	*Gram-positive bacteria*
	Lipoteichoic acid (LTA)	*Gram-positive bacteria*
	Lipoarabinomannan	*mycobacteria*
	A phenol-soluble modulin	*Staphylococcus epidermidis*
	Glycosylphosphatidylinositol anchors	*Trypanosoma Cruzi*
	Glycolipids	*Treponema maltophilum*
	Zymosan	*Fungi*
	Atypical lipopolysaccharide (LPS)	*Leptospira interrogans,*
		Porphyromonas gingivalis
TLR3	Double-stranded RNA	*virus*
TLR4	Lipopolysaccharide (LPS)	*Gram-negative bacteria*
	Taxol	*Taxus brevifolia*
	HSP60	*Chlamydia pneumoniae, host*
	HSP70	*host*
	Extra domain A of fibronectins	*host*
	Oligosaccharides of hyaluronic acid	*host*
	Heparan sulfate	*host*
	Fibrinogen	*host*
TLR5	Flaggelin	*bacterial flagella*
TLR6	Di-acyl lipopeptides	*mycoplasma*
TLR7	Imidazoquinoline	*synthetic compound*
	Loxoribine	*synthetic compound*
	ssRNA	*viruses*
TLR8	Imidazoquinoline	*synthetic compound*
	ssRNA	*viruses*
TLR9	CpG DNA	*bacteria, viruses*
TLR10	*?*	*?*
TLR11	*unknown components*	*uropathogenic bacteria*

The family of human TLRs consists of 10 members, TLR1-10, while twelve TLRs have been found in mice (TLR1-9 and TLR11-13). Each of them signals the presence of one or more PAMPs as illustrated in Table 1. Expression of TLRs in DCs varies between different subsets. Myeloid DCs express high levels of TLR1, 2, 4, 5 and 8, and low levels of TLR6,

while TLR 3, 7, 9 and 10 are not detectable in these cells. In contrast, plasmacytoid DCs express high levels of TLR7 and 9, as well as low levels of TLR1, 6 and 10. TLR2, 3, 4, 5 and 8 are absent in this DC subset [23]. While TLR1, 2, 4, 5 and 6 are located on the cell surface, TLR3, 7, 8 and 9 are expressed on endosome membranes [24].

TLR2 recognizes the broadest range of bacterial compounds (Table 1). Furthermore, TLR2 forms complexes with other TLRs such as TLR1 and TLR6 to recognize microbial lipoproteins and lipopeptides. The TLR1/TLR2 complex detects triacylated lipoproteins, while the TLR2/TLR6 complex recognizes acylated lipoproteins and peptidoglycans (PGN) [25,26]. PGN is a very well known ligand of TLR2 and a major component of the bacterial cell wall. It consists of a glycan backbone with alternating β1-4-linked residues of muramic acid and N-acetyl-D-glucosamine [27,28]. The structure of PGN differs between Gram-positive and Gram-negative bacteria. For example, the PGN layer in Gram-positive bacteria is much thicker and more cross-linked as compared to Gram-negative bacteria [29]. PGN includes a minimal motif, muramyl dipeptide (MDP), common to both Gram-positive and Gram-negative bacteria [30] that allows recognition of both types of PGN via TLRs. Recently, involvement of TLR2 in PGN recognition has become a matter of debate: although it has been described that PGN sensing through TLR2 is lost after removal of lipoproteins or lipoteichoic acid (LTA) from cell walls [31], this finding could not be confirmed by another group [32].

Besides TLR2, other PGN-binding PRRs have been identified, such as PGN recognition proteins (PGRPs). The Gram-negative binding protein 1 (GNBP1) and PGRP-SA serve to recognize Gram-positive bacteria upstream of TLRs [33,34]. Additionally, PGRP-SD enhances the interaction between GNBP1 and PGRP-SA and therefore the binding of GNBP1 to Gram-positive bacteria [34]. Other sensors of bacterial infection are the cytosolic proteins Nod1 and Nod2. They belong to the family of NBS-LRR (nucleotide-binding site and leucine-rich repeat) proteins and are involved in the intracellular recognition of microbes and microbial products [35,36].

1.3   TLR signaling pathways

1.3.1 MyD88-dependent pathway

Signaling pathways activated by TLR engagement are similar to signaling pathways induced by IL-1R activation. The adaptor protein MyD88 has been identified as a component of both

IL-1R and TLR signaling pathways [2,37]. All TLRs except for TLR3 signal through MyD88 and their engagement activates NFκB and JNK [24]. MyD88 is characterized by a C-terminal Toll/IL-1 receptor-like domain (TIR) and a N-terminal death domain (MyDN). Both TLR and IL-1R interact with MyD88 via their TIR domains. Upon stimulation, the serine-threonine kinase IL-1R-associated kinase (IRAK) is recruited to the complex and activated by phosphorylation. This is followed by an association of IRAK with TRAF6 protein and subsequent activation of either MAP-kinases, such as JNK and p38, or the NFκB pathway [1,38,39], as illustrated schematically in Figure 2. The activity of NFκB is regulated by association with inhibitory molecule κB (IκB) that traps NFκB in the cytoplasm. Phosphorylation of IκB by IκB-kinase (IKK) leads to dissociation of the complex, nuclear translocation of NFκB [2,39], and subsequent gene expression.
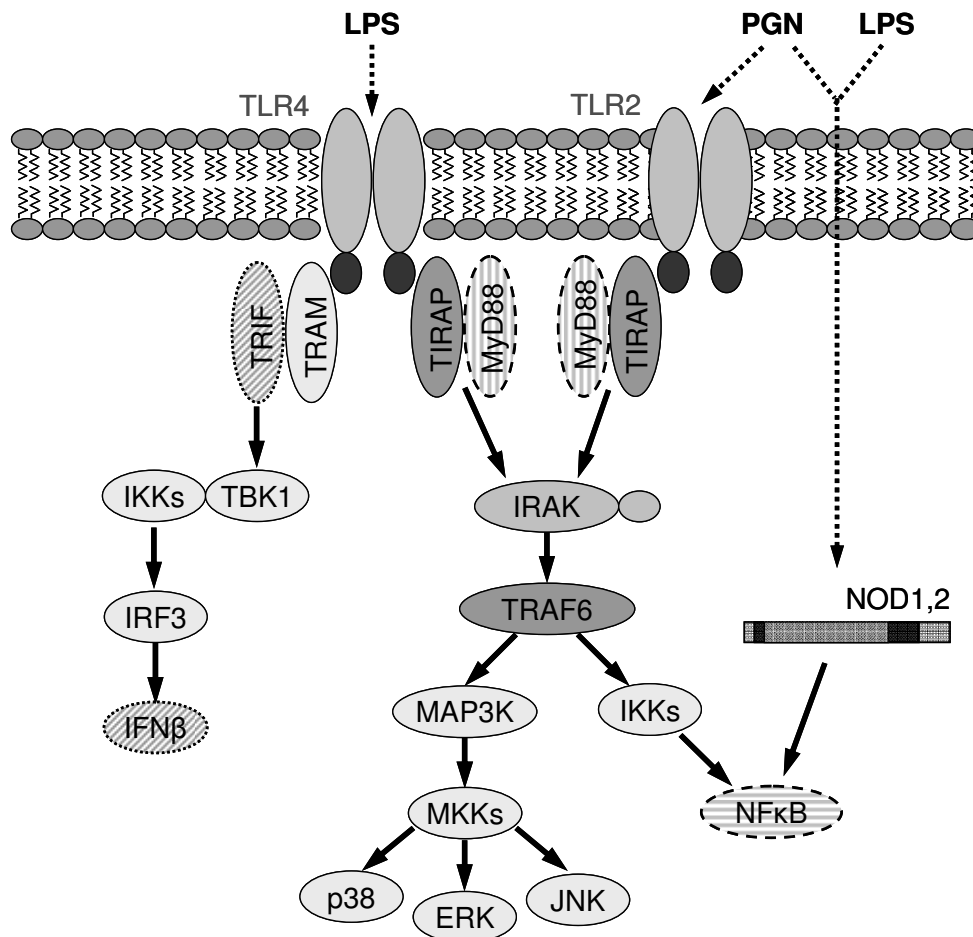
Figure 2. TLR dependent and independent recognition of LPS and PGN
Modified after [22,24,40].

1.3.2 MyD88-independent pathway

Investigation of MyD88-deficient mice revealed the existence of another, MyD88-independent signaling pathway [38,41], that still leads to activation of either MAP-kinases or NFκB. On the one hand, LPS-induced cytokine production from DCs is dependent on MyD88, pointing to an essential role for MyD88 in LPS signaling. However, DCs derived from MyD88-deficient mice still showed LPS-induced activation of NFκB and MAP-kinases, although with delayed kinetics, indicating that LPS still induced functional maturation of these cells via a MyD88-independent pathway downstream of TLR4. On the other hand, bacterial DNA, which signals through TLR9, did not induce maturation of MyD88-deficient DCs, showing that MyD88 is differentially required for TLR signaling [41,42]. MyD88-independent, LPS-induced up-regulation of co-stimulatory molecules CD80, CD86 and CD40 in macrophages was shown to be dependent on another adaptor molecule, called TIR-domain-containing adapter-incucing interferon-β (TRIF) (Figure 2) [24,43,44]. It was further shown that Nod1 is required for sensing bacterial LPS and is involved in LPS-induced, MyD88-independent activation of transcription factor NFκB [45], while Nod2 senses PGN through detection of MDP [30].

1.4 Role of TLR signaling in DC function

1.4.1 Cytokine production

TLR signaling-induced activation of transcription factor NFκB results in expression of NFκB-controlled genes for inflammatory cytokines [20]. The membrane-permeable peptide SN-50 is known to inhibit translocation of NFκB to the nucleus and therefore NFκB-controlled gene transcription. In bone marrow-derived DCs (BMDCs), the presence of SN-50 led to a reduced production of TNFα and IL-12 in response to parasites [39]. Both PGN and LPS, ligands for TLR2 and TLR4, respectively, led to increased levels of TNFα and IL-6, and a decreased level of IL-12, by different subsets of human DC precursors [23]. Langerhans cells (LCs), a DC subset located in the skin, are not able to produce IL-12p70 or type I interferons. Instead, LCs were shown to produce the pro-inflammatory cytokines IL-6 and IL-8, as well as the anti-inflammatory cytokine IL-10, in response to TLR2-stimulation by PGN. Double-stranded RNA, an activator of TLR3, increased production of IL-6, IL-8 and TNFα by LCs [18]. In BMDCs, stimulation with PGN induced production of IL-6, IL-10, TNFα, IL-12p40 and IL-

12p70, whereby cytokine production was markedly impaired in DCs derived from TLR2 deficient mice [46,47].

1.4.2 Cell surface marker expression

Activation of TLR signaling in DCs also leads to NFκB-controlled expression of co-stimulatory molecules required for activation of naïve T lymphocytes [20]. Together with the antigenic peptide presented by MHC I and II proteins, co-stimulatory molecules serve to activate T lymphocytes and thereby activate adaptive immunity [42]. Stimulation of TLR4 by LPS was shown to induce expression of CD80 and CD86 in APCs such as macrophages [44]. In BMDCs, stimulation with PGN induced cell maturation, indicated by an increased expression of CD25, CD40 and CD86, as well as MHC I and MHC II [46,47]. This effect was markedly impaired in TLR2 deficient DCs [47]. In contrast, BMDCs derived from mice deficient for either TLR4, TLR9, or MyD88, showed impaired up-regulation of CD40, CD86 and MHC II expression in response to parasite-induced stimulation. Furthermore, nuclear translocation of NFκB in response to parasites was abolished in BMDCs derived from the respective knock-out mice. Inhibition of NFκB translocation by SN-50 peptide resulted in reduced up-regulation of CD80, CD86 and MHC II after stimulation of the cells with parasites [39].

1.4.3 Phagocytic capacity

A characteristic feature of immature DCs is their high phagocytic activity, which is measureable by the uptake of different particles such as FITC-dextran [48], latex microspheres [49], stained bacteria [50], or zymosan [49]. Phagocytosis induces DC maturation [48], which subsequently leads to a decrease of DC phagocytosis [6,51]. In mouse DCs derived from $tlr2^{-/-}$ mice, PGN stimulation did not reduce their phacocytic activity, indicating that loss of TLR signaling results in a functionally immature phenotype [47].

1.5 Regulation of intracellular calcium concentration

The calcium ion (Ca^{2+}) is an important second messenger that regulates multiple cellular functions. In addition, many key processes require a controlled regulation of the intracellular calcium concentration ($[Ca^{2+}]_i$) [52]. Under resting conditions, $[Ca^{2+}]_i$ is maintained in the order of 50-100 nM in almost all cells [53,54]. In consequence of an extracellular free Ca^{2+} concentration in the millimolar range, a concentration gradient of about 10^4 between the intracellular and extracellular compartment results [54,55]. Energy-consuming pumps and ion exchangers are needed to build up this transmembrane Ca^{2+} gradient, while ion channels spend this energy and lead to a rapid influx of extracellular Ca^{2+} when needed [56].

1.5.1 Removal and storage of Ca^{2+}

Increases in $[Ca^{2+}]_i$ during stimulation of the cell are temporarily and locally restricted. Following raises in $[Ca^{2+}]_i$, the cell uses different strategies to reduce the cytosolic Ca^{2+} levels again in order to avoid a permanent activation of cellular mechanisms. In particular, Ca^{2+} can be chelated by Ca^{2+}-binding proteins, compartmentalized, or extruded [55].

1.5.1.1 Ca^{2+}-ATPases and Ca^{2+} exchangers

Two mechanisms with different affinities and capacities operate in parallel to export Ca^{2+} from cells (Figure 3). Ca^{2+}-ATPases have a high affinity, but low capacity for Ca^{2+}. Plasma membrane Ca^{2+}-ATPases (PMCA) serve to extrude Ca^{2+} across the plasma membrane by exchanging protons for one Ca^{2+}. In contrast, sarco/endoplasmic reticulum Ca^{2+}-ATPases (SERCA) transport two Ca^{2+} in exchange for protons from cytosol into the endoplasmic reticulum (ER) [55,57]. Although the ER serves as an intracellular store for Ca^{2+}, its storage capacity is limited and has to be refilled after depletion [52]. Therefore, the main function of SERCA pumps is to charge up intracellular Ca^{2+} stores, which in turn can release an internal Ca^{2+} signal.
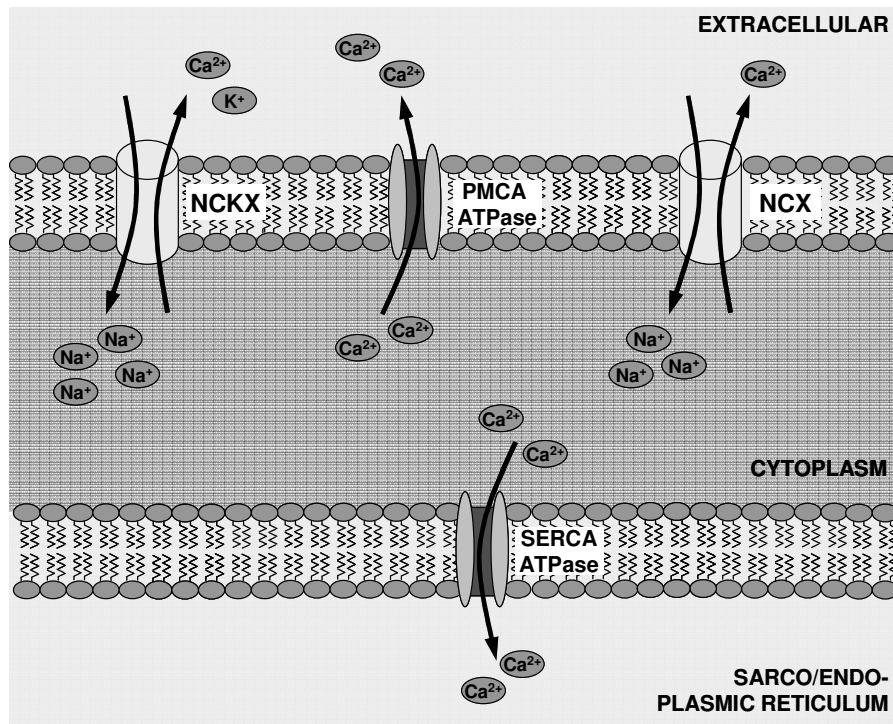
Figure 3. Ca^{2+} extrusion mechanisms in DCs

Cytoplasmic Ca^{2+} levels are kept low in resting cells by extrusion via plasma membrane Ca^{2+}-ATPase (PMCA) and sarco/endoplasmic reticulum Ca^{2+}-ATPase (SERCA). K$^+$-dependent Na$^+$/Ca^{2+} exchangers (NCKX) exchange one Ca^{2+} and one K$^+$ for four Na$^+$, K$^+$-independent Na$^+$/Ca^{2+} exchangers (NCX) exchange one Ca^{2+} for three Na$^+$ (modified after [55]).

A second mechanism of Ca^{2+} extrusion is accomplished by Na$^+$/Ca^{2+} exchangers (Figure 3). Their affinity to Ca^{2+} is lower compared to Ca^{2+}-ATPases, but show a much higher turnover rate [57,58]. Two families of Na$^+$/Ca^{2+} exchangers have been identified, K$^+$-independent (NCX) and K$^+$-dependent (NCKX) Na$^+$/Ca^{2+} exchangers [55,57,59,60]. NCX exchange three Na$^+$ for one Ca^{2+}, while NCKX co-transport one K$^+$ and one Ca^{2+} in exchange of four Na$^+$ [59]. Three NCX and five NCKX isoforms have been identified by molecular cloning [58,60]. Both exchanger families are electrogenic bidirectional transporters and translocate Ca^{2+} either out of or into cells. Direction of transport depends on the dominant electrochemical driving forces, determined by the Na$^+$ and Ca^{2+} concentrations and the membrane potential [61,62]. The expression and function of K$^+$-independent Na$^+$/Ca^{2+} exchangers NCX1 and NCX3 has recently been demonstrated in human lung macrophages and blood monocytes. In these cells, the Ca^{2+} signals generated by the activity of NCX1 and NCX3 resulted in the production of TNFα [63]. So far, the function and regulation of Na$^+$/Ca^{2+} exchangers in DCs have not been described.

1.5.1.2 Ca^{2+}-sensing mechanisms

Ca^{2+} sensing or Ca^{2+} buffering is another important cellular mechanism to modulate changes in [Ca^{2+}]$_i$ and their effects on cell physiology. Under resting or non-activated conditions, Ca^{2+} buffering proteins are present in the Ca^{2+}-free form. Following a rise in [Ca^{2+}]$_i$ due to Ca^{2+} influx or Ca^{2+} release from intracellular stores, these proteins modulate the spatial and temporal aspects of Ca^{2+} signaling [53].

Calmodulin is the primary cellular receptor for Ca^{2+}. Binding of Ca^{2+} to calmodulin is induced by an increase in [Ca^{2+}]$_i$ and results in the conformational change of the protein, leading subsequently to an interaction of the Ca^{2+}/calmodulin complex with target proteins. Important targets downstream of Ca^{2+}/calmodulin signaling are calmodulin kinases (CaMKs). Similar to the MAP-kinase pathway, CaMKs are phosphorylated and therefore activated by CaMK-kinases (CaMKKs) [64,65]. Calmodulin kinase II (CaMKII) has recently been identified as important downstream effector of Ca^{2+} signaling required for DC maturation. It is a multifunctional serine/threonine kinase and an important element of Ca^{2+} signaling in mammalian cells. CaMKII is activated upon DC stimulation by diverse soluble antigens. Inhibition of CamKII results in suppression of cytokine production [64]. Besides CamKII, DCs express another CamK, CaMKIV. Pharmacological inhibition of CaMKIV decreased the viability of monocyte-derived DCs stimulated with LPS. These data indicate that CaMKIV plays a central role in the pathway linking TLR4 to the control of DC life span. However, DCs derived from mice lacking CaMKIV were still able to differentiate and secrete cytokines such as IL-6 and TNFα in response to LPS [66].

Besides calmodulin, the calcineurin/NFAT (nuclear factor of activated T cells) -pathway is also activated and stimulates gene expression in response to rises in [Ca^{2+}]$_i$ [67]. Calcineurin is a calmodulin-dependent serine/threonine phosphatase and contains a catalytic and a regulatory subunit. It is activated through binding of the Ca^{2+}/calmodulin complex to the calcineurin regulatory subunit and displacement of the calcineurin autoinhibitory domain from the enzyme's active site. Activated calcineurin then dephosphorylates and thereby activates NFAT and NFAT-controlled gene expression in response to Ca^{2+} entry. NFAT plays a crucial role in long-term Ca^{2+} signaling, and thus NFAT-driven gene expression is highly dependent on sustained Ca^{2+} influx and calcineurin activity [68,69]. In addition to the role of calcineurin in activating adaptive immune responses, it has been demonstrated to be further involved in regulating the TLR pathway in some cell types, such as monocytes and macrophages [69]. In BMDCs, treatment with inhibitors of calcineurin resulted in increased production of inflammatory mediators like IL-12, TNFα, and IL-1. Furthermore, inhibition of calcineurin led to activation of NFκB in these cells [69]. In contrast, a recent study demonstrated that

stimulation of BMDCs with LPS resulted in an increase in $[Ca^{2+}]_i$ that was linked to activation of NFAT in a TLR-4 independent, but CD14-dependent manner [70].

Calbindin-D9K and calbindin-D28K represent two intracellular Ca^{2+}-binding proteins that buffer Ca^{2+} and furthermore facilitate intracellular Ca^{2+} diffusion. Despite their similar names, they belong to different EF-hand protein subfamilies and thus share little sequence homology [53,54]. Calbindin-D9K has a molecular mass of 9 kDa and was first discovered in the intestinal mucosa of rats [71], while calbindin-D28K, with an apparent molecular mass of 28 kDa, was first found in the chicken duodenal mucosa [72]. Expression of calbindin-D9K and calbindin-D28K is regulated by vitamin D [53]. Pharmacological doses of the active metabolite $1,25(OH)_2D_3$ increase the expression of renal calbindin-D28K, while its expression is reduced under conditions with low levels of circulating $1,25(OH)_2D_3$. Furthermore, calbindin-D28K expression is influenced by the Ca^{2+} concentration in blood [73].

1.5.2 Entry of extracellular Ca^{2+}

The huge concentration gradient for Ca^{2+} across the plasma membrane is accompanied by a negative resting membrane potential. Both provide the electrical driving force for Ca^{2+} entry [55,74]. One of the main functions of Ca^{2+} entry is to charge up intracellular stores, which in turn can release an intracellular Ca^{2+} signal. Ca^{2+} entry occurs via different Ca^{2+}-permeable channels co-existing in the plasma membrane. Voltage-gated channels open in response to membrane depolarization or changes in membrane potential. Activation of ligand-gated channels occurs by binding of an agonist to the extracellular domain of the channel. Receptor-operated channels open upon binding of intracellular second messenger to the channel molecule. Mechanically activated channels respond to mechanical stress. Store-operated channels (SOCs) are activated in response to depletion of intracellular Ca^{2+} stores.

1.5.2.1 Store-operated Ca^{2+} channels

SOCs are characterized by their activation in response to store depletion, even when $[Ca^{2+}]_i$ is buffered to low levels. Activation of SOCs is mediated by activation of phospholipase C (PLC), that triggers the cleavage of phosphatidylinositol-(4,5)-bis-phosphate (PtdIns(4,5)P$_2$) into diacylglycerol (DAG) and inositol-(1,4,5)-trisphosphate (IP$_3$) [52,75]. IP$_3$ binds to its receptor IP$_3$R in the ER membrane and thus stimulates Ca^{2+} release from the ER with subsequent activation of SOCs [55]. IP$_3$R-mediated store depletion is accompanied by the activity of PMCAs, the pumps that release Ca^{2+} out of the cell and therefore prevent the

refilling of ER Ca^{2+} stores. The process subsequently activates slowly over seconds the entry of extracellular Ca^{2+} and is referred to as store-operated Ca^{2+} entry (SOCE) [55,74,76]. Besides IP_3R-mediated store depletion, other mechanisms can lead to lowered ER Ca^{2+} concentration. Blocking of SERCA pumps within the ER membrane, e.g. by thapsigargin, is followed by an increase in $[Ca^{2+}]_i$ with subsequent store depletion [55,77]. Furthermore, low extracellular Ca^{2+} concentrations activate PMCAs in the plasma membrane to extrude leaked Ca^{2+}, depleting ER Ca^{2+} [55].

SOCE is one of the main Ca^{2+} entry mechanisms in many non-excitable cells and plays an essential role in Ca^{2+} signaling and a wide range of other cellular processes, e.g. proliferation, gene transcription, and apoptosis [52]. Many SOCs with different biophysical properties have been described. The best characterized SOCs are the Ca^{2+} release-activated Ca^{2+} (CRAC) channels. CRAC channels represent an ubiquitous signaling mechanism in non-excitable and excitable cells. [74]. In DCs, CRAC channels serve as the major Ca^{2+} entry pathway in response to different antigens. Furthermore, activation of CRAC was shown to be involved in DC maturation and migration. In contrast to voltage-gated Ca^{2+} channels, which are discussed below, Ca^{2+} influx through CRAC is enhanced by membrane hyperpolarization [78]. The mechanisms how intracellular stores sense their depletion to CRAC channels in the plasma membrane have recently become clearer. One of the key players in this mechanism is stromal interaction molecule 1 (STIM1). It is located in the ER membrane and functions as Ca^{2+} sensor [79-81]. STIM1 interacts with Orai1 (or CRACM1), the pore-forming subunit of the CRAC channel [82-84]. Three mammalian homologous CRAC channel proteins have been identified, CRACM1, CRACM2 and CRACM3 [83]. A model of STIM1-Orai1-interaction is illustrated in Figure 4. STIM1 possesses an EF-hand domain with a Ca^{2+}-binding pocket reaching into the ER. Upon store depletion, STIM1 releases the bound Ca^{2+} and forms a junction with the N-terminus of Orai1 in the plasma membrane. This interaction is proposed to subsequently activate SOCE [52,85]. However, little is known about the exact mechanism of interaction of STIM1 and Orai1. It has recently been shown for T lymphocytes that interaction of STIM1 and Orai1 occurs via colocalization of STIM1 in so-called puncta near the site of stimulation, and subsequent interaction with Orai1-containing CRAC channels [86,87]. Another model of STIM1-Orai1-interaction proposes the trafficking of STIM1 to and insertion into the plasma membrane upon store-depletion, thereby activating CRAC channels [52,81].
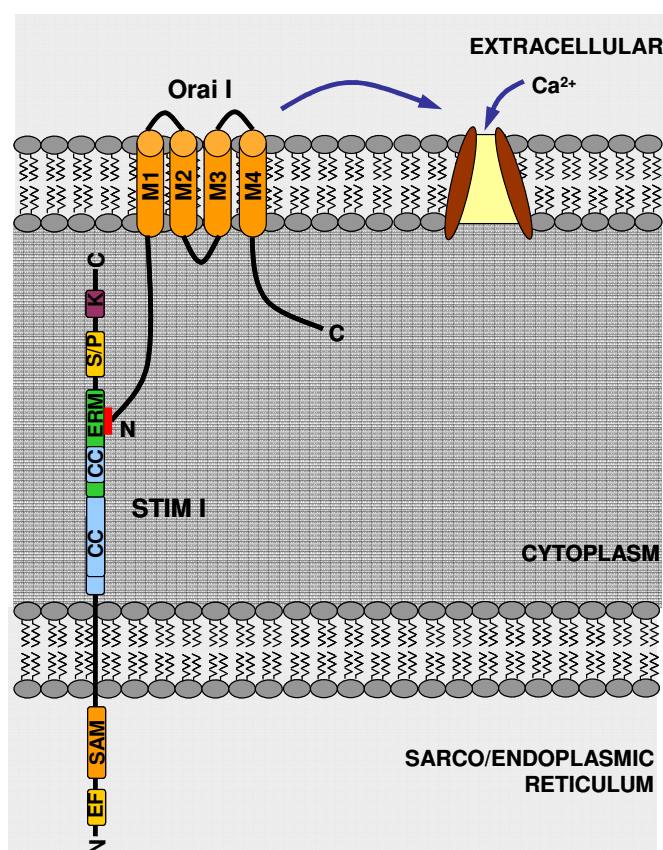
Figure 4. STIM1-Orai1-interaction activates store-operated calcium entry (SOCE)

STIM1 is primarily localized in the ER membrane, with a small fraction in the plasma membrane. Orai1 consists of four domains spanning the plasma membrane, and an intracellular N- and C-terminus. It is possible that interaction of Orai1 N-terminus with the ERM-domain of STIM1 activates SOCE. CC – coiled-coil domain, ERM – ezrin-radixin-moesin domain, K – lysine-rich domain, SAM – sterile-alpha motiv, S/P – serine/proline-rich domain [52].

1.5.2.2 TRP channels

Transient receptor potential (TRP) channels are a superfamily of cation channels that display a greater diversity in activation mechanisms and selectivities than any other group of ion channels [88]. The six TRP channel families known so far share less than 20 % sequence homology. TRP channels consist of six transmembrane domains and are almost ubiquitously expressed [56]. A unifying motif in this superfamily of ion channels is that TRP proteins play critical roles in sensory physiology, contributing to vision, taste, olfaction, hearing, touch, as well as thermo- and osmosensation. In addition, TRP channels enable individual cells to sense changes in their local environment. Many TRP channels are activated by a variety of different stimuli and function as signal integrators. Nematodes use TRP channels at the tips of neuronal dendrites in their "noses" to detect and avoid noxious chemicals. Male mice use pheromone-sensing TRP channels to discriminate between males and females. Humans use

TRP channels to appreciate different tastes and to discriminate temperatures. Some TRP channels, such as TRPV1, respond to a variety of stimuli including proinflammatory agents and exocytosis [88].

Most TRP channels are weakly voltage-sensitive, non-selective ion channels [55]. Some of the TRP channels are highly selective for Ca^{2+}, such as the TRP-vanilloid receptors TRPV5 and TRPV6. They are both activated by raises in $[Ca^{2+}]_i$. The classic TRP channels TRPC3, 6, and 7, are also sensitive to $[Ca^{2+}]_i$, with a relatively low selectivity of Ca^{2+} over Na^+. TRP-melastatin (TRPM) channels TRPM4 and TRPM5 are the only monovalent-selective ion channels of the TRP family and may account for Ca^{2+}-activated, non-selective channel activities [56]. In DCs, Ca^{2+} activates the non-selective cation channel TRPM4, which is essential for DC migration [89].

1.5.2.3 Voltage-gated Ca^{2+} channels

Voltage-gated Ca^{2+} channels (Ca_v channels) provide the fastest way of Ca^{2+} entry into the cell. Their opening is triggered by voltage changes and can lead to more than a 10-fold increase in $[Ca^{2+}]_i$ [55]. They are predominantly expressed in excitable cells like nerve and muscle cells [52], but Kupffer cells also have been shown to contain L-type Ca_v channels [90] and thus depolarization of the cell membrane is required for the Ca^{2+} influx into these cells. In human DCs, the L-type Ca^{2+} channel $Ca_v1.2$ was shown to be involved in Ca^{2+} entry [91]. However, in mouse DCs neither Ca^{2+} currents nor changes in intracellular Ca^{2+} were detected following membrane depolarization, suggesting the absence of functional Ca_v channels in these cells [78].

1.5.2.4 Voltage-gated K^+ channels

Voltage-gated K^+ channels (Kv channels) are transmembrane proteins selective for K^+ over other cations. Their activity is sensitive to changes in the cell membrane potential, as they are activated by depolarization. DCs were shown to possess functionally active voltage-gated K^+ channels, belonging to Kv1 channel family, namely Kv1.3 and Kv1.5. Furthermore, Kv channel activity is involved in LPS-induced DC maturation and cytokine production [92,93]. In human T lymphocytes, inhibition of Kv channels impaired intracellular Ca^{2+} signaling and Ca^{2+}-dependent gene expression [94]. A correlation between Kv channels and Ca^{2+} channels in DCs has not been investigated by now.

1.5.3 Relevance of Ca^{2+}-signaling for DC function

Ca^{2+} signaling plays a central regulatory role in DC maturation and function in response to diverse antigens, including TLR ligands, intact bacteria, and microbial toxins [64,95]. In human monocyte-derived DCs, the PLC-Ca^{2+} pathway is involved in DC activation and maturation induced by different agonists such as LPS, cholera toxin, dibutyryl-cAMP and prostaglandin E_2. Therefore, inhibition of PLC-Ca^{2+} signaling blunts DC maturation [96]. Furthermore, addition of Ca^{2+} ionophore to immature DCs results in the acquisition of many morphological and functional properties associated with a mature DC phenotype, such as co-stimulatory molecule expression [77,96,97]. Thapsigargin, which increases $[Ca^{2+}]_i$ by Ca^{2+}-release from intracellular stores, induces a similar phenotype as the Ca^{2+} ionophore A23187 [77]. In addition, stimulation of DCs by lysophosphatidic acid resulted in a rapid increase in $[Ca^{2+}]_i$ which was not dependent on the presence of extracellular Ca^{2+} [98]. Similarly, ligation of DC-SIGN, a C-type lectin in DCs that mediates capture and internalization of viral, bacterial and fungal pathogens, triggered rapid and transient intracellular Ca^{2+} mobilization [99]. In macrophages and Kupffer cells it was further shown that LPS treatment causes an increase in $[Ca^{2+}]_i$ which was related to TNFα production [100,101].

1.6 Immunoregulation by Vitamin D

The nutrient Vitamin D is a secosteroid hormone that plays a major role in the regulation of calcium homeostasis and normal bone growth. However, recent investigations demonstrated further effects of vitamin D, among which are immunoregulatory properties. Vitamin D deficiency is also involved in the development of autoimmune diseases such as inflammatory bowel disease, ulcerative colitis, and Crohn's disease [102]. The physiological active form of vitamin D is 1,25-dihydroxyvitamin D_3 (1,25(OH)$_2$D$_3$) or calcitriol [102]. It is photochemically synthesized in the skin, where the provitamin 7-dehydrocholesterol is converted to previtamin D_3 in response to sunlight. Previtamin D_3 is further converted into cholecalciferol (vitamin D_3) by isomerization, bound to vitamin D-binding protein (DBP) and transported in the bloodstream to the liver. Cholecalciferol is hydroxylated in the liver by 25-hydroxylase [103]. The resulting 25-hydroxycholecalciferol (25(OH)$_2$D$_3$) is finally converted to its active form 1,25(OH)$_2$D$_3$ in the kidney by the mitochondrial cytochrome P450 enzyme 25(OH)$_2$D$_3$-1α-hydroxylase (1α-hydroxylase), as illustrated in Figure 5 [104,105]. In addition, 1α-hydroxylase activity has been described in several other tissues. Immune cells such as B lymphocytes [106], activated DCs [107], and macrophages [108,109] have been shown to synthesize 1,25(OH)$_2$D$_3$. In B lymphocytes, activation of the cells through CD40 and IL-4 signals induce

expression of 1α-hydroxylase and therefore 1,25(OH)$_2$D$_3$ production, which in turn enhances IL-10 production and inhibits the expression of immunoglobulin E (IgE) [106].
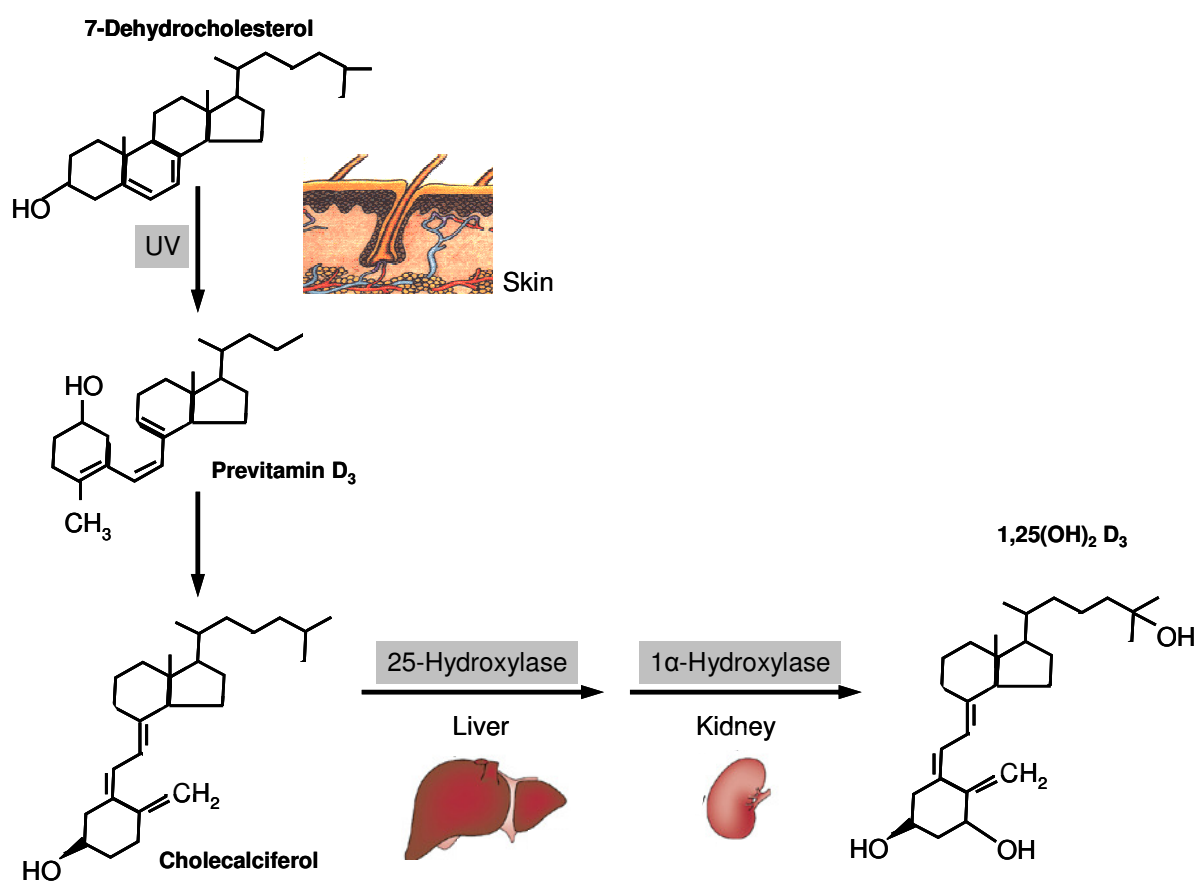
Figure 5. Synthesis of Vitamin D$_3$
Modified after [103].

DCs are primary targets for the immunomodulatory activity of 1,25(OH)$_2$D$_3$, indicated by its inhibitory effect on DC maturation and differentiation [110]. In the resting state, DCs show low levels of 1,25(OH)$_2$D$_3$ production. Activation of the cells by LPS is associated with increased 1α-hydroxylase activity and subsequent increase in 1,25(OH)$_2$D$_3$ production. Terminal maturation makes DCs unresponsive to the effects of 1,25(OH)$_2$D$_3$, but enables them to suppress differentiation of their own precursor cells by a paracrine loop through the production of 1,25(OH)$_2$D$_3$ [107-109]. Furthermore, 1,25(OH)$_2$D$_3$ leads to decreased LPS-induced production of the Th1-polarizing cytokine IL-12 as well as to down-regulation of co-stimulatory molecules and MHC II expression. Moreover, 1,25(OH)$_2$D$_3$ increases the production of IL-10 and promotes DC apoptosis [110-112]. In addition, myeloid DCs treated with 1,25(OH)$_2$D$_3$ show a reduced chemotactic response to inflammatory and lymph node-homing chemokines [111]. Production of CCL22, a chemokine attracting regulatory T

lymphocytes, is up-regulated in myeloid DCs, but not in plasmacytoid DCs, upon $1,25(OH)_2D_3$ exposure [112]. The effects of $1,25(OH)_2D_3$ on DC maturation and function are summarized in Figure 6.
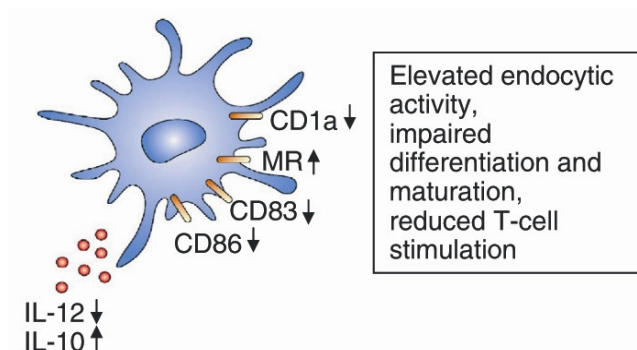
Figure 6. Effects of $1,25(OH)_2D_3$ on DC maturation and function
Taken from [8].

$1,25(OH)_2D_3$ exerts its function by binding to its receptor, the nuclear vitamin D receptor (VDR). VDR was discovered in DCs and other immune cells such as macrophages and activated T and B lymphocytes [113]. Moreover, VDR expression is required for normal development and function of natural killer T lymphocytes [114]. Immunomodulation via the VDR occurs through interference with nuclear transcription factors such as NFAT and NFκB, or through direct interaction with $1,25(OH)_2D_3$-responsive elements in the promoter region of genes encoding for cytokines [110,115]. In activated B lymphocytes, $1,25(OH)_2D_3$ enhances IL-10 expression at least partially through interaction of VDR with the IL-10 promoter region [106]. The NFκB family member RelB, which plays an essential role in DC maturation and differentiation, is selectively suppressed by VDR ligation and subsequent binding of the receptor to the RelB promoter. This mechanism is abolished by LPS-induced DC activation, which results in up-regulation of RelB [115]. In addition, $1,25(OH)_2D_3$ has been shown to inhibit nuclear translocation of NFκB in myeloid, but not in plasmacytoid DCs [112]. Monocyte-derived DCs were further shown to be able to turn on $1,25(OH)_2D_3$-sensitive genes in early phases of cell differentiation if the precursor $25(OH)_2D_3$ is present [116].

Numerous physiological functions require a constant and therefore tight regulation of extracellular Ca^{2+} concentration. Ca^{2+} homeostasis is mainly controlled by kidneys, intestine, skeleton and parathyroid glands. Furthermore, several hormones are involved in its regulation, e.g. calcitonin, parathyroid hormone, and $1,25(OH)_2D_3$ [117]. Thus, the *in vivo* effects of $1,25(OH)_2D_3$ depend on the Ca^{2+} status of the host [102] and, vice versa, $1,25(OH)_2D_3$ is required for Ca^{2+} homeostasis by acting on all three processes of Ca^{2+}

homeostasis: Ca^{2+} entry, diffusion, and extrusion [54]. In epithelial cells, Ca^{2+} transport is regulated by $1,25(OH)_2D_3$ [102]. Furthermore, disturbances in $1,25(OH)_2D_3$-regulated Ca^{2+} homeostasis are involved in autoimmune diseases. In the experimental autoimmune encephalomyelitis (EAE) model of multiple sclerosis, $1,25(OH)_2D_3$ was shown to prevent clinical signs of disease as well as to suppress disease progression [118,119]. These findings suggest a potent immunosuppressive role for $1,25(OH)_2D_3$ *in vivo*. Moreover, $1,25(OH)_2D_3$ was effective to prevent EAE in mice on a high-calcium diet, but not in mice on a low-calcium diet. The data indicate that the role of $1,25(OH)_2D_3$ in preventing EAE and in regulating the immune response to EAE involves Ca^{2+} [120]. Nevertheless, the calcemic effect of $1,25(OH)_2D_3$ *in vivo* limits its therapeutic applications [121]. It was shown recently that a combination of $1,25(OH)_2D_3$ with calcitonin additively suppressed EAE without causing hypercalcemia, thus eliminating a major disadvantage in the use of $1,25(OH)_2D_3$ as a therapeutic agent in multiple sclerosis [122].

1.7 Selective suppression of Th1 immune responses by glucocorticoids

Glucocorticoids belong to the class of steroid hormones and are part of the neuroendocrine system. They are small lipophilic molecules that are involved in numerous physiologic and pathologic processes, among which are immunological responses [123]. Glucocorticoids as well as other steroid hormones (e.g. aldosterone, androgens, and oestrogens) are synthesized in the adrenal cortex out of cholesterol via a common precursor pregnenolone. Dexamethasone, or 9α-fluor-16α-methyl-prednisolone, is a synthetic member of the class of glucocorticoids and approx. ~30 times more effective as cortisol. It is generated out of prednisolone by insertion of a fluor atom at position 9 and a methyl group at position 16 (Figure 7).

Cortisol   **Prednisolone**   **Dexamethasone**
                                                (9α-Fluor-16α-Methyl-Prednisolone)
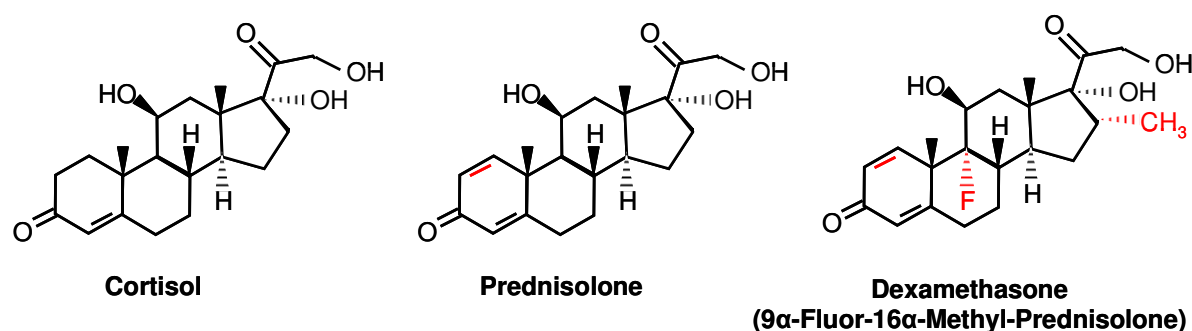
Figure 7. Chemical structures of cortisol, prednisolone and dexamethasone

Glucocorticoids have been shown to act as powerful regulators of the immune response [123-127]. They exert their action directly on T lymphocytes, but are also able to modulate DC maturation and function [8,125,128-132]. Therefore, one major approach for the pharmacological use of glucocorticoids is to promote the tolerogenic effects of DCs [132]. In particular, exposure of DCs to glucocorticoids results in a decreased ability to present antigens and to elicit a T cell response. This effect is primarily due to the inhibitory effects of glucocorticoids on the up-regulation of MHC II and co-stimulatory molecules such as CD86 [125,133]. Moreover, glucocorticoids impair the production of several cytokines by DCs in response to LPS-treatment, including IL-6, IL-12 and TNFα [124,128,130]. On the other hand, glucocorticoid treatment of monocyte-derived DCs increased IL-10 production [131]. The endocytic uptake of antigens by DCs is enhanced by glucocorticoids [133,134], further demonstrated by an inhibitory effect of glucocorticoids on LPS-induced down-regulation of DC endocytosis [128]. These findings are in line with the immature phenotype of glucocorticoid-treated DCs with high antigen capture, low antigen presentation and low ability to stimulate T lymphocytes. The effects of glucocorticoids on DCs are paralleled by an up-regulation of the production of cytokines such as IL-4 and IL-10 by Th2 cells. Taken together, glucocorticoids are not simply immunosuppressive in general, but selectively suppress cellular Th1 immune responses while inducing a shift towards humoral Th2 immunity [124,125,131]. In addition, glucocorticoids such as dexamethasone promote antigen capture, thereby reducing external antigen concentration and availability and further inhibiting the capacity to activate T lymphocytes [134]. The immunomodulatory effects of glucocorticoids on DCs are summarized in Figure 8. They show many parallels to $1,25(OH)_2D_3$-induced immunomodulation and could at least partially be due to an influence on Ca^{2+}-dependent signaling in DCs.
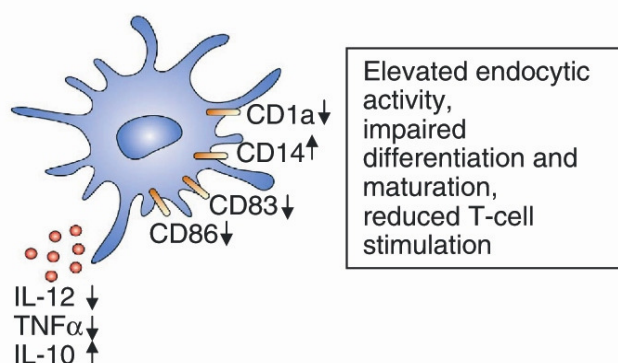
Figure 8. Effects of glucocorticoids on DC maturation and function
Taken from [8].

Glucocorticoids exert their anti-inflammatory and immunomodulatory effects predominantly via genomic mechanisms. Their low molecular mass and lipophilic structure enables them to

pass the membrane and bind to cytosolic glucocorticoid receptors (GCRs), which are ligand-dependent transcription factors. Upon glucocorticoid binding, GCRs are activated and further regulate gene expression [123,135]. GCRs are members of a large superfamily that includes receptors for other steroid hormones, such as thyroid hormone, vitamin D_3, retinoic acid, and a number of orphan receptors [123]. To date, the molecular mechanisms involved in the glucocorticoid-induced impairment of DC maturation are poorly understood. One possible target for glucocorticoid-mediated immunosuppression is the transcription factor NFκB. Glucocorticoids have been shown to induce expression of IκB, which traps active NFκB in the cytosol, inhibits translocation of NFκB to the nucleus, and thus deactivates NFκB-driven gene transcription [136,137]. Since many immunoregulatory genes are activated by NFκB in response to pro-inflammatory stimuli, this mechanism is likely to be at least partially involved in the immunoregulatory activities of glucocorticoids [136]. Another axis of glucocorticoid action is the rapid induction of **g**lucocorticoid-**i**nduced **l**eucine **z**ipper (GILZ) gene, which is expressed by lymphocytes and APCs such as DCs. GILZ is needed for the induction of Tregs by APCs [129,138]. Furthermore, GILZ was shown to contribute to glucocorticoid-mediated inhibition of NFκB [138]. The immunoregulatory enzyme indolamine-2,3-dioxygenase (IDO) may act as a bridge between DCs and Tregs [127]. IDO is a key enzyme in the metabolism of tryptophan [8] and regulates immune responses through its capacity to degrade tryptophan into kynurenine and other metabolites, that suppress the function of effector T lymphocytes and favour the differentiation of Tregs. IDO was shown to be expressed by DCs, whereby induction of IDO-expression occurs in a NFκB-dependent manner [127,139].

1.8 Aim of the study

Lymphocyte priming and the type of induced T cell immunity is controlled by DCs. Several aspects of DC biology are involved in this process, including DC migration and maturation [7]. Moreover, Ca^{2+} signaling plays a major regulatory role in DC maturation and function in response to diverse antigens [64,95]. Although CRAC channels have been shown to be the major Ca^{2+} entry pathway in DCs [78], their role in these cells remains ill-defined. Therefore, the first aim of the present study was to explore the mechanism of Ca^{2+} entry into DCs upon activation in respect to its importance for DC function. Kv channels serve to maintain the electrochemical driving force for Ca^{2+} entry [140]. Therefore, the second aim of the present work was to investigate the role of these channels in the regulation of Ca^{2+}-dependent DC functions. Ca^{2+} entry into a cell is followed by signal termination, which is extremely important

for determination of duration, amplitude and intracellular location of a particular Ca^{2+} signal [141]. Signal termination is accomplished by ion pumps and exchangers, such as Na^+/Ca^{2+} exchangers in the plasma membrane. Nothing is known about the function of Na^+/Ca^{2+} exchangers in DCs. Thus, the third aim of the present study was to investigate if DCs express Na^+/Ca^{2+} exchangers and whether they play a role in DC maturation and function. The fourth aim of the present work was to explore the pharmacological regulation of Na^+/Ca^{2+} exchangers in DCs. Immunosuppressive effects of glucocorticoids could at least partially be due to an influence on Ca^{2+}-dependent signaling in DCs. Moreover, since $1,25(OH)_2D_3$ is a potent regulator of cytosolic Ca^{2+} concentration, it seems to be plausible that some immunomodulatory effects of $1,25(OH)_2D_3$ in DCs are mediated through Ca^{2+} transporting ion channels and transporters.

New insights into the regulation of Ca^{2+}-dependent DC functions might contribute to the development of possible new starting points to modulate immune responses directed against different pathogens.

2   Materials and Methods

2.1   Materials

2.1.1 Tissue culture

2.1.1.1 Equipment

Centrifuge RotiFix 32	Hettich Zentrifugen, Tuttlingen, Germany
Eppendorf pipettes 1000 µl, 100 µl, 10 µl	Eppendorf AG, Hamburg, Germany
Heraeus Incubator	Thermo Electron Corporation, Dreieich, Germany
Neubauer counting chamber	Brand, Wertheim, Germany
Pipetus® pipetting aid	Hirschmann Laborgeräte, Eberstadt, Germany
Syringe BD 10 ml, Luer-Lok™ Tip	Becton Dickinson Labware, Franklin Lakes, USA
Tissue Culture Dishes 60x15 mm	Becton Dickinson Labware, Franklin Lakes, USA
Vortex Genie	Scientific Industries, Bohemia NY, USA
Eppendorf cups 1.5 ml	Eppendorf AG, Hamburg, Germany
Needles BD Microlance™ 3, 0.55x25 mm	Becton Dickinson Labware, Franklin Lakes, USA
PP-Test tubes 15, 50 ml	Greiner bio-one, Frickenhausen, Germany
Stripette® 5, 10, 25 ml	Corning Incorporated, Corning NY, USA

2.1.1.2 Chemicals

1,25-(OH)$_2$ Vitamin D$_3$	Sigma, Taufkirchen, Germany
24,25-(OH)$_2$ Vitamin D$_3$	Sigma, Taufkirchen, Germany
3',4'-dichlorobenzamyl	Sigma, Taufkirchen, Germany
Dexamethasone	Sigma, Taufkirchen, Germany
Foetal Bovine Serum (FBS)	GIBCO, Carlsbad, Germany
GMCSF mouse recombinant	Peprotech/Tebu, Cölbe, Germany
ICAGEN-4	Aventis Pharma, Frankfurt, Germany
KB-R7943	Calbiochem, Schwalbach, Germany
L-Glutamine	GIBCO, Carlsbad, Germany
Lipopolysaccharide E.coli (LPS)	Sigma, Taufkirchen, Germany
Margatoxin	Alomone Labs, Jerusalem, Israel
MEM Non-Essential Amino Acids	Invitrogen, Karlsruhe, Germany

Penicillin-Streptomycin	Invitrogen, Karlsruhe, Germany
Perhexiline maleate (PM)	Sigma, Taufkirchen, Germany
PGN from *Staphylococcus aureus*	InvivoGen, San Diego, California, USA
Phosphate buffered saline (PBS)	GIBCO, Carlsbad, Germany
RPMI 1640	GIBCO, Carlsbad, Germany
SKF-96365	Sigma, Taufkirchen, Germany
Trypan blue solution 0,4%	Sigma, Taufkirchen, Germany
β-mercaptoethanol	Invitrogen, Karlsruhe, Germany

2.1.1.3 Culture medium composition

Complete medium

RPMI-1640	
Fetal bovine serum (FBS)	10 %
L-Glutamine	1 %
Non-essential amino acids (NEAA)	1 %
Penicillin/streptomycin (P/S)	1 %
ß-mercaptoethanol	0.05 %

2.1.2 Intracellular Calcium Imaging

2.1.2.1 Technical equipment

Camera Proxitronic	Proxitronic, Bensheim, Germany
Centrifuge RotiFix 32	Hettich Zentrifugen, Tuttlingen, Germany
Discofix® Stopcock for Infusion Therapy	B. Braun, Melsungen, Germany
Filter Set for Fura-2	AHF Analysentechnik AG, Tübingen, Germany
Filter tips 10, 100, 1000µl	Biozym Scientific, Hess. Oldendorf, Germany
Filter wheel	Sutter Instrument Company, Novato, USA
Infusion Regulator Dosi-Flow 10	Dahlhausen, Köln/Sürth, Germany
Lambda 10-2	Sutter Instrument Company, Novato, USA
Lamp XBO 75	Leistungselektronik Jena GmbH, Jena, Germany
Metafluor software	Universal Imaging, Downingtown, USA
Microscope Axiovert 100	Zeiss, Oberkochen, Germany

Microscope cover glasses round, 30mm diameter, 0.13-0.16 mm	Karl Hecht KG, Sondheim, Germany
Neutral densitiy filters 10, 20, 40, 60%	AHF Analysentechnik AG, Tübingen, Germany
Objective fluar 40x/1.3 oil	Carl Zeiss, Oberkochen, Germany
Syringe BD 10 ml, Luer-Lok™ Tip	Becton Dickinson Labware, Franklin Lakes, USA
Syringe BD Perfusion™ 50 ml	Becton Dickinson Labware, Franklin Lakes, USA
Tissue Culture Dishes 35x10 mm	Becton Dickinson Labware, Franklin Lakes, USA
Winged Needle Infusion Set Butterfly®-21	Hospira Venisystems, Donegal Town, Ireland

2.1.2.2 Chemicals

Ampuwa	Fresenius KABI, Bad Homburg, Germany
$CaCl_2$ x 2 H_2O	Carl Roth, Karlsruhe, Germany
Ethylene glycol tetraacetic acid (EGTA)	Sigma, Taufkirchen, Germany
Fura-2 AM	Invitrogen, Karlsruhe, Germany
Glucose	Carl Roth, Karlsruhe, Germany
HEPES	Sigma, Taufkirchen, Germany
Immersol 518F	Carl Zeiss, Göttingen, Germany
Ionomycin	Sigma, Taufkirchen, Germany
KCl	Carl Roth, Karlsruhe, Germany
$MgCl_2$ x 6 H_2O	Sigma, Taufkirchen, Germany
$MgSO_4$ x 7 H_2O	Sigma, Taufkirchen, Germany
Na_2HPO_4 x 2 H_2O	Sigma, Taufkirchen, Germany
NaCl	Sigma, Taufkirchen, Germany
N-methyl-D-glucamine (NMDG)	Sigma, Steinheim, Germany
Poly-L-Lysine	Sigma, Taufkirchen, Germany
Silicone grease	Carl Roth, Karlsruhe, Germany
Thapsigargin	Molecular Probes, Leiden, The Netherlands

2.1.2.3 Buffer composition

Standard Ringer

NaCl	125 mM/l	
KCl	5 mM/l	
MgSO$_4$ x 7 H$_2$O	1.2 mM/l	
HEPES	32.2 mM/l	
Na$_2$HPO$_4$ x 2 H$_2$O	2 mM/l	
Glucose	5 mM/l	
CaCl$_2$ x 2 H$_2$O	2 mM/l	pH 7.4 (NaOH)

Ca^{2+}-free Ringer

NaCl	125 mM/l	
KCl	5 mM/l	
MgSO$_4$ x 7 H$_2$O	1.2 mM/l	
HEPES	32.2 mM/l	
Na$_2$HPO$_4$ x 2 H$_2$O	2 mM/l	
Glucose	5 mM/l	
EGTA	0.5 mM/l	pH 7.4 (NaOH)

Standard Na$^+$, high K$^+$ Ringer

NaCl	90 mM/l	
KCl	40 mM/l	
MgCl$_2$ x 6 H$_2$O	2 mM/l	
CaCl$_2$ x 2 H$_2$O	2 mM/l	
HEPES	10 mM/l	
Glucose	10 mM/l	pH 7.4 (NaOH)

Standard Na$^+$, low K$^+$ Ringer

NaCl	130 mM/l	
KCl	5 mM/l	
MgCl$_2$ x 6 H$_2$O	2 mM/l	
CaCl$_2$ x 2 H$_2$O	2 mM/l	
HEPES	10 mM/l	
Glucose	10 mM/l	pH 7.4 (NaOH)

Standard Na⁺, K⁺-free Ringer

NaCl	130 mM/l
$MgCl_2$ x 6 H_2O	2 mM/l
$CaCl_2$ x 2 H_2O	2 mM/l
HEPES	10 mM/l
Glucose	10 mM/l pH 7.4 (NaOH)

Na⁺-free, high K⁺ Ringer

NMDG	90 mM/l
KCl	40 mM/l
$MgCl_2$ x 6 H_2O	2 mM/l
$CaCl_2$ x 2 H_2O	2 mM/l
HEPES	10 mM/l
Glucose	10 mM/l pH 7.4 (HCl)

Na⁺-free, low K⁺ Ringer

NMDG	130 mM/l
KCl	5 mM/l
$MgCl_2$ x 6 H_2O	2 mM/l
$CaCl_2$ x 2 H_2O	2 mM/l
HEPES	10 mM/l
Glucose	10 mM/l pH 7.4 (HCl)

Na⁺-free, K⁺-free Ringer

NMDG	130 mM/l
$MgCl_2$ x 6 H_2O	2 mM/l
$CaCl_2$ x 2 H_2O	2 mM/l
HEPES	10 mM/l
Glucose	10 mM/l pH 7.4 (HCl)

2.1.3 Patch Clamp

2.1.3.1 Technical Equipment

Borosilicate glass filaments	Harvard Apparatus, March-Hugstetten, Germany
DMZ puller	Zeitz, Augsburg, Germany
EPC-9 amplifier	Heka, Lambrecht, Germany
ITC-16 Interface	Instrutech, Port Washington, N.Y., USA
Microscope Axiovert 100	Zeiss, Oberkochen, Germany
MS314 electrical micromanipulator	MW, Märzhäuser, Wetzlar, Germany
Pulse software	Heka, Lambrecht, Germany

2.1.3.2 Chemicals

Some of the chemicals mentioned above are also used for Patch Clamp, therefore the additional chemicals are listed here only.

CsCl	Sigma, Taufkirchen, Germany
HCl	Sigma, Taufkirchen, Germany
K^+-gluconate	Sigma, Taufkirchen, Germany
LiCl	Sigma, Taufkirchen, Germany
MgATP	Sigma, Taufkirchen, Germany
Tetraethylammonium (TEA)	Sigma, Taufkirchen, Germany

2.1.3.3 Bath solutions

I_{CRAC} – Standard bath

NaCl	140 mM/l	
KCl	5 mM/l	
$MgCl_2$	0.1 or 10 mM/l	
$CaCl_2$	0.1 or 10 mM/l	
HEPES/NaOH	10 mM/l	
Glucose	20 mM/l	pH 7.4

I_{CRAC} – Na$^+$-free bath

NMDG-Cl	145 mM/l
MgCl$_2$	1 mM/l
CaCl$_2$	10 mM/l
HEPES/NMDG	10 mM/l
Glucose	20 mM/l pH 7.4

K_V – Standard bath

NaCl	140 mM/l
KCl	5 mM/l
MgCl$_2$	1 mM/l
CaCl$_2$	2 mM/l
HEPES/NaOH	10 mM/l
Glucose	20 mM/l pH 7.4

Na+/Ca2+ exchange – bath I

NaCl	130 mM/l
TEA-Cl	20 mM/l
MgCl$_2$	2 mM/l
EGTA	0.5 mM/l
HEPES/CsOH	10 mM/l
Glucose	10 mM/l pH 7.2

Na+/Ca2+ exchange – bath II

TEA-Cl	20 mM/l
LiCl	130 mM/l
KCl	0 or 40 mM/l
MgCl$_2$	2 mM/l
CaCl$_2$	2 mM/l
HEPES/CsOH	10 mM/l
Glucose	10 mM/l pH 7.2

2.1.3.4 Pipette solutions

CsCl/NaCl pipette solution

NaCl	35 mM/l
CsCl	120 mM/l
MgATP	1 mM/l
EGTA	10 mM/l
HEPES/CsOH	10 mM/l pH 7.4

KCl/K⁺-gluconate pipette solution

KCl	80 mM/l
K$^+$-gluconate	60 mM/l
MgATP	1 mM/l
MgCl$_2$	1 mM/l
EGTA	1 mM/l
HEPES/KOH	10 mM/l pH 7.2

Na⁺-based pipette solution

NaCl	120 mM/l
KCl	40 mM/l
MgATP	2 mM/l
MgCl$_2$	2 mM/l
TEA-Cl	20 mM/l
HEPES/CsOH	10 mM/l
Glucose	8 mM/l pH 7.2

2.1.4 Immunostaining and phagocytosis

2.1.4.1 Technical equipment

FACS Calibur	Becton Dickinson, Heidelberg, Germany
FACS tubes, 1.3 ml, PP, round bottom	Greiner bio-one, Frickenhausen, Germany

2.1.4.2 Antibodies and chemicals

Annexin-V-Fluos	Roche Diagnostics, Penzberg, Germany
FITC-conjugated anti-mouse CD11c, clone HL3 (Armenian Hamster IgG$_1$, λ2)	BD Pharmingen, Heidelberg, Germany
FITC-conjugated dextran	Sigma, Taufkirchen, Germany
PE- conjugated anti mouse ICAM-1 (CD-54), clone 3E2 (Armenian Hamster IgG1, κ)	BD Pharmingen, Heidelberg, Germany
PE-conjugated anti-mouse CD86, clone GL1 (Rat IgG$_{2a}$, κ)	BD Pharmingen, Heidelberg, Germany
PE-conjugated rat anti-mouse I-A/I-E, clone M5/114.15.2 (IgG2b, κ)	BD Pharmingen, Heidelberg, Germany
Sodium azide	Sigma, Taufkirchen, Germany

2.1.4.3 Buffers

FACS buffer

PBS

0.1 % heat-inactivated FBS

2.1.5 Migration and cytokine production

2.1.5.1 Technical equipment

Magellan™ software	Tecan Group Ltd., Männedorf, Switzerland
multi well plates; 24, 96 well	Corning Inc., Corning NY, USA
Sunrise™ Microplate Reader	Tecan Trading AG, Switzerland

2.1.5.2 Chemicals and Kits

Calcein-AM	Calbiochem, Schwalbach, Germany
CCL21	Peprotech/Tebu, Cölbe, Germany
InnoCyte™ Cell Migration Assay Kit	Calbiochem, Schwalbach, Germany
Mouse IL-10 ELISA Set	BD Pharmingen, Heidelberg, Germany

Mouse IL-12p70 ELISA Set	BD Pharmingen, Heidelberg, Germany
Mouse IL-6 ELISA Set	BD Pharmingen, Heidelberg, Germany
Mouse TNF (Mono/Mono) ELISA Set	BD Pharmingen, Heidelberg, Germany
TMB substrate reagent	BD Pharmingen, Heidelberg, Germany

2.1.5.3 Buffers and solutions

Coating buffer

0.2 M sodium phosphate   pH 6.5

Assay diluent

1x PBS

10 % heat-inactivated FBS

Stop Solution

2 N H_2SO_4

2.1.6 Immunoblotting

2.1.6.1 Technical equipment

Agarose gel electrophoresis chamber	BioRad, München, Germany
Centrifuge 5415R	Eppendorf, Hamburg, Germany
Densitometer Quantity One	BioRad, München, Germany
Gel tips	Alpha Laboratories, Hampshire, UK
Kodak film	Sigma, Hannover, Germany

2.1.6.2 Chemicals

Acrylamide/bisacrylamide	Carl Roth, Karlsruhe, Germany
BenchMark prestained protein ladder	Invitrogen, California, USA
Cell lysis buffer	Pierce, Bonn, Germany
Detection reagent	GE Healthcare, München, Germany
Glycine	Sigma, Taufkirchen, Germany

Loading buffer (4x)	Carl Roth, Karlsruhe, Germany
Milk powder	Carl Roth, Karlsruhe, Germany
Nitrocellulose membrane	VWR, Darmstadt, Germany
Ponceau S	Sigma, Taufkirchen, Germany
Protease inhibitor	Sigma, Taufkirchen, Germany
Sodium dodecyl sulfate (SDS)	Sigma, Hannover, Germany
TEMED	Carl Roth, Karlsruhe, Germany
Triethanolamine-buffered saline (TBS)	Sigma, Taufkirchen, Germany
Tween-20	Böhringer Ingelheim, Mannheim, Germany

2.1.6.3 Antibodies and Kits

Anti-α/β tubulin	Cell Signaling/ New England Biolabs, Frankfurt am Main, Germany
Anti-phospho-IκBα	Santa Cruz Biotechnology, Heidelberg, Germany
Enhanced chemiluminescence (ECL) Kit	Amersham, Freiburg, Germany
Monoclonal (mouse) anti-calbindin D-28K	Swant, Bellinzona, Switzerland
Goat anti-mouse Alexa 488	Molecular Probes, Leiden, The Netherlands

2.1.6.4 Buffers

Running buffer

Tris	25 mM/l
Glycine	250 mM/l
SDS	0,1 %

Transfer buffer

Tris	25 mM/l	
Glycine	192 mM/l	
Methanol	20 %	pH 8.3

Wash buffer (PBS-T)

1x PBS	
Tween-20	0.05 %

2.1.7 RNA measurements

2.1.7.1 Technical equipment

Densitometer	BioRad, München, Germany
LightCycler System	Roche Diagnostics, Mannheim, Germany
Mastercycler®	Eppendorf AG, Hamburg, Germany

2.1.7.2 Chemicals

10x reaction buffer	Biolabs, Frankfurt, Germany
Agarose	Sigma, Taufkirchen, Germany
DEPC water	Ambion, Darmstadt, Germany
dNTP mix	Promega, Mannheim, Germany
Ethanol 99.7%	VWR, Darmstadt, Germany
Ethidium bromide	Sigma, Taufkirchen, Germany
Master Sybr Green I Mix	Roche, Mannheim, Germany
M-MuLV reverse transcriptase	Biolabs, Frankfurt, Germany
Primer mix	Search LC, Heidelberg, Germany
puReTaq Ready-To-Go PCR bead	Amersham Biosciences, Freiburg, Germany
Recombinant RNase inhibitor	Roche, Mannheim, Germany
RLT lysis buffer	Qiagen, Hilden, Germany

2.1.7.3 Kits

QIAshredder	Qiagen, Hilden, Germany
Murine MRPS9 Kit	Search LC, Heidelberg, Germany
RNase-free DNase Set	Qiagen, Hilden, Germany
Rneasy Mini Kit	Qiagen, Hilden, Germany

2.1.8 Animals

The mice (NMRI, female) were obtained from Charles River, Sulzfeld, Germany. Alternatively, any wild type mice breeded in the institute could be used because a comparison between cells from wild type and knock out animals was not performed. For PGN experiments, DCs were additionaly isolated form $tlr2^{-/-}$ mice of C57BL/6 background and their wild-type littermates.

2.2 **Methods**

2.2.1 Cell culture

Dendritic cells (DCs) were cultured from mouse bone marrow following an established protocol [142] with slight modifications. The cells were isolated from femur and tibias of 7-11 weeks old mice. After removing skin and muscle mass from the bone, the bone marrow-derived cells were flushed out off the bone marrow cavity from the femur and tibia with sterile, icecold PBS using a small needle fixed on a syringe. The extracted cells were centrifuged at 1500 rpm for 5 min at 4°C. The supernatant was discharged and the cells were resuspended in complete cell culture medium and centrifuged. Subsequently, the DCs were resuspended again and counted using a Neubauer counting chamber. Cells were seeded out into 60x15 mm petri dishes at a density of 2×10^6 cells per dish. Finally, GM-CSF (35 ng/mL) was added to the culture media.

The cells were cultured for 1 week with changes of the medium on days 3 and 6. For the first medium change, fresh medium as well as GM-CSF was added to the culture. On day 6, nonadherent and loosely attached cells were harvested and the removed volume of the culture medium was replaced by fresh medium and GM-CSF. At day 7, the cells were seeded out into several petri dishes in an amount of 5×10^5 cells per dish. For cell treatment, the substances of interest were added to the respective dishes for a certain time period indicated in the respective experiments. Experiments were performed on mature DCs and carried out on days 7-9. The expression of CD11c and maturation markers was monitored by FACS analysis.

2.2.2 Immunostaining and flow cytometry

Maturation of the DCs was confirmed by flow cytometry using a FACS Calibur. Measurements were carried out on day 7 of DC culture as well as after time periods indicated in the particular experiments. Cells (4×10^5) were incubated in 100 µl FACS buffer containing fluorochrome-conjugated antibodies at a concentration of 10 µg/ml. DCs were stained for their surface markers CD11c, CD86, CD54 (ICAM-1), and MHCII (I-A/I-E). The amount of apoptotic cells was verified by estimating the amount of Annexin-V binding. After incubating with the respective antibodies for 60 minutes at 4^0C, the cells were washed twice and resuspended in FACS buffer for flow cytometry analysis. A total of 2×10^4 cells were analyzed for each experiment.

2.2.3 Intracellular Calcium Imaging

The measurements of intracellular calcium concentration $[Ca^{2+}]_i$ were performed using an inverted phase-contrast microscope connected to the following accessories: a camera, a light source, a filter wheel with different excitation filters, a shutter element, a perfusion system inserted into a measuring chamber, a water bath, and a pump to allow a continous exchange and removal of the added bath solutions (Figure 9). The cells were continously superfused during each experiment. Experiments were performed at 37°C in Ringer solution.
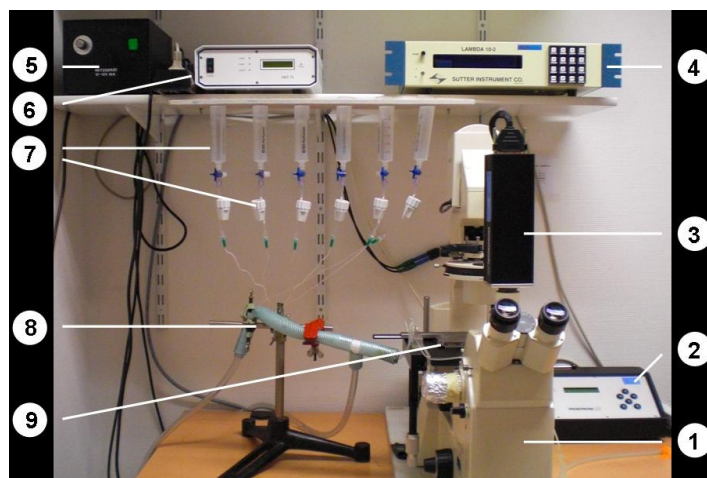
Figure 9. Intracellular Calcium Imaging Setup
1 – Microscope, 2 – Camera control panel, 3 – Camera, 4 – Shutter, 5 – Light source, 6 – Xenon lamp control panel, 7 – Perfusion system, 8 – Flow heating system, 9 – measuring chamber.

Cells were incubated with 2 µM Fura-2/AM for 30 minutes at 37℃. The chamber was then mounted onto the microscope and both inlet and outlet equipment for exchanging the bath solution were fixed to the chamber cavity. To generate a Fura-2 fluorescence ratio, cells were excited alternatively at 340 and 380 nm and the light was deflected by a dichroic mirror into either the camera or the objective. For the latter, an oil-immersion objective suitable for fluorescence microscopy was used. When the light was deflected into the camera, the emitted fluorescence intensity was recorded at 505 nm and data acquisition was performed every 6-10 seconds by using Metafluor computer software. For data analysis, the obtained data were converted to Excel for further evaluation. As a measure for the increase of cytosolic Ca^{2+} activity, the slope and peak of the changes in the 340/380 nm ratio in response to changing the measurement conditions were calculated for each cell and experiment. Though, the deviation between the lowest and the highest point of the increase in $[Ca^{2+}]_i$ reflected the peak, whereas the ratio change per time represented the slope of the reaction.

For intracellular calibration purposes, 10 µM ionomycin was applied at the end of each experiment. Adding of ionomycin to the Ca^{2+}-containing Ringer solution yielded a maximum value R_{max} at saturating free Ca^{2+} levels. Administration of ionomycin in Ca^{2+}-free Ringer solution yielded a minimum value R_{min} at zero free Ca^{2+} levels. The obtained ratios were converted into nanomolar Ca^{2+} concentrations using the equation according to Grynkiewicz et al. [143]. The equation describes the interrelationship of the free Ca^{2+} concentration and the fluorescence emission intensity ratio of any experimental sample (Figure 10).

$$[Ca^{2+}]_{free} = K_d \times \left(\frac{R - R_{min}}{R_{max} - R} \right) \times S_f$$

K_d = Dissociation constant of Fura-2 (inverse logarithm of the x-intercept)

R = Ratio of emission intensity, exciting at 340 nm, to emission intensity, exciting at 380 nm

R_{min} = Ratio at zero free Ca^{2+}

R_{max} = Ratio at saturating Ca^{2+}

S_f = instrumental constant

$$= \frac{\text{Fluorescence intensity, exciting at 380 nm, for zero free } Ca^{2+}}{\text{Fluorescence intensity, exciting at 380 nm, at saturating free } Ca^{2+}}$$

Figure 10. Calibration Equation for the calculation of intracellular calcium concentrations
Referring to Grynkiewicz et al. [143].

The dissociation constant of the dye K_d and the instrumental constant S_f were determined using a Fura-2 Calcium Imaging Calibration Kit. For K_d, the obtained values were used to generate a standard curve, which then allowed to calculate K_d (Figure 11). On the basis of

the calibration equation and the obtained K_d value, the free Ca^{2+} concentration for any experimental sample was calculated from the corresponding R value of each sample.
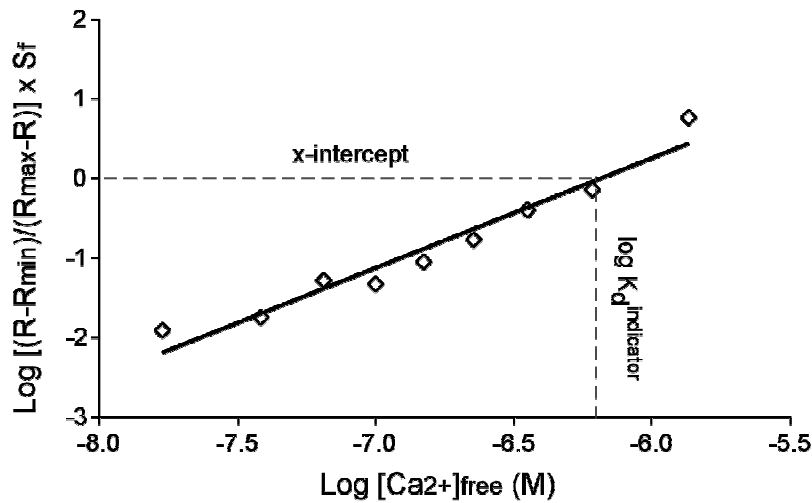
Figure 11. Standard curve to calculate the dissociation constant K_d of Fura-2

2.2.4 Patch clamp

Patch clamp experiments were performed at room temperature in voltage-clamp, fast-whole-cell mode according to Hamill et al. [144]. The cells were continuously superfused through a flow system inserted into the dish. The bath was grounded via a bridge filled with NaCl Ringer solution. Borosilicate glass pipettes, manufactured by a microprocessor-driven DMZ puller, were used in combination with a MS314 electrical micromanipulator. The currents were recorded by an EPC-9 amplifier using Pulse software and an ITC-16 Interface.

For I_{CRAC} measurements whole-cell currents were elicited by 200 ms square wave voltage pulses from -100 to +80 mV in 20 mV steps delivered from a holding potential of 0 mV. Alternatively, the currents were recorded with 200 ms voltage ramps from -120 to +100 mV. Kv whole-cell currents were elicited by 200 msec square wave voltage pulses from -90 to +90 mV in 20 mV steps delivered at 20 ms intervals from a holding potential of -70 mV. The currents were recorded with an acquisition frequency of 10 kHz and 3 kHz low-pass filtered. For measurements of Na^+/Ca^{2+}-exchanger voltage clamp steps were applied every 2 s to potentials between -100 and +50 mV from a holding potential of 0 mV. The currents were recorded with an acquisition frequency of 10 kHz and 3 kHz low-pass filtered.

Composition of the bath solution differed depending on whether I_{CRAC}, Kv currents or Na^+/Ca^{2+}-exchange currents were measured (see section 2.1.3.3). The patch clamp pipettes were filled with an internal solution, which composition differed between K_v current (KCl/K^+-gluconate pipette solution), Na^+/Ca^{2+} exchange current (Na^+-based pipette solution, 1 µM free Ca^{2+}) and I_{CRAC} measurements (CsCl/NaCl pipette solution).

2.2.5 RT-PCR

Total RNA was isolated from mouse DCs by using the Qiashredder and RNeasy Mini Kit from Qiagen according to the manufacturer's protocol. For cDNA first strand synthesis, 1 µg of total RNA in 12.5 µl DEPC-H_2O was mixed with 1 µl of oligo-dT primer (500 µg/ml) and heated for 2 min at 70°C. A RT mix of 2 µl 10x reaction buffer, 1 µl dNTP mix (dATP, dCTP, dGTP, dTTP, 10 mM each), 0.5 µl recombinant RNase inhibitor, 0.1 µl M-MuLV reverse transcriptase, and 2.9 µl DEPC-H_2O was then added and the reaction mixture was incubated for 60 min at 42°C. The reaction was stopped by heating the mixture for 5 min at 94°C. The cDNA was stored at -80 °C until PCR analysis. PCR analysis was then performed with 1 µl of the reverse transcription product in a total volume of 25 µl of a PCR mix containing 22 µl of sterile bi-distilled H_2O, 1 µl of sense primer (100 pmol/µl), 1 µl of antisense primer (100 pmol/µl), and 1 puReTaq Ready-To-Go PCR bead through 40 cycles as indicated in Table 2.

Table 2. RT-PCR protocols

	denaturation	annealing	synthesis
CRACM1	30 s at 95°C	20 s at 58°C	45 s at 72°C
CRACM2	30 s at 95°C	20 s at 56°C	45 s at 72°C
CRACM3	30 s at 95°C	20 s at 52°C	45 s at 72°C
NCKX1	15 s at 95°C	45 s at 56°C	45 s at 72°C
NCKX2	15 s at 95°C	45 s at 60°C	45 s at 72°C
NCKX3	15 s at 95°C	45 s at 60°C	45 s at 72°C
NCKX4	15 s at 95°C	90 s at 52°C	90 s at 72°C
NCKX5	15 s at 95°C	45 s at 56°C	45 s at 72°C
NCX1	15 s at 95°C	45 s at 56°C	45 s at 72°C
NCX2	15 s at 95°C	45 s at 60°C	45 s at 72°C
NCX3	15 s at 95°C	60 s at 56°C	90 s at 72°C

The following primers were used to amplify specific cDNA fragments from mouse DCs. PCR products were analysed by agarose gel electrophoresis.

NCX1 *(440 bp)*   sense primer: 5'-GCTTCATTGTCTCCATCCTCATG-3'
     antisense primer: 5'-GGAAGATGTGAGGAGCTTGGC-3'

NCX2 *(436 bp)*   sense primer: 5'-CTTTGGTGTCTGCATCCTGGTC-3'
     antisense primer: 5'-GGTGGTGGCCAGCTTGGGTC-3'

NCX3 *(437 bp)*   sense primer: 5'-CTTCGTGGTCTCCATCCTCATC-3'
     antisense primer: 5'-ATGTCGTGGCAAGCTTGCAGC-3'

NCKX1 *(456 bp)*   sense primer: 5'-CACCTTCCTGGGATCCATCATC-3'
     antisense primer: 5'-CGATCTTCTAACATCACACTGATC-3'

NCKX2 *(370 bp)*   sense primer: 5'-TTATCATGTGGTGGGAAAGC-3'
     antisense primer: 5'-GCTTTTTCTCTGAACCTCCC-3'

NCKX3 *(456 bp)*   sense primer: 5'-GACATTCGCTTCCTCTACGCTAT-3'
     antisense primer: 5'-AACTCCGTCATGATGGAGAAA-3'

NCKX4 *(349 bp)*   sense primer: 5'-ATTCTCAGCTCTAGCCCTCC-3'
     antisense primer: 5'-ACTTAGCCTTGTCGCCTTTT-3'

NCKX5 *(410 bp)*   sense primer: 5'-CAGTTCATTTTAATGGCTGGA-3'
     antisense primer: 5'-GTTTTCCCGACCTTGGTGTA-3'

Mouse **CRACM1**   sense primer: 5'-CATGGTAGCGATGGTGGAAGTC-3'
     antisense primer: 5'-TGCTCATCGTCTTTAGTGCCT-3'

Mouse **CRACM2**   sense primer: 5'-ATGGTGGCCATGGTGGAGGT-3'
     antisense primer: 5'-ATTGCCTTCAGCGCCTGCA-3'

Mouse **CRACM3**   sense primer: 5'-AAGCTCAAAGCCTCCAGCCGC-3'
     antisense primer: 5'-GGTGGGTATTCATGATCGTTCT-3'

2.2.6 Real time-PCR

Isolation of total RNA and cDNA first strand synthesis was performed as mentioned above (section 2.2.5). Subsequently, quantitative real time-PCR was performed to determine transcript levels of NCX1, NCX2, and NCX3, using a LightCycler System. PCR reactions were performed in a final volume of 20 µl containing 2 µl cDNA, 2.4 µl $MgCl_2$ (3 µM), 1 µl primer mix (0.5 µM of both primers), 2 µl cDNA Master SybrGreen I mix, and 12.6 µl DEPC-treated water. The following primers were used to quantify mRNA transcripts:

NCX1 *(200 bp)*	sense primer:	5'-TCCGAGTTCTTAAATGGTTAAGGC-3'
	antisense primer:	5'-TGGGTGGATCACTACTTTCTATAAGGA-3'
NCX2 *(174 bp)*	sense primer:	5'-GCCATCCATCTCTGCCCTTA-3'
	antisense primer:	5'-CCTGGGGGACAGATACTCCA-3'
NCX3 *(185 bp)*	sense primer:	5'-TGACAGCTGCTAGCCCACA-3'
	antisense primer:	5'-CTCAGCCTCCAGAGCTCGAT-3'

MRPS9 was used as housekeeping gene, and transcript levels were determined for each sample using a commercial primer kit. To this end, each PCR reaction for MRPS9 was performed in a final volume of 20 µl containing 2 µl cDNA, 2 µl MRPS9 primer mix, 2 µl cDNA Master Sybr Green I mix, and 14 µl DEPC-treated water. The target DNA was amplified during 50 cycles of 95ºC for 10 s, 68ºC for 10 s, and 72ºC for 16 s, each with a temperature transition rate of 20ºC/s, a secondary target temperature of 58ºC, and a step size of 0.5ºC. In order to determine the melting temperature of primer dimers and the specific PCR products, as well as to confirm the amplified products, melting curve analysis was performed at 95ºC/0 s, 58ºC/15 s, and 95ºC/0 s. mRNA expression for each signal was calculated using the $\Delta\Delta C_t$ method.

2.2.7 Immunoblotting

To generate samples from mouse DCs for Western Blot analysis, 2×10^6 cells were washed twice in PBS and subsequently solubilized in lysis buffer containing a protease inhibitor cocktail. The amount of protein was measured using the Bradford method. Samples were mixed with 4x loading buffer in a 1:4-ratio. 80 µg of each sample was separated by SDS-PAGE, using a 5 %-stacking gel and a 12 %-resolving gel. The preparation of one stacking gel and one resolving gel is shown in Table 3. The gel was run at 80 V for 15 minutes first, then the voltage was increased to 120 V for 1 hour. Subsequently, the separated proteins were transferred to a nitrocellulose membrane for 1 hour at 82 V. Transfer was checked by Ponceau S-staining. The membrane was blocked with 5 % nonfat-milk in TBS-buffer containing 0.1 % Tween-20. The blot was then probed overnight with either anti-phospho-IκBα, or monoclonal (mouse) anti-calbindin D-28K, diluted 1:1000 in 5 % milk made up with TBS-buffer containing 0.1 % Tween-20. Membranes were washed 5 times in PBS-T and probed with secondary antibodies conjugated to horseradish peroxidase for 1 h at room temperature. After 5 final washes, antibody binding was detected with the enhanced chemiluminescence (ECL) kit and densitometer scans were performed.

Table 3. Gel preparation

	Stacking gel (5 %)	*Resolving gel (12 %)*
H_2O	2.7 ml	3.3 ml
30 % acrylamide	670 µl	4.0 ml
1.5 M Tris (pH 8.8)	-	2.5 ml
1.0 M Tris (pH 6.8)	500 µl	-
10 % SDS	40 µl	100 µl
10 % ammonium persulfate	40 µl	100 µl
TEMED	4 µl	4 µl

2.2.8 Cytokine measurement

To determine the production of TNFα, IL-6, IL-10, and IL-12p70 by mouse DCs, the enzyme-linked immunosorbent assay (ELISA) was performed using the respective ELISA Set from BD Biosciences (see section 2.1.5.2). Samples were obtained by incubating mouse DCs with a certain substance for a certain time point at 37°C and 5 % CO_2. Afterwards the cells were harvested and centrifuged for 5 min at 1500 rpm. The supernatant was collected and stored at -20°C until usage. The amount of the respective cytokines in the supernatant were analysed according to the manufacturer's protocol. Briefly, a 96-well plate was coated with 100 µl of Capture Antibody diluted in Coating Buffer and kept overnight at 4°C. Subsequently, the plate was aspirated and washed 3 times. The wells were blocked for 1 hour at room temperature (RT) with 200 µl Assay Diluent. Afterwards, the plate was aspirated and washed again 3 times. 100 µl of the standards and samples were added to each well and incubated for 2 hours at RT. The plate was aspirated and washed for 5 times and 100 µl Working Detector were added to each well. After incubation at RT for 1 hour, the plate was aspirated and washed for 7 times. 100 µl Substate Solution were added to each well and incubated for 30 min at RT in the dark. Subsequently, 50 µl Stop Solution was added to each well. Absorbance was recorded at 450 nm.

2.2.9 Phagocytosis assay

DCs of each experimental condition were suspended in prewarmed serum-free RPMI 1640 medium in a concentration of 10^6 cells/ml. The samples were then pulsed with FITC-conjugated dextran at a final concentration of 1 mg/ml and incubated for 3h at 37°C. Uptake of FITC-conjugated dextran was stopped by adding ice-cold PBS. The cells were then washed three times with ice cold PBS supplemented with 5% FCS and 0.01% sodium azide and analysed by FACS for the uptake of FITC-dextran.

2.2.10 Migration assay

DCs were washed twice with PBS and resuspended in RPMI 1640 medium. Migration was assessed in triplicate in a mulitwell chamber with 8 µm-pore size filter contained in the InnoCyte™ Cell Migration Assay Kit. The cells were adjusted to 5 x 10^5 cells/ml and the cell suspension was placed in the upper chamber to migrate into the lower chamber in which either 250 ng/ml CCL21 or medium alone as a control for spontaneous migration were included. The chamber was placed into an incubator at 5% CO_2 and 37°C for 4h. Subsequently, the cells that migrated into the lower chamber were detached using the provided cell detachment buffer containing Calcein-AM fluorescent dye. The results were read using a standard fluorescence plate reader. For data analysis, the mean fluorescence of spontaneously migrated cells was substracted from the total fluorescence of migrated cells.

2.2.11 Statistics

Data are provided as means ± SEM, *n* represents the number of independent experiments. All data were tested for significance using Student's unpaired two-tailed *t*-test or ANOVA. *P*<0.05 was considered to indicate statistical significance.

3   Results

3.1 LPS- and PGN-induced Ca^{2+} entry

Intracellular Calcium Imaging was used to assess changes in intracellular free Ca^{2+} concentration ([Ca^{2+}]$_i$) upon treatment of mouse dendritic cells (DCs) with either lipopolysaccharide (LPS, 100 ng/ml) or peptidoglycan (PGN, 25 µg/ml). Images of the cells stained with 2 µM Fura-2 were taken every 6-10 seconds in a pseudocolor mode. A change of the color from blue to red indicates an increase in [Ca^{2+}]$_i$. Figure 12 shows a representative experiment using PGN for acute treatment of the cells.
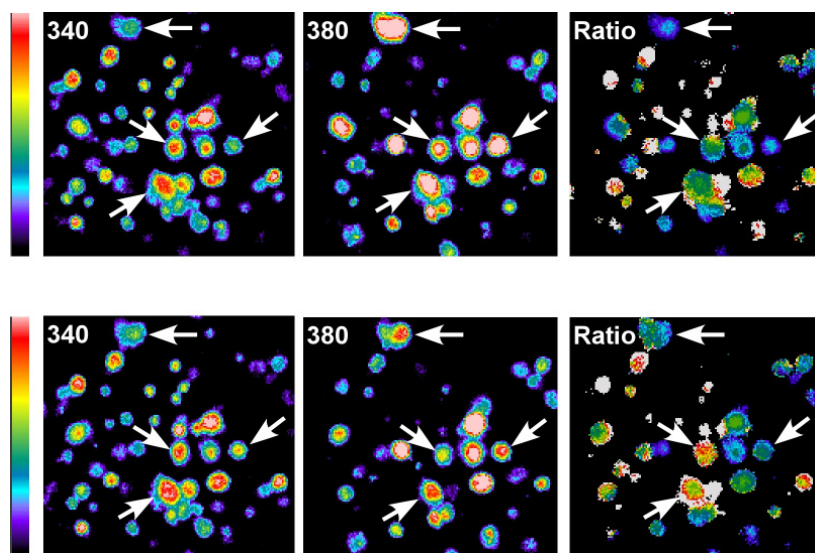
Figure 12. Pseudocolor images of Fura-2 loaded DCs

Left panels: pseudocolor images at 340nm excitation. *Central panels:* pseudocolor images of the same cells at 380 nm excitation. Right panels: pseudocolor images resulting from the ratio of both excitation wavelengths of the respective cells. *Upper panels* were recorded before addition of 25 µg/ml PGN. *Lower panels* were recorded after addition of PGN and subsequent influx of extracellular Ca^{2+}. White arrows indicate example cells that show a shift from dark blue (low intracellular Ca^{2+}) to red (high intracellular Ca^{2+}) upon addition of PGN.

Acute stimulation of mouse DCs with either LPS (100 ng/ml, Figure 13A) or PGN (25 µg/ml, Figure 13B) resulted in a rapid increase in [Ca^{2+}]$_i$. This increase was due to Ca^{2+} release from intracellular stores and influx of extracellular Ca^{2+}, since the increase of [Ca^{2+}]$_i$ was significantly blunted but not fully abrogated when LPS or PGN was applied in the absence of extracellular Ca^{2+} (Figure 13C, D). The same effect was achieved when LPS or PGN were

applied in the presence of SKF-96365 (10 µM, Figure 13A, B, E, F), a blocker of store-operated Ca^{2+} channels.

Figure 13. LPS or PGN exposure increases [Ca^{2+}]$_i$ in mouse DCs

A, B Representative original tracings showing the change in [Ca^{2+}]$_i$ in Fura-2/AM loaded control and SKF-96365 (10 µM)-pretreated DCs prior to and following acute addition (white arrow) of **(A)** LPS (0.1 µg/ml) or **(B)** PGN (25 µg/ml). For quantification of Ca^{2+} entry the slope (Δ nM/s) and peak (Δ nM) of [Ca^{2+}]$_i$ increase following addition of either LPS or PGN were calculated. **C, D** Representative original tracing showing the changes in [Ca^{2+}]$_i$ prior to and following acute addition of **(C)** LPS or **(D)** PGN in the absence of extracellular Ca^{2+}. To yield a Ca^{2+}-free environment, EGTA (0.5 mM) was added to the Ca^{2+}-free bath solution. **E, F** Mean ($\pm$ SEM) of the peak value (left) and slope (right) of the change in intracellular Ca^{2+} concentrations following addition of **(E)** LPS (100 ng/ml) or **(F)** PGN (25 µg/ml) in the absence (n=8-11, open bars) and presence (n=8-12, closed bars) of SKF-96365. * (p<0.05) and *** (p<0.001) indicate significant difference between treated and untreated cells (two-tailed unpaired *t*-test).

While the optimum concentration of LPS (100 ng/ml) was already established in the laboratory, the ideal concentration of PGN had to be assessed. Figure 14 shows that the PGN-induced increase in $[Ca^{2+}]_i$ positively correlated with PGN concentration. In order to keep the used PGN concentration as low as possible but at the same time to induce a clear effect on $[Ca^{2+}]_i$, 25 µg/ml PGN was considered as the optimum concentration for all experiments.
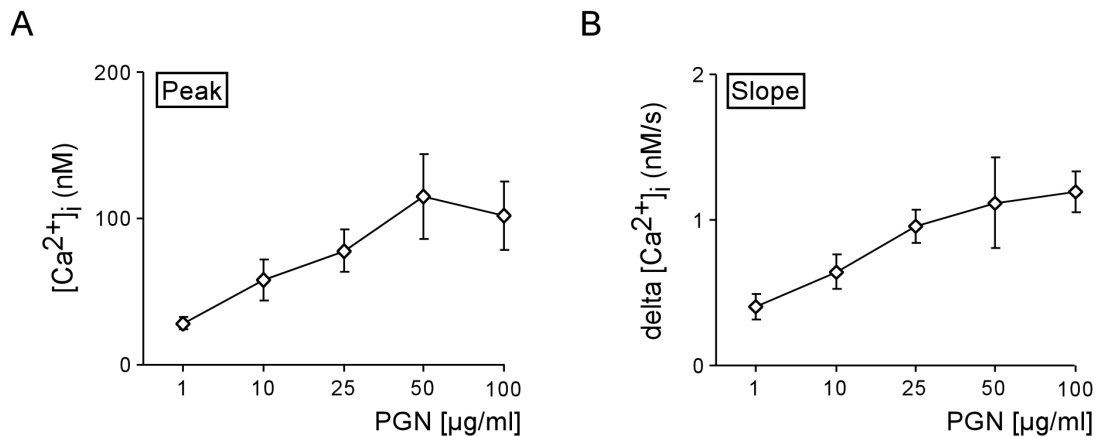
Figure 14. The effect of PGN on $[Ca^{2+}]_i$ is concentration-dependend
Concentration dependence of the effect of PGN on $[Ca^{2+}]_i$ as calculated from the peak value **(A)** and slope **(B)** of the change in $[Ca^{2+}]_i$ following addition of PGN to the bath solution (n = 6-11).

3.2 Involvement of TLR2 in PGN-induced effects on $[Ca^{2+}]_i$

It has been well established that PGN binds to TLR2 [145,146]. Since a recent study questioned this view [31], DCs were isolated from *tlr2*^{-/-} mice and their wild-type littermates. The PGN-induced increase in $[Ca^{2+}]_i$ was markedly impaired in DCs isolated from *tlr2*^{-/-} mice, indicating that TLR2 is one of the main receptors for PGN in DCs (Figure 15).
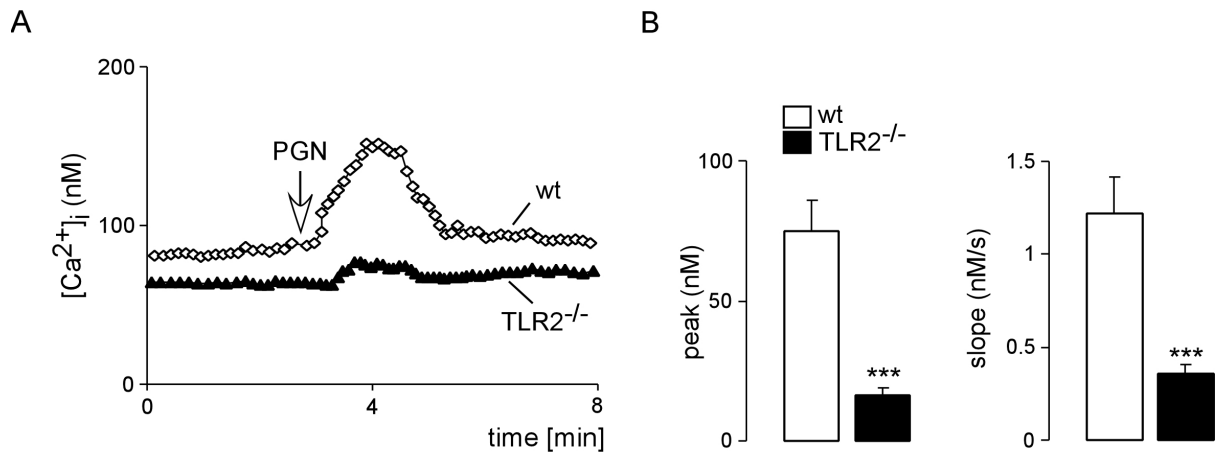
Figure 15. Effect of PGN exposure on [Ca^{2+}]$_i$ depends on TLR2

(A) Representative original tracings showing the change in [Ca^{2+}]$_i$ in Fura-2/AM loaded DCs from wild type and TLR2$^{-/-}$ mice prior to and following acute addition of peptidoglycan (PGN, 25 µg/ml). White arrow indicates the timepoint of acute addition of PGN. **(B)** Mean (± SEM) of the peak value (left) and slope (right) of the change in [Ca^{2+}]$_i$ following addition of PGN (25 µg/ml) to the bath solution to wild type DCs (n=8, open bars) and *tlr2$^{-/-}$* DCs (n=13, closed bars). *** (p<0.001) indicate significant difference between two genotypes (two-tailed unpaired *t*-test).

3.3 Activation of calcium release-activated calcium (CRAC) channels is measurable upon store depletion

To further analyse the above findings, store-operated Ca^{2+} entry was measured upon store depletion by inhibiting vesicular Ca^{2+}-ATPase by thapsigargin (1 µM). Figure 16 shows that under Ca^{2+}-free conditions, depleting of intracellular Ca^{2+} stores leads to a distinguishable increase in [Ca^{2+}]$_i$. Subsequent re-addition of extracellular Ca^{2+} in the continued presence of thapsigargin induces a much more pronounced increase in [Ca^{2+}]$_i$, representing influx of extracellular Ca^{2+} and indicating activation of CRAC channels.
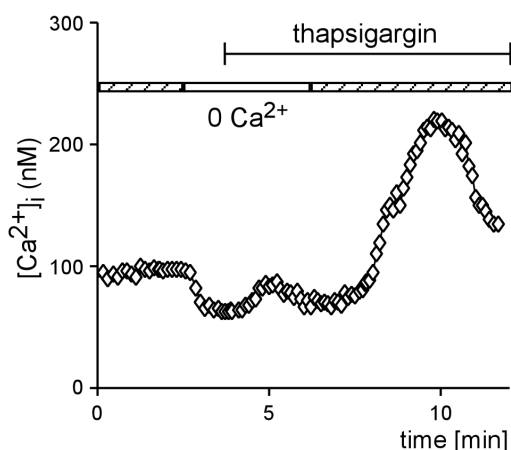
Figure 16. Activation of CRAC channels in mouse DCs

Representative tracing showing the changes in $[Ca^{2+}]_i$ in Fura-2/AM loaded DCs. Experiments were carried out prior to and during exposure to Ca^{2+}-free bath solution. Where indicated, thapsigargin (1 µM) was added to the Ca^{2+}-free bath solution. Readdition of extracellular Ca^{2+} in the continued presence of thapsigargin reflects the entry of Ca^{2+} through CRAC channels.

3.4   CRAC channels are expressed and active in mouse DCs

To ensure that the observed effects are mediated by CRAC channels, RT-PCR was performed to confirm that CRAC channels are expressed in mouse DCs and therefore can be responsible for the observed changes in $[Ca^{2+}]_i$ upon treatment with LPS or PGN. The proteins involved in store-operated Ca^{2+} entry have been identified recently, namely STIM1 and Orai1. STIM1 is a Ca^{2+} sensor in the ER [79-81], while Orai1, also called CRACM1, is a pore subunit of the CRAC channel [82,84,147]. Moreover, there are three mammalian homologous CRAC channel proteins, CRACM1, CRACM2 and CRACM3 [83]. To test if and which CRAC channels are expressed in mouse DCs, DNA fragments specific for the cloned mouse CRACM1, CRACM2 and CRACM3 channels were amplified by RT-PCR. The RT-PCR data demonstrated endogenous expression of all three channels in mouse DCs (Figure 17).
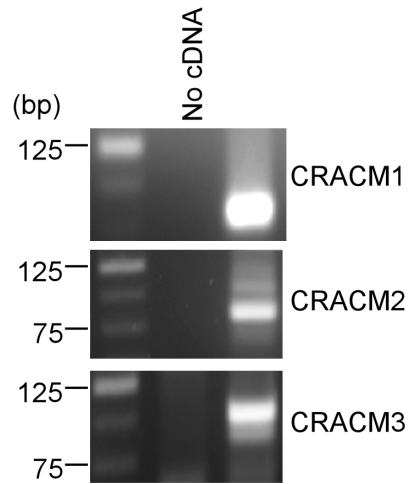
Figure 17. All three CRAC channels CRACM1, CRACM2 and CRACM3 are expressed in mouse DCs

Agarose gels with PCR products specific for CRACM1, CRACM2 and CRACM3 channels amplified from cDNA of mouse DCs.

To further validate the hypothesis that LPS or PGN treatment activates CRAC channels in mouse DCs, whole-cell voltage clamp experiments were performed in order to study the entry of extracellular Ca^{2+} upon TLR stimulation of DCs. Experiments were exemplary performed using 100 ng/ml LPS. LPS addition activated an inward current within 1.5-3 min, with properties similar to I_{CRAC} (Figure 18A, B). The typically high selectivity for Ca^{2+} was indicated by the fact that the LPS-stimulated current reversed at > +50 mV, when Ca^{2+} was the charge carrier in the bath (10 mM Ca^{2+}). When extracellular Na^+ was replaced by $NMDG^+$, neither reversal potential of the current/voltage (I/V) relationship nor current amplitude were altered in LPS-stimulated cells (Figure 18A). The I/V curve of the LPS-stimulated current fraction revealed a prominent inward rectification at negative voltages. A reduction in the concentration of extracellular Ca^{2+} in the continued presence of external Na^+ and Mg^{2+} reduced the inward current (Figure 18C, D, F).
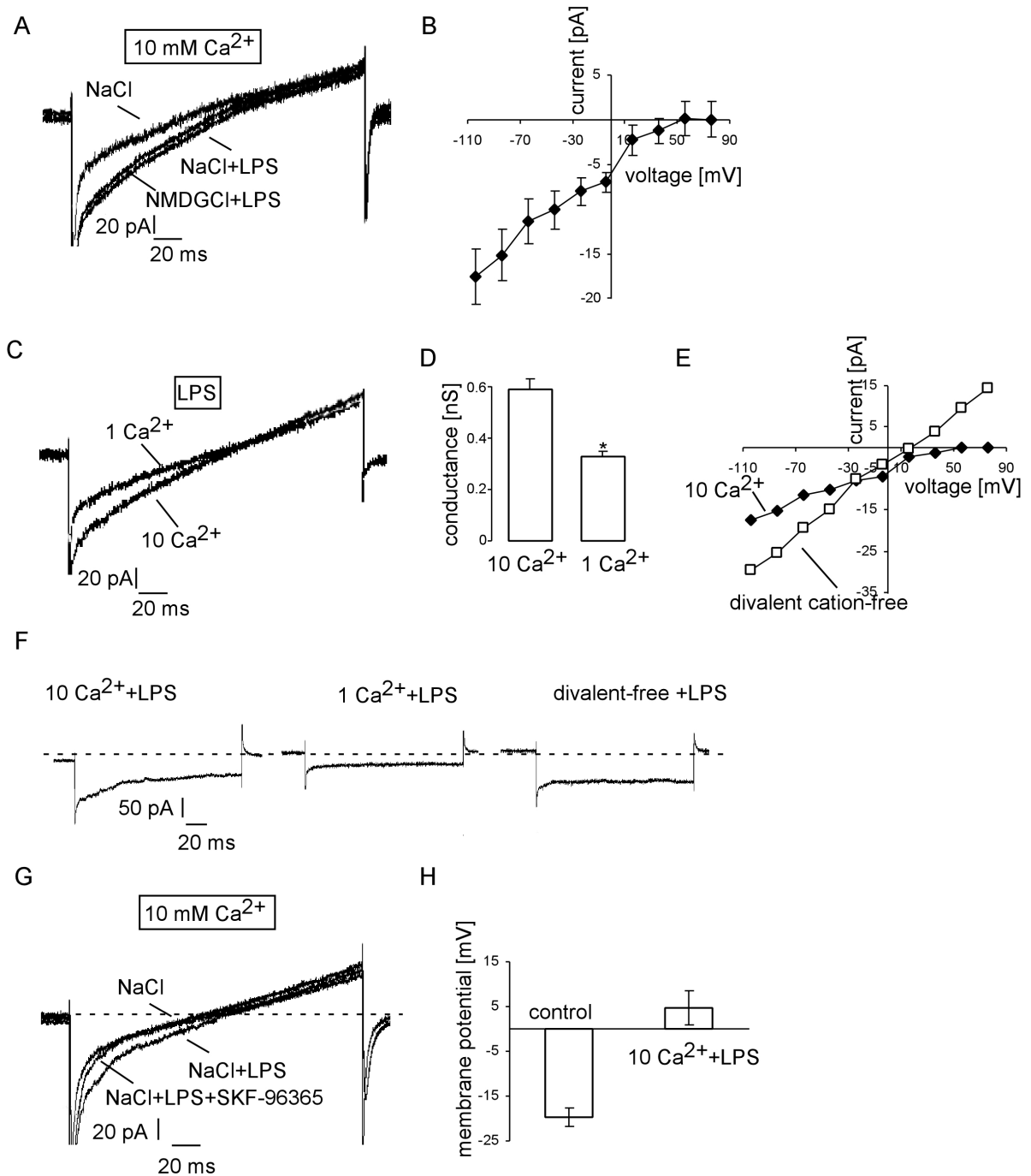
Figure 18. Entry of extracellular Ca²⁺ upon LPS-stimulation of DCs is mediated by CRAC channels

(A) Original ramp currents recorded with CsCl/NaCl pipette solution under control conditions (NaCl/10 Ca²⁺), 2 min after addition of LPS (100 ng/ml) and then upon substitution of Na⁺ by NMDG⁺. **(B)** Mean current-voltage (I/V) relationships (± SEM, n=9) of current fraction activated by LPS recorded in NaCl/10 mM Ca²⁺ bath solution. **(C)** LPS-induced original ramp currents recorded in response to voltage ramps in NaCl bath solution containing either 1 mM Ca²⁺ (and 9 mM Mg²⁺) or 10 mM Ca²⁺. **(D)** Mean whole-cell conductance of inward currents (± SEM, n=3) in NaCl bath solution containing either 10 mM Ca²⁺ or 1 mM Ca²⁺. Data were calculated by linear regression of I/V curves between -100 and -20 mV. * (p<0.05) indicates significant difference (two-tailed paired *t*-test). **(E)** I/V curves of the LPS-

activated current fractions obtained in NaCl/10 mM Ca^{2+}- containing or divalent cation-free bath solutions. **(F)** Original current traces at -100 mV obtained upon LPS stimulation in NaCl bath solution containing 10 mM Ca^{2+} (left), 1 mM Ca^{2+}, 9 mM Mg^{2+} (middle) or no divalent cations (right). **(G)** Original ramp currents recorded in NaCl bath solution containing 10 mM Ca^{2+} under control conditions (NaCl), 2 min after addition of LPS (100 ng/ml, NaCl+LPS) and then upon inhibition of the current by SKF-96365 (10 µM, NaCl+LPS+SKF-96365). **(H)** Mean membrane potential (± SEM, n=9) in DCs prior to (control) and after stimulation with LPS (10 Ca^{2+} + LPS).

One feature of CRAC channels is the so called anomalous mole fraction. It describes the property of CRAC channels to exhibit large Na^+ currents when external Ca^{2+} concentration is in the submicromolar range and therefore very low [74]. Figure 18E and F show that the LPS-stimulated channels exhibited anomalous mole fraction in a Na^+-containing but divalent cation-free environment, becoming permeable for Na^+. The invard current of LPS-stimulated cells inactivated fast during hyperpolarizing voltage pulses in the presence of extracellular Ca^{2+}, another distinguishable feature of CRAC channels, while this inactivation was missing in a divalent cation-free solution (Figure 18F). Furthermore, the current was inhibited when the currents were recorded in the presence of 10 µM SKF-96365, a blocker of store-operated channels (Figure 18G). In order to analyse changes in membrane potential upon treatment of mouse DCs with LPS, the current-clamp mode of the patch-clamp technique was used. As shown in Figure 18H, the cell membrane depolarized from -19.5 ± 2.5 mV to 1.8 ± 3.5 mV when LPS was applied to the cells.

3.5 Modulation of Ca^{2+} entry through CRAC channels by Kv channel blockers

It has been shown before that DCs express voltage-gated K^+ channels belonging to the Shaker (Kv1) family, presumably Kv1.3 and Kv1.5 [92,93]. In patch-clamp experiments different Kv channel blockers were tested in order to find an effective combination of blockers that could completely inhibit Kv currents in DCs. Figure 19A shows an effect of margatoxin (MgTx, 0.1 nM) and ICAGEN-4 (10 µM, [140]) blockers of Kv1.3 and Kv1.5 channels, respectively. Alternatively, another Kv1.5 channel inhibitor perhexiline maleate (PM, 5 µM) was used in combination with MgTx (1 nM) (Figure 19B). The current fraction sensitive to MgTx (0.1 nM) alone was 54.1±11.8 % (n=4, calculated for the current at +60 mV), to ICAGEN-4 (10 µM) alone 65.7±3.4 % (n=8), and when MgTx (0.1 nM) and ICAGEN-4 (10

µM) were applied together 84.2±3.4 % (n=4) of the current was inhibited. Neither acute application of nor incubation with LPS or PGN modified Kv currents in DCs. Thus, the current density at +90 mV was 22.1 ± 2.9 pA/pF (n = 13) in control cells, and was not significantly changed after acute application of PGN: 22.4 ± 1.5 pA/pF (n = 5) or after a 24 h incubation with 25 µg/ml PGN: 22.8 ± 3.0 pA/pF (n = 16).
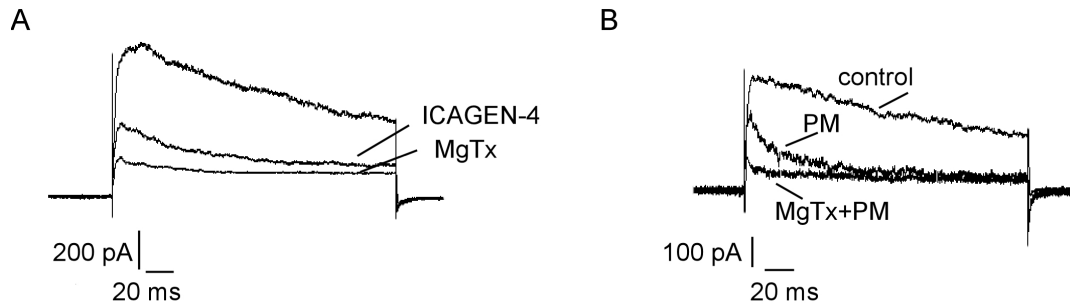
Figure 19. Blockers of Kv1.3 and Kv1.5 inhibit Kv-like currents in mouse DCs

Original Kv current traces recorded at +90 mV with KCl/K-gluconate pipette solution before and after application of **(A)** ICAGEN-4 (10 µM) and then MgTx (0.1 nM) or **(B)** PM (5 µM) and then MgTx (1 nM).

To test whether Kv channels can modulate the Ca^{2+} entry through CRAC channels, additional experiments have been performed using intracellular Ca^{2+} imaging in Fura-2/AM loaded DCs. The influence of Kv channel blockers on LPS- or PGN-induced increase in $[(Ca^{2+})_i]$ is shown in Figure 20. As can be seen, a combination of MgTx and ICAGEN-4 (Figure 20A, B) or of MgTx and PM (Figure 20C, D) leads to a significant reduction in LPS- or PGN-induced increase in $[(Ca^{2+})_i]$, respectively. Separate application of either MgTx or PM similarly resulted in significant inhibition of PGN-induced increase in $[(Ca^{2+})_i]$ (Figure 20E-H). However, this effect was more prominent when both blockers were used in combination, pointing to an involvement of both Kv1.3 and Kv1.5 channels in maintaining the Ca^{2+} entry.
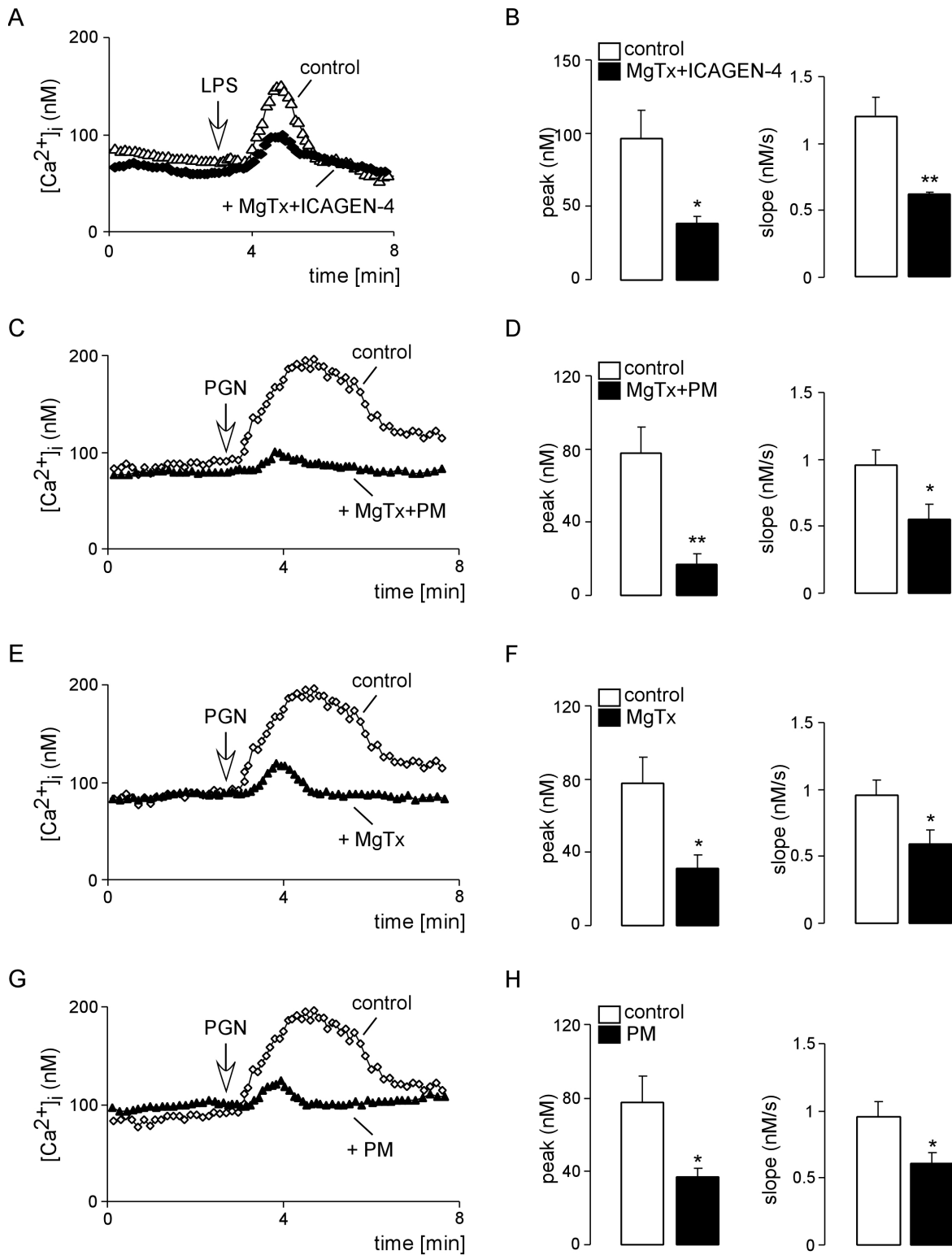
Figure 20. Blocking of Kv channels attenuates the increase in [Ca^{2+}]$_i$ upon TLR stimulation of DCs

(A), **(C)**, **(E)**, **(G)** Representative tracing showing [Ca^{2+}]$_i$ in Fura-2/AM loaded control DCs and DCs preteated with MgTx (1 nM)+ICAGEN-4 (10 µM) **(A)** or with MgTx (1 nM) + PM (10 µM) **(C)** or MgTx **(E)** or PM **(G)** prior to and following acute addition of either LPS (100 ng/ml) **(A)** or PGN (25 µg/ml). **(C)**, **(E)**, **(G)** to the bath solution. **(B)**, **(D)**, **(F)**, **(H)** Mean (± SEM, n = 6-8) of the peak value (left) and slope (right) of the change in [Ca^{2+}]$_i$ for control cells (open bars) and DCs pretreated (closed bars) with

either MgTx+ICAGEN-4 **(B)** or MgTx+PM **(D)** or MgTx **(F)** or PM **(H)** following addition of either LPS **(B)** or PGN **(D)**, **(F)**, **(H)** to the bath solution. * (p<0.05) and ** (p<0.01) indicate significant difference between both groups (two-tailed unpaired *t*-test).

3.6 Effect of CRAC and Kv channel blockers on DC maturation and function

To further investigate the impact of store-operated Ca^{2+} and Kv channels on DC functions, several parameters, namely cytokine production, maturation and phagocytosis, were examined in the absence and presence of the Kv channel blockers MgTx, ICAGEN-4 and PM, and the blocker of store-operated Ca^{2+} channels, SKF-96365.

3.6.1 LPS- and PGN-induced cytokine production

The production of cytokines by LPS- and PGN-treated DCs in the presence or absence of channel blockers was assessed by using the ELISA technique. DCs were either pretreated with 10 µM SGK-96365 for 30 min or left untreated prior to stimulation with either 25 µg/ml PGN or 100 ng/ml LPS. Figure 21 shows that inhibition of store-operated Ca^{2+} channels by SKF-96365 significantly blunted the release of TNF-α and IL-6 or TNF-α and IL-10 from LPS- or PGN-stimulated mouse DCs, respectively.
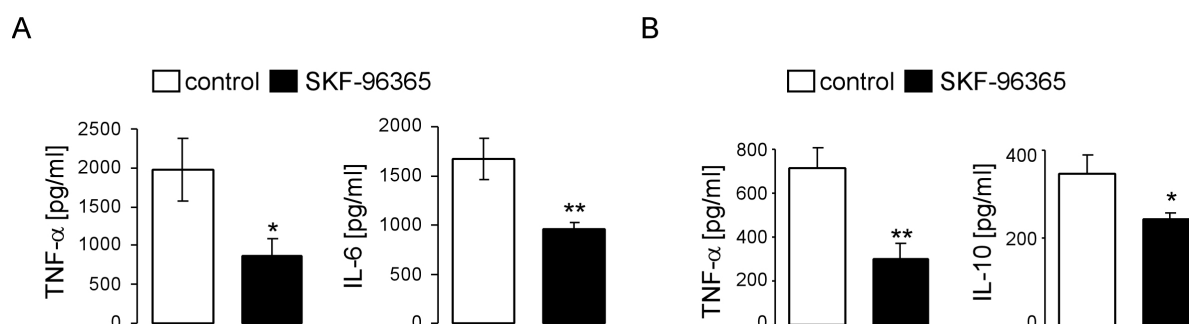
Figure 21. Inhibition of SOCE impairs LPS- and PGN-induced cytokine production by DCs
DCs were incubated for 30 min in the presence or absence of 10 µM SKF-96365 prior to stimulation with **(A)** 100 ng/ml LPS or **(B)** 25 µg/ml PGN. Supernatants were collected after 4 hours to measure TNFα, after 24 hours to measure IL-6, and after 48 hours to measure IL-10 by ELISA. The results are representative for 3 to 7 independent experiments. Each experiment was performed in duplicates; values represent the mean ± SEM of duplicates, * (p<0.05) and ** (p<0.01) indicate significant differences between treated and untreated cells (two-tailed unpaired *t*-test).

Next, the relevance of Kv channels for LPS- and PGN-induced cytokine production by DCs was considered. To this end, the cells were treated with either a combination of MgTx (1 nM) and ICAGEN-4 (10 μM) or a combination of MgTx (1 nM) and PM (10 μM) to block both Kv1.3 and Kv1.5 channel activity. As shown in Figure 22, inhibition of Kv1.3 by MgTx together with inhibition of Kv1.5 by ICAGEN-4 or PM led to a marked decrease in the production of TNFα and IL-6 in response to LPS-stimulation (Figure 22A), as well as to a significant reduction in the PGN-induced production of TNFα and IL-10 (Figure 22B). The results suggest a critical role of Kv channels in regulating DC cytokine production in response to TLR triggering.
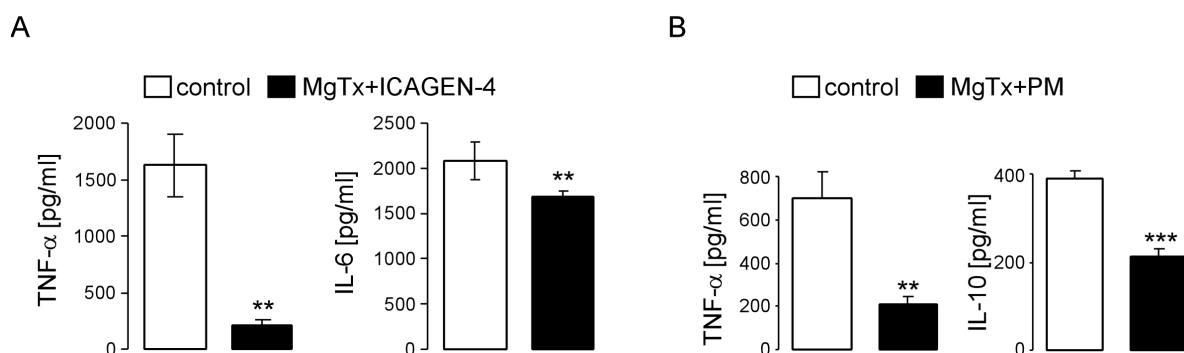
Figure 22. Kv channel blockers attenuate cytokine production by LPS- and PGN-stimulated DCs

DCs were incubated for 30 min in the presence or absence of **(A)** MgTx (1 nM)+ICAGEN-4 (10 μM) or **(B)** MgTx (1 nM) or PM (10 μM) prior to stimulation with **(A)** 100 ng/ml LPS or **(B)** 25 μg/ml PGN. Supernatants were collected after 4 hours to measure TNFα, after 24 hours to measure IL-6, and after 48 hours to measure IL-10 by ELISA. The results are representative for 3 to 7 independent experiments. Each experiment was performed in duplicates; values represent the mean ± SEM of duplicates, ** (p<0.01) and *** (p<0.001) indicate significant differences between treated and untreated cells (two-tailed unpaired *t*-test).

Since cytokine production in DCs is regulated by the transcription factor NFκB [148], the effect of store-operated Ca^{2+} and Kv channel blockers on NFκB activation was investigated. To this end, DCs were treated with 25 μg/ml PGN for 1 hour in the presence or absence of either SKF-96365 or a combination of MgTx and PM and subsequently analyzed for phosphorylation of inhibitory molecule IκBα by western blotting. As illustrated in Figure 23, the level of phosphorylated IκBα was increased by PGN-stimulation, but was not significantly altered upon store-operated Ca^{2+} or Kv channel inhibition.
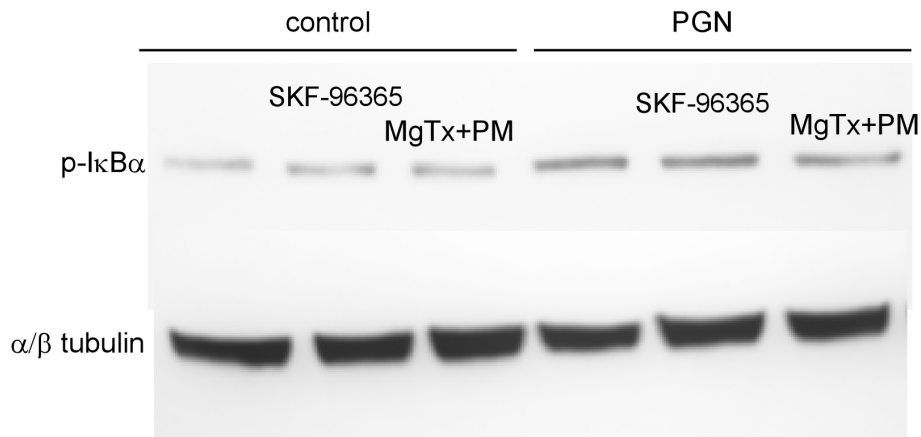
Figure 23. CRAC and Kv channel blockers do not affect IκBα phosphorylation in mouse DCs
Original Western blot of unstimulated (control) and PGN (25 µg/ml, 60 min)-stimulated DCs untreated or treated (60 min) with either SKF-96365 (10 µM) or MgTx (1 nM) + PM (5 µM). Protein extracts were analyzed by direct Western blotting using antibodies directed to phosphorylated IκBα. Protein loading was controlled by anti-α/β tubulin antibody. One representative experiment out of three is shown.

3.6.2 LPS- and PGN-induced DC maturation

Upon maturation, DCs express on their surface antigen-presenting molecules (such as MHC class II), costimulatory (CD86) and adhesion (CD54) molecules. Expression of CD86 and CD54 was not affected by SKF-96365 (10 µM) or Kv channel blockers MgTx (1 nM), ICAGEN-4 (10 µM) and PM (5 µM) upon LPS- or PGN-induced DC maturation. However, the up-regulation of MHC class II by LPS was significantly reduced by SKF-96365 and MgTx + ICAGEN-4 (Figure 24A), indicating that Ca^{2+} and Kv channels can be involved in LPS-induced DC maturation. The same tendency could be observed for PGN-treatment, however, this effect was not significant (Figure 24B).
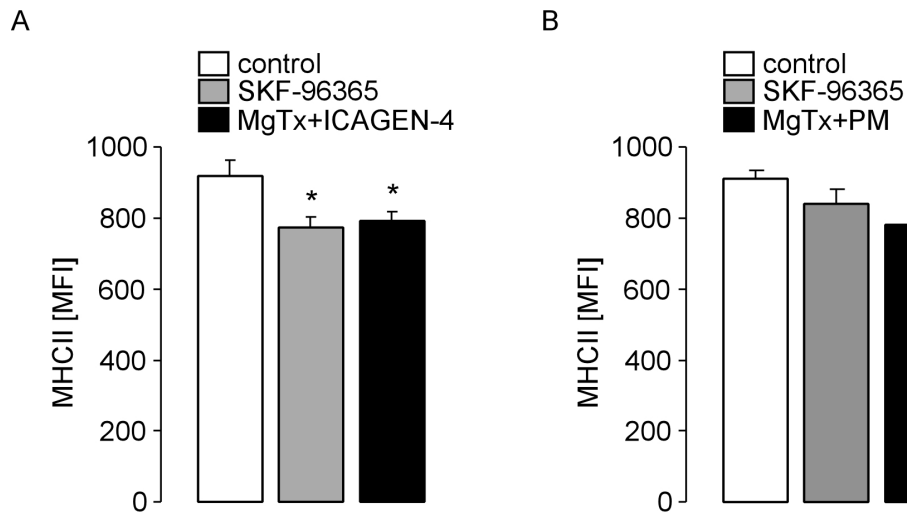
Figure 24. SKF-96365 and Kv channel blockers MgTx and ICAGEN-4 reduce LPS- but not PGN-induced up-regulation of MHC class II

Mean fluorescence intensity (MFI ±SEM; n=5-6) of MHC class II molecule in **(A)** LPS (100 ng/ml, 48 h)-stimulated DCs and **(B)** PGN (25 µg/ml, 48h)-stimulated DCs incubated in the absence (control, open bar) or in the presence of either SKF-96365 (10 µM, grey bar, **A,B**), MgTx (1 nM)+ICAGEN-4 (10 µM) (closed bar, **A**), or MgTx (1 nM)+PM (5 µM) (closed bar, **B**).* (p<0.05) indicate significant difference from control (ANOVA).

3.6.3 Phagocytic capacity

The capacity of DCs to phagocytose antigen is one of DC functions in innate immunity and is down-regulated during DC maturation [6,49]. Phagocytic capacity of DCs assessed as FITC-dextran uptake was measured in the presence of Ca^{2+} and Kv channel blockers. As a result, SKF-96365 as well as MgTx in combination with either ICAGEN-4 or PM significantly increased the FITC-dextran uptake by LPS- or PGN-stimulated mouse DCs (Figure 25). The data indicate that inhibition of CRAC or Kv channels lead to a less mature DC phenotype with higher phagocytic activity.
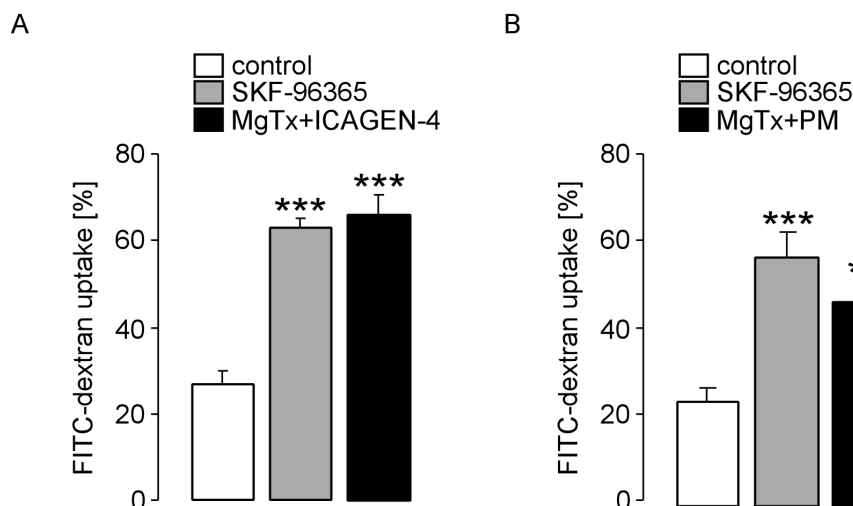
Figure 25. SKF-96365 and Kv channel blockers MgTx, ICAGEN-4 and PM enhance phagocytic activity of LPS- and PGN-stimulated DCs

(A) Bar diagram representing mean percent (±SEM; n=3) of FITC-dextran uptake by LPS (100 ng/ml, 48 h)-stimulated DCs incubated in the absence (control, open bar) or in the presence of either SKF-96365 (10 µM) or MgTx (1 nM)+ICAGEN-4 (10 µM). *** (p<0.001) indicates significant difference from control (ANOVA). **(B)** Bar diagram representing mean percent (± SEM; n=3-6) of FITC-dextran uptake by PGN (25 mg/ml, 48 h)-stimulated DCs incubated in the absence (control, open bar) or in the presence of either SKF-96365 (10 µM) or MgTx (1 nM)+ PM (5 µM). ** (p<0.01) and *** (p<0.001) indicate significant difference from control (ANOVA).

3.6.4 DC migration

The migration of DCs to lymphoid tissues is essential for the activation and coordination of immune responses [7]. The influence of CRAC and Kv channel blockers on DC migration was exemplary analysed in LPS-stimulated DCs. Figure 26 shows that DC migration in response to CCL21, a CCR7 ligand, was markedly impaired when the cells were treated for 24 hours with LPS in the presence of either SKF-96365 or MgTx and ICAGEN-4, compared to untreated, LPS-stimulated cells.
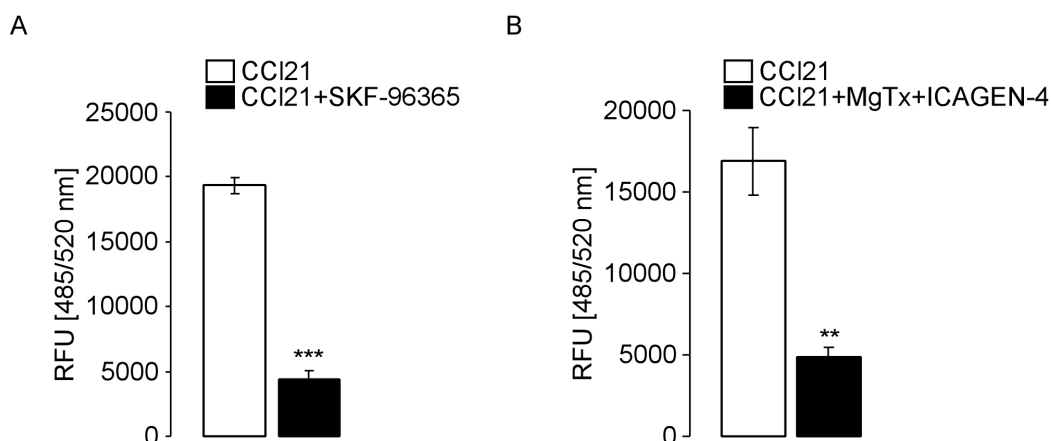
Figure 26. SKF-96365 and Kv channel blockers MgTx and ICAGEN-4 impair CCL21-dependent migration of LPS-stimulated DCs

Mean fluorescence (RFU, relative fluorescence units, ±SEM; n=3-4) of migrating DCs in response to CCL21. DCs were stimulated with LPS (100 ng/ml, 24 h) either in the absence (open bars) or presence of either **(A)** SKF-96365 (10 µM, closed bar) or **(B)** MgTx (1 nM)+ICAGEN-4 (10 µM) (closed bar). ** (p<0.01) and *** (p<0.001) indicate significant difference between both groups (two-tailed unpaired *t*-test).

3.7 1,25(OH)$_2$D$_3$ and dexamethasone impair the LPS-induced increase in [Ca^{2+}]$_i$

Incubation of mouse DCs with dexamethasone (10 nM, overnight, Figure 27A, B) or with 1,25(OH)$_2$D$_3$, the active form of vitamin D (Figure 27C, D, E), resulted in a strong impairement of LPS-induced increase in [Ca^{2+}]$_i$. 1,25(OH)$_2$D$_3$ was added exemplary to the DC culture for several timepoints and in different concentrations, whereby an effect on [Ca^{2+}]$_i$ was observed after 16 hours of incubation with concentrations ≥ 25 nM (Figure 27D, E). To test whether also vitamin D derivates are capable to modulate cytosolic Ca^{2+} concentration, DCs were incubated with 100 nM 24,25(OH)$_2$D$_3$ for 24 hours prior to addition of LPS. 24,25(OH)$_2$D$_3$ had no effect on LPS-induced increase in [Ca^{2+}]$_i$ (Figure 27F).
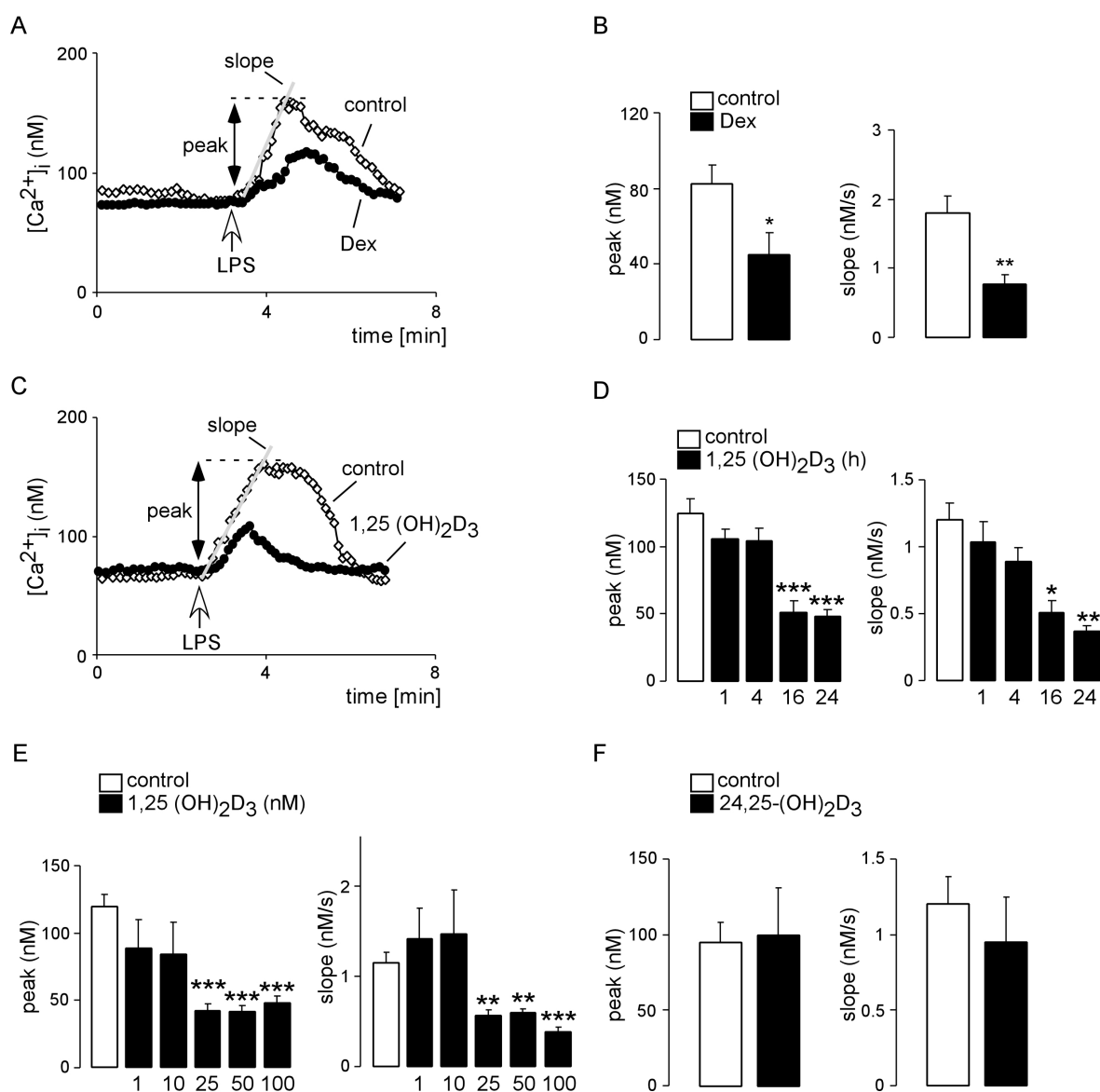
Figure 27. Effect of dexamethasone and 1,25(OH)$_2$D$_3$ on LPS-induced increase in [Ca^{2+}]$_i$ in DCs

(A) Representative tracing showing [Ca^{2+}]$_i$ in Fura-2/AM loaded control and dexamethasone (10 nM, overnight)-incubated DCs prior to and following acute addition of LPS (100 ng/ml; white arrow). **(B)** Mean (± SEM) of the peak value (left) and slope (right) of the change in [Ca^{2+}]$_i$ following addition of LPS to control (n=7, open bars) and dexamethasone-incubated (n=7, closed bars) DCs. * (p<0.05) and ** (p<0.01) indicate significant difference between two groups (two-tailed unpaired *t*-test). **(C)** Representative tracing showing [Ca^{2+}]$_i$ in Fura-2/AM loaded control and 1,25(OH)$_2$D$_3$ (100 nM, 24 h)-incubated DCs prior to and following acute addition of LPS (0.1 µg/ml; white arrow). **(D)** Mean (± SEM) of the peak value (left) and slope (right) of the change in [Ca^{2+}]$_i$ following addition of LPS to control DCs (n=17, open bars) and to DCs incubated for 4, 16 and 24 h with 1,25(OH)$_2$D$_3$ (100 nM, n=5-19, closed bars). * (p<0.05), ** (p<0.01) and *** (p<0.001) indicate significant difference from control DCs (ANOVA). **(E)** Mean (± SEM) of the peak value (left) and slope (right) of the change in intracellular Ca^{2+} following addition of LPS to control DCs (n=17, open bars) and to DCs incubated for 24 h with different concentrations of 1,25(OH)$_2$D$_3$ (1-100 nM, n=5-23, closed bars). * (p<0.05), ** (p<0.01) and *** (p<0.001) indicate significant difference from control DCs (ANOVA). **(F)** Mean (± SEM) of the peak

value (left) and slope (right) of the change in $[Ca^{2+}]_i$ following addition of LPS to control DCs (n=21, open bars) and to DCs incubated for 24 h with 100 nM $24,25(OH)_2D_3$ (n=9, closed bars).

The inhibitory effect of dexamethasone and $1,25(OH)_2D_3$ could have been due to several mechanisms, acting alone or in parallel. First, the entry of extracellular Ca^{2+} itself could have been blunted. Second, the extrusion of cytosolic Ca^{2+} out of the cell could have been increased. And/or third, the cytosolic Ca^{2+} buffering could have been increased. For cells of the collecting ducts and connecting tubules of the kidney it has been shown, that $1,25(OH)_2D_3$ stimulates, rather than inhibits, Ca^{2+} entry [149]. Therefore, the possibility of $1,25(OH)_2D_3$ stimulating Ca^{2+} extrusion, which could be accomplished by Na^+/Ca^{2+} exchangers, was investigated first.

3.8 Expression of Na^+/Ca^{2+} exchangers in mouse DCs

Because it has never been shown before, whether Na^+/Ca^{2+} exchangers are expressed in DCs, their expression was determined using RT-PCR. Figure 28A shows that mouse DCs express high amounts of all three K^+-independent isoforms, namely NCX1, NCX2, and NCX3. Regarding the K^+-dependent Na^+/Ca^{2+} exchangers, three out of five isoforms: NCKX1, NCKX3, and NCKX5 were strongly expressed in mouse DCs. Additionally, low expression levels of NCKX4 could be detected (Figure 28B).
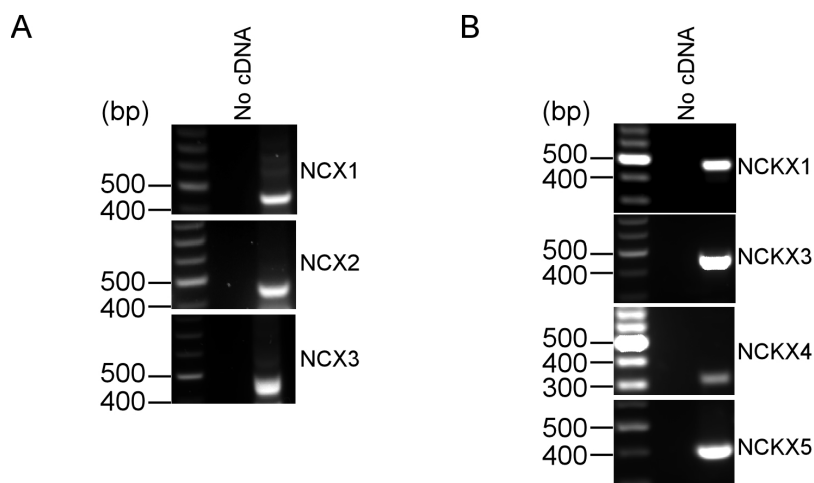
Figure 28. Expression of Na^+/Ca^{2+} exchanger isoforms in mouse DCs
Agarose gels with PCR products specific for NCX1, NCX2, NCX3 and NCKX1, NCKX3, NCKX4, NCKX5 exchangers amplified from cDNA of mouse DCs.

3.9   Effect of 1,25(OH)$_2$D$_3$ and dexamethasone on Na$^+$/Ca^{2+} exchangers

The effect of dexamethasone and 1,25(OH)$_2$D$_3$ on Na$^+$/Ca^{2+} exchanger expression levels was investigated by real time PCR. To this end, total RNA was isolated from mouse DCs incubated with dexamethasone (10 nM, overnight) or with 1,25(OH)$_2$D$_3$ (100 nM, 24 h) or left untreated. Treatment with dexamethasone resulted in significantly enhanced transcript levels for two Na$^+$/Ca^{2+} exchangers, namely NCX2 and NCX3 (Figure 29). There was no effect of dexamethasone treatment on expression levels of K$^+$-dependent Na$^+$/Ca^{2+} exchangers and no effect of 1,25(OH)$_2$D$_3$ on any of these exchangers.

In addition to monitoring the expression levels, the activity of Na$^+$/Ca^{2+} exchangers was investigated using intracellular Ca^{2+} imaging. Activity of K$^+$-independent Na$^+$/Ca^{2+} exchangers was assessed in K$^+$-free environment only. The effect of 1,25(OH)$_2$D$_3$ was tested in the presence of either 5 mM K$^+$ or 40 mM K$^+$ to ensure an activation of both K$^+$-dependent and K$^+$-independent Na$^+$/Ca^{2+} exchangers. Activity of Na$^+$/Ca^{2+} exchangers could be measured by assessing changes in [Ca^{2+}]$_i$, since removal of external Na$^+$ in the presence of external Ca^{2+}, leads to inversion of the direction of Na$^+$/Ca^{2+} exchanger activity and subsequently to a carrier-mediated Ca^{2+} entry [61].
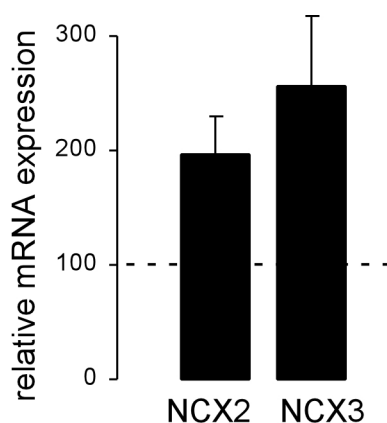
Figure 29. Effect of dexamethasone on Na$^+$/Ca^{2+} exchanger expression
Total RNA was isolated from control cells and DCs pretreated with 10 nM dexamethasone overnight, and NCX 1-3 mRNA levels were assessed by real-time PCR using MRPS9 mRNA as a reference gene. Relative mRNA expression of NCX2 and NCX3 is shown as percent of increase in dexamethasone-treated versus control cells (100%, dotted line) in comparison to the reference gene (n=12).
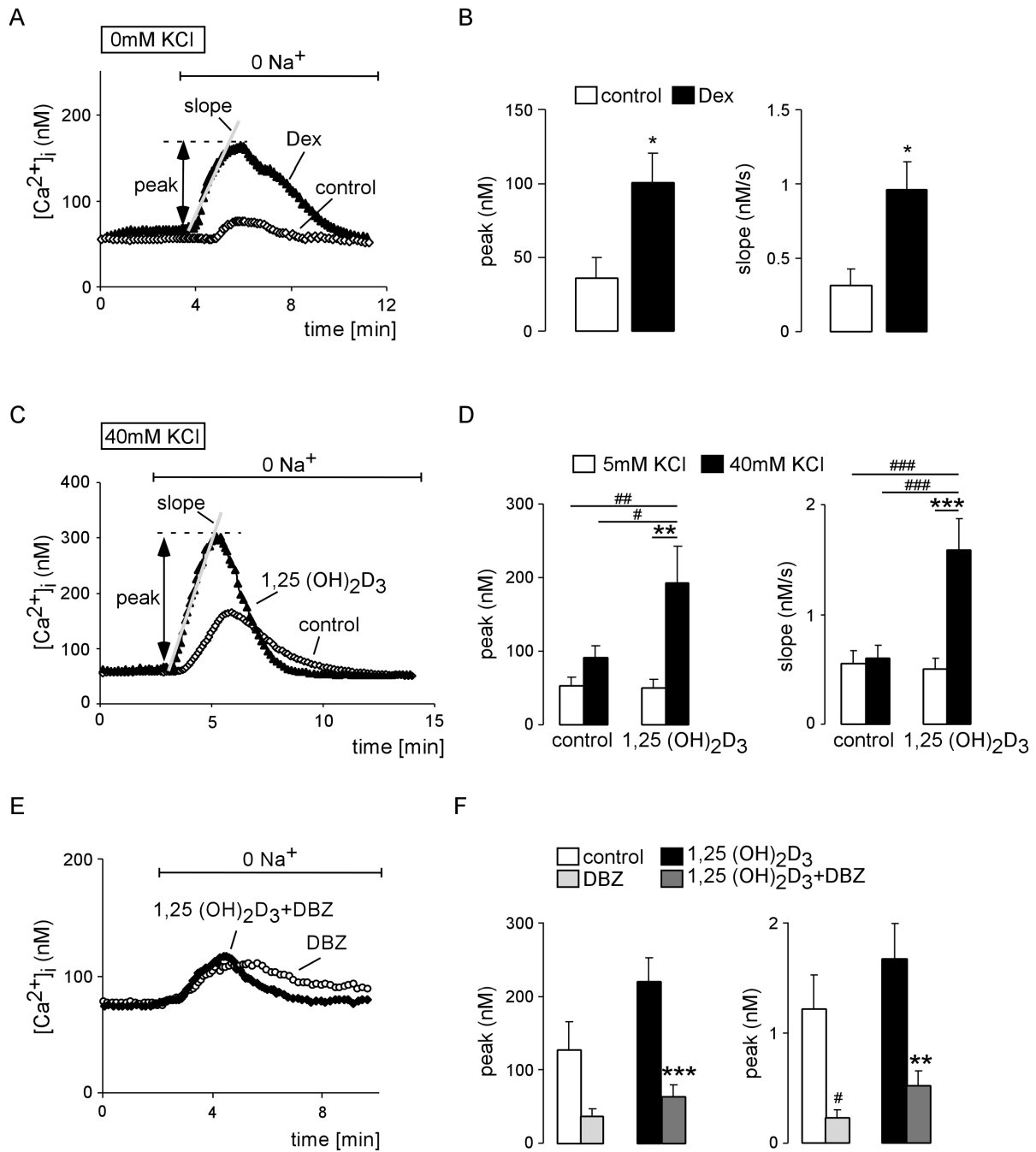
Figure 30. Activity of Na$^+$/Ca^{2+} exchangers in mouse DCs is modulated by dexamethasone and 1,25(OH)$_2$D$_3$

(A) Representative tracing showing [Ca^{2+}]$_i$ in Fura-2/AM loaded control and dexamethasone (Dex, 10 nM, overnight)-incubated DCs prior to and following removal of external Na$^+$ (0 Na$^+$) in the absesence of extracellular K$^+$. **(B)** Mean (± SEM) of the peak value (left) and slope (right) of the change in [Ca^{2+}]$_i$ following removal of external Na$^+$ in control (n=8-12) and dexamethasone-treated (Dex, 10 nM, overnight) DCs. * (p<0.05) indicates significant difference between the two groups (two-tailed unpaired *t*-test). **(C)** Representative tracing showing [Ca^{2+}]$_i$ in Fura-2/AM loaded control and 1,25(OH)$_2$D$_3$ (100 nM, 24 hours)-incubated DCs prior to and following removal of external Na$^+$ (0 Na$^+$) in the presesence of 40 mM K$^+$. **(D)** Mean (± SEM) of the peak value (left) and slope (right) of the change in [Ca^{2+}]$_i$ following removal of external Na$^+$ in the presence of either 5 mM K$^+$ (open bars) or 40 mM K$^+$ (closed

bars) in control (n=12-14) and $1,25(OH)_2D_3$ (100 nM, 24 h)-incubated (n=10) DCs. [#] ($p<0.05$), [##] ($p<0.01$) and [###] ($p<0.001$) indicate significant differences between control and $1,25(OH)_2D_3$-treated DCs; ** ($p<0.01$) and *** ($p<0.001$) indicate significant differences between 5 mM K^+ and 40 mM K^+ (ANOVA). **(E)** Representative tracing showing $[Ca^{2+}]_i$ in Fura-2/AM loaded DCs treated with either $1,25(OH)_2D_3$ (100 nM, 24 hours) alone or a combination of $1,25(OH)_2D_3$ and 3',4'-dichlorobenzamyl (DBZ, 10 μM), prior to and following removal of external Na^+ (0 Na^+) in the presence of 40 mM K **(F)** Mean (± SEM) of the peak value (left) and slope (right) of the change in $[Ca^{2+}]_i$ following removal of external Na^+ in the presence of 40 mM K^+ (closed bars) in control and $1,25(OH)_2D_3$ (100 nM, 24 h)-incubated DCs either in the absence (n=8-10) or in the presence (n=13-14) of DBZ (10 μM). # ($p<0.05$) indicates significant differences between control and DBZ-incubated DCs; ** ($p<0.01$) and *** ($p<0.001$) indicate significant differences between $1,25(OH)_2D_3$ and $1,25(OH)_2D_3$ + DBZ-treated DCs (ANOVA).

Removal of external Na^+ either in the presence or absence of K^+ induced an increase in $[Ca^{2+}]_i$ in mouse DCs (Figure 30A, C). Overnight treatment of the cells with 10 nM dexamethasone significantly enhanced Na^+/Ca^{2+} exchanger activity when measured in the absence of extracellular K^+ (Figure 30A, B). Likewise, 24 hours treatment of mouse DCs with 100 nM $1,25(OH)_2D_3$ led to a significantly enhanced Na^+/Ca^{2+} exchanger activity compared to untreated DCs when extracellular K^+ concentration of 40 mM was used upon the measurements (Figure 30C, D). These observation suggests an action of $1,25(OH)_2D_3$ on at least one K^+-dependent Na^+/Ca^{2+} exchanger NCKX in mouse DCs. In human platelets it has been shown that the activity of K^+-dependent Na^+/Ca^{2+} exchangers was inhibited by 3',4'-dichlorobenzamyl (DBZ) [150]. Therefore, mouse DCs were incubated with 10 μM DBZ for 24 hours either in the presence or absence of $1,25(OH)_2D_3$. In both cases, the increase in $[Ca^{2+}]_i$ induced by removal of extracellular Na^+ in the presence of extracellular Ca^{2+} was markedly impaired compared to sole treatment with 100 nM $1,25(OH)_2D_3$ (Figure 30E, F).

In addition to Ca^{2+} imaging experiments, Na^+/Ca^{2+} exchanger activity was further assessed using the patch clamp technique. An important feature of all Na^+/Ca^{2+} exchangers is that they are electrogenic bidirectional transporters and therefore can be measured electrophysiologically. Na^+/Ca^{2+} exchange currents can be assessed by patch clamp by switching between the Ca^{2+} influx and Ca^{2+} efflux mode [61]. Removing of external Ca^{2+} in the presence of external Na^+ leads to efflux of intracellular Ca^{2+}, while removing of external Na^+ in the presence of external Ca^{2+} triggers an influx of extracellular Ca^{2+}. Whole-cell membrane currents were recorded continuously at -80 mV (Figure 31). Negative currents were recorded at negative membrane potentials independently of the bath solutions used. Removal of external Na^+ in the presence of external Ca^{2+} induced an upward shift, which was reversed by removal of external Ca^{2+} and readdition of external Na^+ (Figure 31A). The

outward current was estimated as difference in currents (ΔI) elicited by the switch from Na^+-containing, Ca^{2+}-free solutions to Na^+-free, Ca^{2+}-containing solutions. Treatment of mouse DCs with either 100 nM $1,25(OH)_2D_3$ for 24 hours or 10 nM dexamethasone overnight enhanced the Na^+/Ca^{2+} exchange currents when measured in the presence or in the absence of 40 mM K^+ in the bath, respectively (Figure 31B, C).
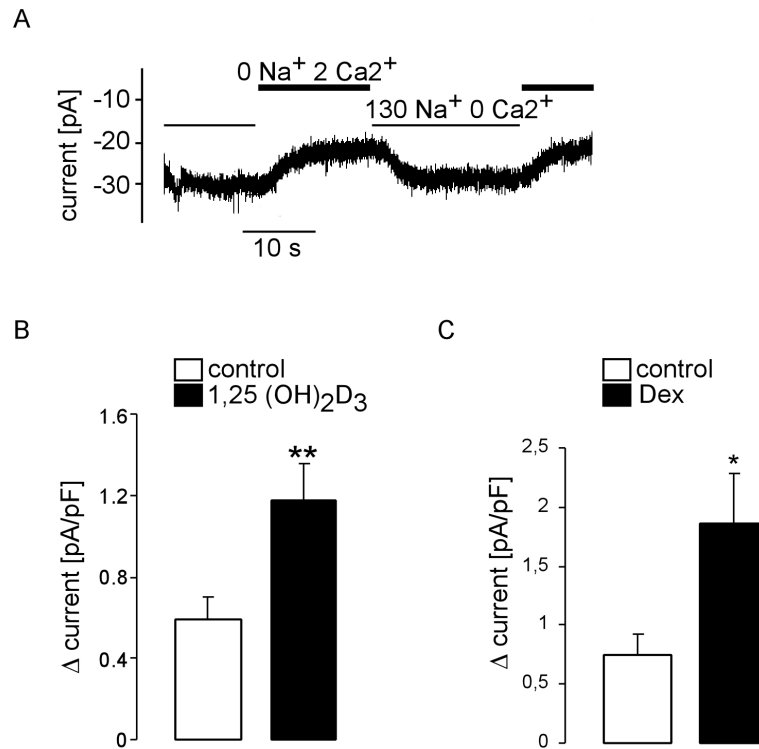
Figure 31. Na^+/Ca^{2+} exchange currents in mouse DCs are enhanced by dexamethasone or $1,25(OH)_2D_3$

(A) Whole cell currents in DCs recorded at -80 mV during the switch between external solutions that contained 40 mM K^+ and either 130 mM Na^+ and no Ca^{2+} (130 Na^+ 0 Ca^{2+}) or 2 mM Ca^{2+} and no Na^+ (0 Na^+ 2 Ca^{2+}). The internal solution stimulated Na^+ overload and Ca^{2+} plateau levels (1 µM free Ca^{2+}, 120 mM Na^+, 40 mM K^+). Cesium and TEA^+ were present in the solutions to block K^+ channel currents. **(B)** Mean current density changes (ΔI, pA/pF) at -80 mV induced by the switch between external solutions containing 130mM Na^+, 0 Ca^{2+}, 40 mM K^+ and 0 Na^+, 2mM Ca^{2+}, 40 mM K^+ in DCs treated (closed bar, n = 13) and untreated (open bar, n = 12) with $1,25(OH)_2D_3$ (100 nM, 24 h). The internal solution was as in A. **(C)** Mean current density changes (ΔI, pA/pF) at -80 mV induced by the switch between external solutions containing 130 mM Na^+, 0 Ca^{2+} and 0 Na^+, 2 mM Ca^{2+} in DCs treated (closed bar, n = 5) and untreated (open bar, n = 5) with dexamethasone (Dex, 10 nM, overnight). The internal solution was as in A. * ($p<0.05$) and ** ($p<0.01$) indicate significant difference between two groups (two-tailed unpaired *t*-test).

3.10 Effect of 1,25(OH)$_2$D$_3$ on LPS-induced Ca^{2+} entry is counteracted by NCKX

As shown above, treatment of mouse DCs for 24 hours with 100 nM 1,25(OH)$_2$D$_3$ reduced the LPS-induced increase in [Ca^{2+}]$_i$ and enhanced the activity of at least one K$^+$-dependent Na$^+$/Ca^{2+} exchanger NCKX. To find out whether these two observations are associated, intracellular Ca^{2+} measurements upon stimulation with LPS were performed in DCs treated with 1,25(OH)$_2$D$_3$ (100 nM, 24 hours) and the blocker of K$^+$-dependent Na$^+$/Ca^{2+} exchanger DBZ (10 µM, 24 hours). Figure 32 illustrates that DBZ counteracted the inhibiting effect of 1,25(OH)$_2$D$_3$ on LPS-induced increase in [Ca^{2+}]$_i$.
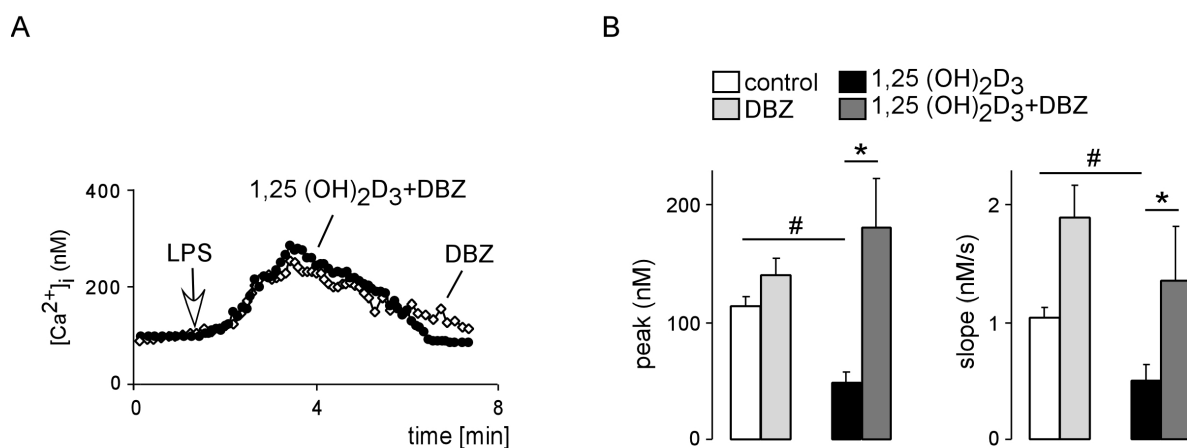
Figure 32. Effect of 1,25(OH)$_2$D$_3$ on LPS-induced increase in [Ca^{2+}]$_i$ is sensitive to NCKX-inhibitor 3',4'-dichlorobenzamyl (DBZ)
(A) Representative tracing showing [Ca^{2+}]$_i$ in Fura-2/AM loaded DCs treated with 10 µM DBZ alone or DBZ + 1,25(OH)$_2$D$_3$ (100 nM) for 24 hours prior to and following acute addition of LPS (100 nM). **(B)** Mean (± SEM) of the peak value (left) and slope (right) of the change in [Ca^{2+}]$_i$ following acute addition of LPS (100 nM) in control and 1,25(OH)$_2$D$_3$ (100 nM, 24 h)-incubated DCs either in the absence or in the presence of DBZ (10 µM) (n=4). [#] (p<0.05) indicates significant difference between control and 1,25(OH)$_2$D$_3$-treated DCs; [*] (p<0.05) indicates significant differences between 1,25(OH)$_2$D$_3$ and 1,25(OH)$_2$D$_3$ + DBZ-treated DCs (ANOVA).

3.11 Effect of 1,25(OH)$_2$D$_3$ on Calbindin-D28K expression in DCs

Besides the action of 1,25(OH)$_2$D$_3$ on Na$^+$/Ca^{2+} exchangers, which leads to a reduction in LPS-induced increase in [Ca^{2+}]$_i$, other mechanisms could operate in parallel to keep the cytosolic Ca^{2+} concentration low. For example, calbindin-D28K facilitates Ca^{2+} diffusion in the kidney and lowers the intracellular Ca^{2+} concentration to avoid Ca^{2+} toxicity [67,151]. Furthermore, studies in several cell models provided evidence that 1,25(OH)$_2$D$_3$ enhances calbindin-D28K expression [152]. Therefore, mouse DCs were analysed for calbindin-D28K expression under control conditions and in response to 24 hour treatment with 100 nM 1,25(OH)$_2$D$_3$. As shown in Figure 33, calbindin-D28K was expressed in mouse DCs, and its expression was up-regulated by 1,25(OH)$_2$D$_3$. The data indicate that the effect of 1,25(OH)$_2$D$_3$ on [Ca^{2+}]$_i$ is not only due to enhanced Ca^{2+} extrusion, but also to enhanced Ca^{2+} buffer capacity.
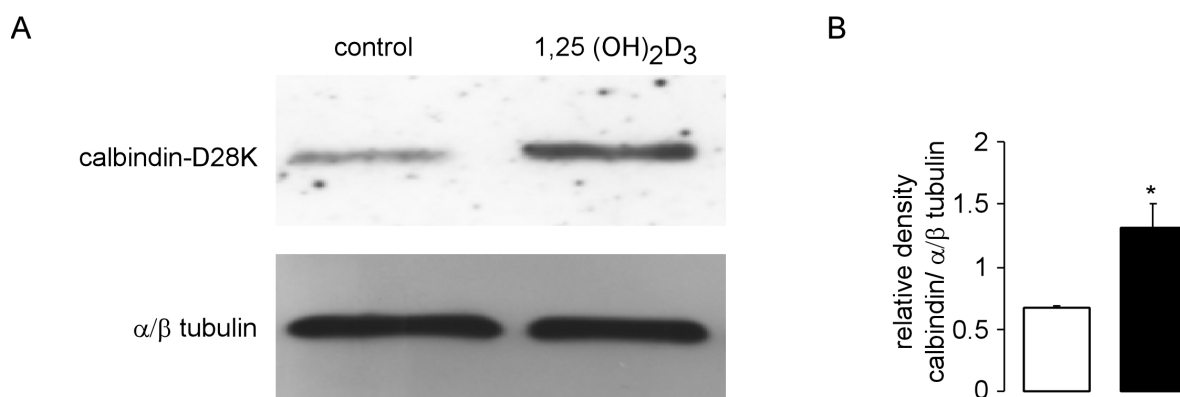
Figure 33. Calbindin-D28K is up-regulated by 1,25(OH)$_2$D$_3$ in mouse DCs
(A) Original Western blot of DCs treated or untreated with 1,25(OH)$_2$D$_3$ (100 nM, 24 h). Protein extracts were analyzed by direct Western blotting using antibodies directed to calbindin-D28K. **(B)** Arithmetic mean ±SEM (n = 3) of the abundance of calbindin-D28K as the ratio of calbindin-D28K: α/β-tubulin. * (p<0.05) indicates significant difference between two groups (two-tailed unpaired *t*-test).

3.12 Effect of 1,25(OH)$_2$D$_3$ and dexamethasone on DC maturation and cytokine production

It has been shown before, that effects of 1,25(OH)$_2$D$_3$ on the immune system include inhibition of DC maturation [115]. Furthermore, it has been shown that DC treatment with glucocorticoids affects DC maturation and function [128,131]. The data presented above

indicate that treatment of mouse DCs with LPS induced expression of maturation markers and production of cytokines. To assess whether this LPS-induced effect can be modulated by dexamethasone or $1,25(OH)_2D_3$, the cells were treated for 24 hours with 100 ng/ml LPS in the presence or absence of either 10 nM dexamethasone or 100 nM $1,25(OH)_2D_3$. As illustrated in Figure 34A-C, both dexamethasone and $1,25(OH)_2D_3$ treatment led to a reduction in LPS-induced expression of the maturation markers CD86 and/or MHC class II. In addition, LPS-induced production of TNFα and IL-12p70 was markedly reduced in the presence of dexamethasone (Figure 34D, E).
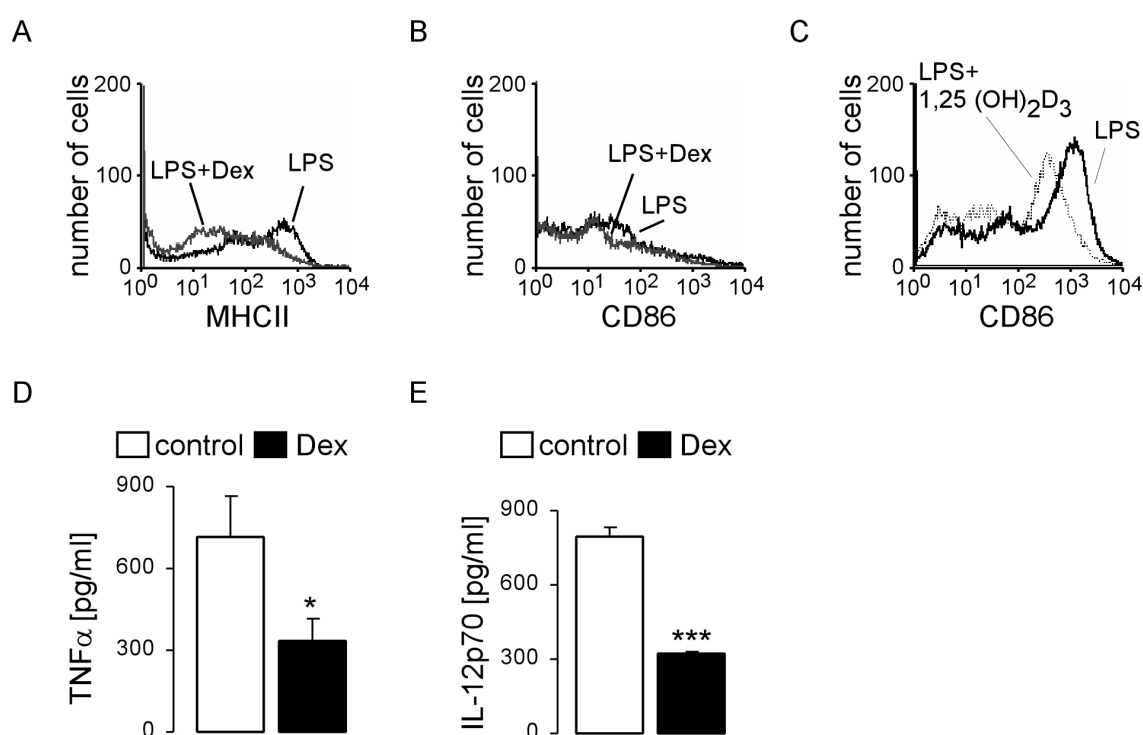
Figure 34. Effect of dexamethasone and $1,25(OH)_2D_3$ on maturation and cytokine production in mouse DCs

(A)-(C) Representative FACS histograms depicting the expression of MHC class II and CD86 in LPS-stimulated (100 ng/ml, 24 hours) mouse DCs in the absence (black line) and in the presence (grey line) of dexamethasone (10 nM, 24 hours, A,B) or $1,25(OH)_2D_3$ (100 nM, 24 hours, C). **(D), (E)** DCs were incubated with LPS (100 ng/ml) in the absence (open bars) or in the presence of dexamethasone (10 nM, closed bars). After 4 hours (C) or 24 hours (D) supernatants were collected to measure TNF-α (C) or IL-12p70 (D), respectively, by ELISA. The results are representative for 4-7 independent experiments. Each experiment was performed in duplicate; values represent the mean ± SEM of duplicates, * ($p<0.05$) and *** ($p<0.001$) show differences from untreated (control) group, two-tailed unpaired *t*-test.

3.13 The inhibitory effect of dexamethasone and 1,25(OH)$_2$D$_3$ is abolished by blockers of Na$^+$/Ca^{2+} exchangers

Since the inhibition of NCKX by DBZ was shown above to restore the LPS-induced increase in [Ca^{2+}]$_i$, it was further tested whether the effect of 1,25(OH)$_2$D$_3$ and dexamethasone on DC maturation could be influenced by blocking Na$^+$/Ca^{2+} exchangers. Treatment of mouse DCs with 100 nM 1,25(OH)$_2$D$_3$ in the presence of the NCKX blocker DBZ (10 µM) restored the 1,25(OH)$_2$D$_3$-induced reduction in CD86 expression (Figure 35A). Similarly, the dexamethasone-induced decrease of CD86 expression was significantly blunted in the presence of the NCX blocker KB-R7943 (10 µM, Figure 35B). The data indicate that K$^+$-dependent and K$^+$-independent Na$^+$/Ca^{2+} exchangers in DCs are at least partially involved in 1,25(OH)$_2$D$_3$- and dexamethasone-mediated suppression of DC maturation, respectively.
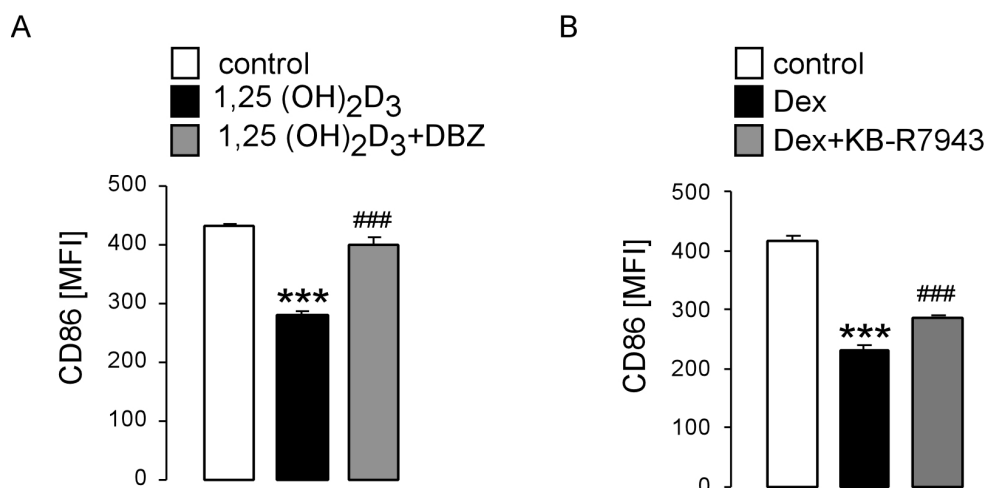
Figure 35. Effect of dexamethasone and 1,25(OH)$_2$D$_3$ on CD86 expression is sensitive to blockers of Na$^+$/Ca^{2+} exchangers

(A) Arithmetic means ± SEM (n = 4) of CD86 expression in LPS (100 ng/ml, 24 hours) -stimulated DCs cultured without (control, white bar) or with 1,25(OH)$_2$D$_3$ (100 nM, 24 hours) in the absence (black bar) or in the presence of 3',4'-dichlorobenzamyl (DBZ, 10 µM, grey bar). *** (p<0.001) indicates difference from control DCs, ### (p<0.001) indicates difference from 1,25(OH)$_2$D$_3$-treated cells (ANOVA). **(B)** Arithmetic means ± SEM (n = 6) of CD86 expression in LPS (100 ng/ml, 24 h) -stimulated DCs cultured without (control, white bar) or with dexamethasone (Dex, 10 nM, 24 h) in the absence (black bar) or in the presence of KB-R7943 (10 µM, grey bar). *** (p<0.001) indicates difference from control DCs, ### (p<0.001) indicates difference from dexamethasone-treated cells (ANOVA).

4 Discussion

4.1 DC culture

The described method to culture mouse bone marrow-derived dendritic cells (BMDCs) in the presence of GM-CSF as external factor is adopted from Inaba et al. [142] and yields a DC culture with a purity of approximately ~80-85%. Cell culture purity is a critical factor for *in vitro* experiments such as the determination of the expression of a new protein. Many different methods and approaches exist to generate DC cultures, e.g. generation of DCs out of peripheral blood monocytes in the presence of GM-CSF and IL-4 [153], IFNα [154], or IL-15 [155], additional activation of the cells with anti-CD3-specific antibody after prior cultivation in the presence of GM-CSF and IL-4 [156], or usage of Transwell chambers based on a one-way migration of blood monocytes through a layer of human umbilical vein endothelial cells in the absence of endogenous factors [157]. Regarding generation of DC cultures out of mouse bone marrow, as it has been done in the present work, protocols are available using not only GM-CSF but also IL-4 as external factor [158]. However, all of the stated approaches use different external factors and/or progenitor cells as in the present work, which may result in altered DC properties. Possible changes in the culturing protocol to increase DC culture purity therefore should not affect the external factors or the progenitor cells used, but the culturing protocol itself. The method of Lutz et al. [159] describes a possibility to generate large quantities of highly pure DCs from mouse bone marrow and involves, among other things, an increased starting culture density, a decreasing dose of GM-CSF over the culturing, and a culture period extended to 10-12 days [159]. Besides a higher purity of the DC culture, which increases the reliability of the data, the yield of mature DCs is higher as with the standard method of Inaba et al. [142], allowing a higher experimental throughput.

4.2 Assessment of changes in [Ca^{2+}]$_i$

The present data on changes in [Ca^{2+}]$_i$ have been obtained by fluorescence optics. LPS- and PGN-induced increases in [Ca^{2+}]$_i$ occur transient, which means that cytosolic Ca^{2+} is subsequently extruded by uptake into the intracellular stores and extrusion across the cell membrane. However, subsequent localized oscillatory increases in [Ca^{2+}]$_i$ can not be ruled out, since they may escape detection by determination of bulk cytosolic Ca^{2+} but may

account for long-lasting effects of Ca^{2+} signaling, such as cell proliferation [160,161] and maturation [162]. Ca^{2+} oscillations require the entry of extracellular Ca^{2+}, whereby Ca^{2+} release from internal stores amplifies the external Ca^{2+} signal [163]. They have been observed in a multitude of cell types and tissues, e.g. kidney [164], neurons [163,165], and oocytes [162], and regulate a wide variety of functions, among which are vasoconstriction, gene transcription, apoptosis, platelet activation, and neuronal function [160,164,166].

4.3 LPS- and PGN-induced Ca^{2+} entry in mouse DCs

The present work investigated the effects of the TLR ligands LPS and PGN on cytosolic Ca^{2+} activity ($[Ca^{2+}]_i$) in BMDCs. Treatment with the respective compounds resulted in a rapid transient increase in $[Ca^{2+}]_i$. The peak and slope of this increase were significantly blunted, but not completely abolished, in the absence of extracellular Ca^{2+} or in the presence of SKF-96365, a blocker of CRAC channels [74]. These findings indicate that both the LPS- and the PGN-induced increase in $[Ca^{2+}]_i$ are partially due to Ca^{2+} influx through Ca^{2+} channels in the plasma membrane and in part due to Ca^{2+} release from intracellular stores. The activation of Ca^{2+} entry in response to store depletion is a characteristic feature of CRAC channels.

It has been demonstrated that, similar to other immune cells, CRAC channels display the major entry pathway for Ca^{2+} in DCs [78]. Hsu et al. further demonstrated that Ca^{2+} release-activated Ca^{2+} currents (I_{CRAC}) could be activated by store depletion induced by dialyzing the cytosol with inositol 1,4,5-trisphosphate (IP_3) and with high concentration of the Ca^{2+} chelator BAPTA, which chelates Ca^{2+} that leaks from the stores and hence prevents store refilling. These findings are in line with the data presented here, showing the same effect by blocking SERCA pumps in the ER using thapsigargin, thereby preventing store refilling. In addition, LPS and PGN have recently been shown to induce $PLC_{\gamma2}$ phosphorylation, resulting in generation of IP_3 and subsequent mobilization of Ca^{2+} from the ER in BMDCs [167]. In addition, the present data show that the effect of PGN on $[Ca^{2+}]_i$ is dramatically reduced in DCs derived from *tlr2*$^{-/-}$ mice, revealing that TLR2 is one of the main receptors for PGN in mouse DCs. Taken together, the present results indicate that LPS and PGN activate CRAC channels and therefore reveal an important mechanism of channel activation by TLR ligands. In the present work, SKF-96365 was used to inhibit CRAC channels. However, the blocker appears to be equally potent in blocking TRP and voltage-gated Ca^{2+} channels [74]. Therefore, SKF-96365 can not be regarded as a specific CRAC channel blocker. However,

this problem may be solved in the nearer future, since the molecules involved in store-operated Ca^{2+} entry (SOCE) have been identified recently. The identification of these molecules should contribute to the development of potent and specific inhibitors of the CRAC channel. Besides CRAC channels, the canonical TRP channels TRPC have also been reported to increase $[Ca^{2+}]_i$ through coupled plasma membrane receptor stimulation or, probably, through store-depletion in different cell types including lymphocytes. But a direct participation of TRPCs in SOCE remains controversial, and moreover, there are no obvious reports of store-operated TRPC Ca^{2+} currents in lymphocytes [168]. However, nothing has been described so far about the function of TRPC channels in DCs.

Voltage-gated K^+ channels such as Kv1.3 are involved in maintaining the membrane potential and are activated upon membrane depolarization. Furthermore, they potentiate the driving force for CRAC-mediated influx of positively charged Ca^{2+} and thereby display indirect modulators of $[Ca^{2+}]_i$ in lymphocytes [168,169]. Thus, the influence of Kv channels on Ca^{2+} entry in DCs was explored by using a combination of Kv1.3 and Kv1.5 channel blockers. The presence of Kv1.3 and Kv1.5 in DCs has recently been demonstated in human blood-derived DCs [92] and mouse BMDCs [93]. As a result, DC Kv channels sustained the increase in $[Ca^{2+}]_i$ upon LPS and PGN stimulation, and this effect was most probably due to the maintenance of a negative membrane potential [170] and provision of the necessary electrical driving force for Ca^{2+} entry through CRAC channels. To quantify whether either Kv1.3 or Kv1.5 alone are sufficient to maintain the membrane potential and thereby the driving force for Ca^{2+} entry in response to TLR activation, blockers of Kv1.3 and Kv1.5 were used separately. It could be shown that the inhibitory effect on $[Ca^{2+}]_i$ was most prominent when both blockers were used in combination. Nevertheless, Kv channels are not the only channels maintaining the electrical driving force for Ca^{2+} entry. The nonselective cation channel TRPM4 was shown to control Ca^{2+} homeostasis in T lymphocytes [171] and mast cells [172]. TRPM4 was recently demonstrated to be also expressed in DCs, where it controls chemokine-dependent DC migration. It induces membrane depolarization by allowing the entry of Na^+, a condition decreasing the driving force for Ca^{2+} entry [89].

4.4   Role of CRAC and Kv channels in DC maturation and function

It has been further shown here that CRAC channels are involved in LPS- and PGN-induced increase in $[Ca^{2+}]_i$ and subsequent production of cytokines. Since the cytokine profile produced by a cell depends, among others, on the type of stimuli [23], the production of TNFα and IL-6 was determined following LPS stimulation, while TNFα and IL-10 were assessed when DCs were stimulated with PGN. PGN-mediated Ca^{2+} entry has already been suggested to upregulate cytokine production in DCs and macrophages [96]. Furthermore, CRAC channels have been suggested to be important for DC maturation, since activation of I_{CRAC} with thapsigargin was shown to induce maturation of mouse myeloid DCs [78], human peripheral blood monocytes and HL-60 cells [77]. Moreover, addition of calcium ionophore to human monocytes or immature DCs leads to acquisition of many properties characteristic of activated myeloid DCs [97]. Therefore, the role of CRAC channels in LPS- and PGN-induced cytokine production has been investigated. Inhibition of CRAC channels by SKF-96365 impaired the secretion of TNFα and IL-6 in response to LPS, and of TNFα and IL-10 in response to PGN treatment. Moreover, LPS-induced upregulation of MHC class II expression and DC migration in response to CCL21 were shown to depend on CRAC channel activity. In addition, the phagocytic capacity of DCs stimulated for 48 hours with LPS or PGN was increased in the presence of CRAC channel blockers.

Besides CRAC channels, Kv channels have also been reported to play a role in DC maturation and cytokine production [92,93]. They are similarly involved in the activation and proliferation of leukocytes [140]. Kv1.3 constitutes the dominant K^+ conductance of resting T lymphocytes [173]. Inhibition of Kv1.3 channels induces membrane depolarization and prevents the activation response of human T lymphocytes [140]. Moreover, Kv channels are regulated during proliferation and activation of macrophages [174]. Therefore, the present work investigated the involvement of Kv channels in LPS- and PGN-induced DC function by using Kv channel blockers. Inhibition of Kv channels blunted the secretion of TNFα, IL-6 and IL-10 in response to LPS or PGN. Moreover, LPS-induced upregulation of MHC class II expression and DC migration in response to CCL21 were shown to depend on Kv channel activity. In addition, the phagocytic uptake of FITC-dextran by DCs stimulated for 48 hours with LPS or PGN was shown to depend on Kv channel activity. At the sites of pathogen entry DCs "sample" their environment by phagocytosis, initiating specific immune responses, when they recognize microbes or tissue damage [6]. The efficient uptake of pathogens is thus essential for generation of immunity against an infectious agent.

Interestingly, both CRAC and Kv channel blockers enhanced antigen uptake only in PGN- and LPS-stimulated cells, which upon LPS- or PGN-induced maturation lost part of their phagocytic capacity. In immature cells that are efficient in antigen uptake the channel blockers did not influence phagocytosis. Ca^{2+} entry is required for the stimulation of DC maturation [77,96,97], and maturation leads in turn to decreased phagocytosis [6,51].

It was further demonstrated that blocking of both CRAC and Kv channels in DCs has no effect on the IκBα phosphorylation, which is in turn known to regulate the transcription factor NF-κB. Ca^{2+} activates opposing nuclear signaling pathways in different cell types and thereby may up- or downregulate NF-κB [175-179]. In T lymphocytes and mesangium cells, phorbol-12-myristate-13-acetate (PMA)-induced activation of NF-κB was stimulated in the presence of Ca^{2+} ionophore [175,178], while Ca^{2+} channel blockers inhibited this effect [178]. NF-κB translocation to the nucleus in osteoblasts was shown to depend on intracellular Ca^{2+} release [176]. Moreover, Ca^{2+} chelation by EGTA inhibited NF-κB activation in retina and microglia [177,179], an effect linked to the production of IL-6 [179]. In contrast, in epithelial cells, NF-κB is repressed by Ca^{2+} signaling [175].

The role of SOCE in DCs remains poorly understood, and there are several important questions still to be solved. In contrast, the role of SOCE in lymphocytes is well established, where it upregulates nuclear factor of activated T-cells (NFAT) [82]. The importance of this process is illustrated by patients with a rare form of hereditary **s**evere **c**ombined **i**mmuno**d**eficiency (SCID). T lymphocytes from these patients show multiple cytokine deficiency and a selective inability to activate NFAT resulting from a pronounced reduction in I_{CRAC} [82]. In calcium ionophore-treated HL-60 cells, which can under certain conditions differentiate to monocyte/macrophage-like cells, antagonists of the protein phosphatase calcineurin, that renders NFAT active, have been shown to attenuate expression of costimulatory molecules [77]. NFAT activation in DCs was demonstrated upon stimulation of the beta-glucan receptor Dectin-1, a C-type lectin, by zymosan [180]. Dectin-1, similar to T cell receptor (TCR) and B cell receptor (BCR), has an immunoreceptor tyrosine-based activation motif (ITAM) in its intracellular tail and thus, it seems likely, that NFAT activation in DCs occurs by similar mechanisms to those used in lymphocytes. NFAT activation was shown to regulate IL-2, IL-10 and IL-12 p70, but not TNFα production in zymosan-stimulated DCs [180]. Moreover, a recent study has demonstrated that LPS-induced Ca^{2+} mobilization in DCs leads to calcineurin-dependent nuclear translocation of NFAT and production of NFAT-dependent cytokines, such as IL-2 [70]. Moreover, LPS-mediated activation of the NFAT pathway was required to induce apoptotic death of terminally differentiated DCs.

Consequently, blocking this pathway *in vivo* causes prolonged DC survival and an increase in T cell priming capability [70].

4.5   Regulation of Ca^{2+} homeostasis by $1,25(OH)_2D_3$ and dexamethasone

Physiological Ca^{2+} signaling occurs through Ca^{2+} oscillations rather than through a long-lasting increase or decrease in $[Ca^{2+}]_i$. Therefore, the activity of signal terminators such as ER- and plasma membrane-localized Ca^{2+} pumps (SERCA and PMCA, respectively), Na^+/Ca^{2+} exchangers in the plasma membrane, and mitochondrial and cytosolic buffer proteins, is extremely important for determination of duration, amplitude and intracellular location of a particular Ca^{2+} signal [141]. A sustained increase of cytosolic Ca^{2+} would be detrimental, as it would induce apoptosis [181,182]. It is shown here that mouse BMDCs express Na^+/Ca^{2+} exchangers for rapid extrusion of cytosolic Ca^{2+}. Their expression has been reported before in other immune cells such as human lymphocytes [183], mast cells [61,184], neutrophils [185], human macrophages and monocytes [61,63]. NCX and NCKX have been furthermore reported to be expressed in non-excitable cells such as epithelial cells [186] and platelets [187]. Moreover, the carriers have been shown to terminate the Ca^{2+} signal following stimulation of Ca^{2+} entry in a variety of excitable cells including neurons [59,188], the heart [189-192], retinal rod photoreceptors and smooth muscle cells [62].

It could be demonstrated that $1,25(OH)_2D_3$ and the glucocorticoid dexamethasone blunt the increase of $[Ca^{2+}]_i$ following LPS treatment. The present data further reveal mechanisms accounting for the altered Ca^{2+} response, among which are Na^+/Ca^{2+} exchangers. The activity of these carriers was measured by assessing changes in $[Ca^{2+}]_i$. It has been shown that at least one K^+-dependent Na^+/Ca^{2+} exchanger is regulated by $1,25(OH)_2D_3$, while the hormone did not act on K^+-independent Na^+/Ca^{2+} exchangers. This was indicated by the observation that $1,25(OH)_2D_3$ had no effect on Na^+/Ca^{2+} exchanger activity in the absence of extracellular K^+. Elevating extracellular K^+ concentration to 40 mM only slightly increased the observed effect on $[Ca^{2+}]_i$ in untreated control cells, but dramatically enhanced cytosolic Ca^{2+} concentration in $1,25(OH)_2D_3$-treated cells. In contrast, the effect of dexamethasone did not depend on extracellular K^+ concentration, indicating an action on K^+-independent Na^+/Ca^{2+} exchangers. The finding was further confirmed by showing an upregulation of transcription levels of NCX2 and NCX3 in dexamethasone-treated DCs. There was no effect of dexamethasone on transcript levels of NCX1. The data are in line with recent findings in

duodenum, where mRNA levels of NCX1 were not altered by dexamethasone [193]. However, in kidney cells, dexamethasone treatment has been shown to increase NCX1 transcript levels [194], pointing to a cell type-specific action of dexamethasone on Na^+/Ca^{2+} exchangers.

The mechanism underlying the immunosuppressive effects of glucocorticoids in T lymphocytes has recently been shown to involve modulation of Ca^{2+} signaling via down-regulation of IP_3 receptors. Upon strong TCR stimulation, dexamethasone converted the Ca^{2+} response from transient increase to sustained oscillations. In contrast, Ca^{2+} oscillations induced by weak TCR stimulation were decreased by dexamethasone, which was associated with the inhibition of IL-2 induction. Those effects were rapid and mediated by nongenomic inhibition of the Src family kinase Lck [195], whereas the effects of dexamethasone presented in this study were largely due to a strong transcriptional activation of NCX.

Enhanced Na^+/Ca^{2+} exchanger activity accelerates extrusion of Ca^{2+} and thereby blunts the increase of cytosolic Ca^{2+} concentration following stimulation of DCs with LPS. As discussed above, $[Ca^{2+}]_i$ regulates a variety of DC functions, including maturation and production of inflammatory cytokines [61,77,95,167,196], thereby regulating DC-dependent immune responses. Previous studies further report an inhibitory effect of $1,25(OH)_2D_3$ on DC differentiation and maturation as well as on IL-12 production [110-112,197]. In the present study, it has been demonstrated that the NCKX blocker 3',4'-dichlorobenzamyl reversed the effect of $1,25(OH)_2D_3$ on $[Ca^{2+}]_i$ and subsequent CD86 expression. The data provide a link between $1,25(OH)_2D_3$-induced activity of Na^+/Ca^{2+} exchangers and LPS-induced DC maturation. Similarly, the NCX blocker KB-R7943 at least partially reversed the inhibitory effect of dexamethasone on DC maturation, which is part of the events underlying the immunosuppressive effects of glucocorticoids. However, the remaining, KB-R7943-insensitive decline of CD86 expression following dexamethasone treatment may be due to a, perhaps, more strong K^+-dependent Na^+/Ca^{2+} exchanger activity. Another explanation could be an incomplete inhibition of the Na^+/Ca^{2+} exchanger by KB-R7943.

It has been shown further that $1,25(OH)_2D_3$ increases the expression of calbindin-D28K in mouse DCs, thereby providing another mechanism accounting for the blunted LPS-induced increase in $[Ca^{2+}]_i$ in the presence of $1,25(OH)_2D_3$. Calbindin-D28K eagerly binds cytosolic Ca^{2+} and thus serves as an intracellular Ca^{2+} buffer. In Ca^{2+} transporting epithelia, the binding of Ca^{2+} to calbindin-D28K is critically important for the cytosolic transport of Ca^{2+} from the apical to the basolateral cell membrane [67]. At the present low cytosolic Ca^{2+} concentration the intracellular diffusion of free Ca^{2+} would not be sufficiently fast for the

transepithelial Ca^{2+}-transport. In DCs, calbindin-D28K could serve to weaken the alterations of $[Ca^{2+}]_i$ following stimulation of Ca^{2+} entry. Taken together, the effects of $1,25(OH)_2D_3$ on the Na^+/Ca^{2+} exchanger and calbindin-D28K blunt the LPS-induced increase of $[Ca^{2+}]_i$. Accordingly, following treatment of DCs with $1,25(OH)_2D_3$, LPS leads to an only slight increase of $[Ca^{2+}]_i$. As reported in previous studies $1,25(OH)_2D_3$ inhibits the differentiation and maturation of DCs as well as IL-12 production [110,111,197,198]. Thus, the suppressive effect of $1,25(OH)_2D_3$ could be at least partially due to its effect on cytosolic Ca^{2+} in DCs.

Effects of glucocorticoids on Ca^{2+} signaling have previously been reported in other cell types. In duodenum, glucocorticoids down-regulate genes encoding for Ca^{2+} transport proteins, resulting in impaired Ca^{2+} absorption. In particular, treatment of mice with dexamethasone for 5 days resulted in decreased expression of transient receptor potential vanilloid 6 (TRPV6) channels with a subsequent reduction in Ca^{2+} entry across the apical membrane and thus reduces intestinal Ca^{2+} absorption. In addition, the expression of the Ca^{2+} binding protein calbindin-D9K was decreased, an effect abolishing intracellular Ca^{2+} transport. However, treatment with dexamethasone for shorter timepoints (e.g. 24 hours) induced duodenal transcript levels of TRPV6, calbindin-D9K and PMCA. A similar action of dexamethasone was reported in kidney cells, with increased transcriptional levels of TRPV5, calbindin-D9K, and NCX1 after 24 hours of treatment, while renal transcript levels of TRPV6 were reduced following treatment with the glucocorticoid [194]. In contrast, in aortic myocytes, dexamethasone was shown to decrease NCX expression and activity [199,200]. This different regulation of NCX by glucocorticoids in distinct tissues may be explained by the model of Lee et al. [201]. According to this model, expression of the same NCX protein is driven by at least three different tissue-specific promoters, allowing the exchangers to respond independently to specific demands of different environments [201]. Thus, tissue or cell type specific promoter elements may at least partially account for the distinct regulation of NCX expression in response to glucocorticoids.

4.6 Conclusions and future experiments

Regarding the initially determined aim of the present work, the nature of the LPS- and PGN-induced Ca^{2+} signal in mouse DCs has been characterized. DCs respond to LPS- and PGN-stimulation with a fast increase in $[Ca^{2+}]_i$. This increase is accomplished by both Ca^{2+} release from intracellular stores and Ca^{2+} influx through CRAC channels, with the latter being dependent on the activity of Kv channels. Inhibition of either CRAC or Kv channels leads to

marked changes in DC functions, including changes in maturation, phagocytosis, migration and cytokine production. The data contribute to an increasing body of evidence that Ca^{2+}-mediated signal transduction pathways serve a central regulatory role in DC responses to diverse antigens, including TLR ligands, intact bacteria, and microbial toxins. Moreover, it could be demonstrated for the first time that mouse BMDCs express Na^+/Ca^{2+} exchangers, and that the carriers are regulated by $1,25(OH)_2D_3$ and dexamethasone. In addition, $1,25(OH)_2D_3$ further modulates the Ca^{2+} signal by increasing calbindin-D28K expression. In respect to the pivotal role of Ca^{2+} signaling in the regulation of DC function, the effects of $1,25(OH)_2D_3$ and dexamethasone on $[Ca^{2+}]_i$ are likely to play a critical role in their known immunosuppressive effects. However, the effect of $1,25(OH)_2D_3$ and dexamethasone on Ca^{2+} entry through CRAC channels remains to be determined. Entry of extracellular Ca^{2+} displays a third possible mechanism besides Ca^{2+} extrusion and Ca^{2+} buffering how the two compounds may modulate $[Ca^{2+}]_i$. It is known, however, from chick skeletal muscle cells that $1,25(OH)_2D_3$ regulates Ca^{2+} entry into these cells by inducing (and not inhibiting) an initial IP_3-dependent Ca^{2+} mobilization from internal stores with subsequent activation of CRAC channels [202]. Similar results have been obtained in jejunal enterocytes, where $1,25(OH)_2D_3$ was shown to promote Ca^{2+} entry via CRAC channels [203].

The experiments focussing on the effects of dexamethasone on DC functions could also be extended and proved further. For example, the effect of dexamethasone treatment on NCX protein expression could be additionaly investigated, since changes in the expression levels of NCX2 and NCX3 do not necessarily indicate a production or more abundant production of the respective proteins. Furthermore, the precise function of Na^+/Ca^{2+} exchangers in mouse DCs is not clear. The data on CD86 expression describing the effect of the NCX blocker KB-R7943 on dexamethasone-induced suppression of DC maturation and function would be further supported by performing additional functional readouts for DC maturation and function. The missing link between NCX2/NCX3 and the dexamethasone-induced increase in Na^+/Ca^{2+} exchange can be established by either a specific blocker or small RNA interference experiments.

4.7 Clinical Relevance

SOCE has been observed in the majority of both immature and mature DCs, pointing to its importance in the regulation of a range of DC functions, e.g. maturation, chemotaxis, and

migration to lymphoid tissues [78]. Since DCs serve as an important link between innate and adaptive immune responses [6,132], activation of DC CRAC channels in response to bacterial components such as LPS or PGN may play a critical role in a range of immune responses by modulating DC function.

Regarding the pivotal role of Ca^{2+} signaling in the regulation of DC function, the observed effects of $1,25(OH)_2D_3$ and dexamethasone are likely to play a critical role in the known immunosuppressive effect of the two compounds. Vitamin D-deficiency is linked to several autoimmune diseases. DCs express the vitamin D receptor (VDR) and are primary targets for the immunomodulatory activity of $1,25(OH)_2D_3$ [110]. Therefore, $1,25(OH)_2D_3$ as well as synthetic VDR agonists with immunomodulatory and anti-inflammatory properties could be used to modulate DC function and thereby the progression and development of a variety of autoimmune diseases such as rheumatoid arthritis, multiple sclerosis, type 1 diabetes, or inflammatory bowel disease [204]. These considerations are supported by the fact that supplementation with $1,25(OH)_2D_3$ not only prevented, but also reduced experimental autoimmune encephalomyelitis (EAE), an animal model of multiple sclerosis, in mice [118,119]. $1,25(OH)_2D_3$ alters DC and T lymphocyte function and regulates macrophages in EAE [205]. That the effects of $1,25(OH)_2D_3$ may at least partially involve modulation of CRAC channel activity is supported by the effects observed in chick sceletal muscle cells [202] and jejunal enterocytes [203], as discussed earlier. Regarding glucocorticoids, it has been suggested from experiments in Jurkat T lymphocytes, that dexamethasone indirectly modulates Ca^{2+} entry through CRAC channels by inhibiting Kv channels [206]. Therefore, the anti-inflammatory and immunomodulatory effects of glucocorticoids may involve modulation of CRAC channel activity and play a role in treatment and prevention of rheumatoid and inflammatory diseases. Another important field of application could be SCID. It could be shown recently that DCs, previously exposed to a combination of dexamethasone and $1,25(OH)_2D_3$, are able to prevent experimental inflammatory bowel disease in mice suffering from SCID [207]. It is likely that this effect is at least partially due to CRAC channel activity, since SCID patients were shown to be defective in SOCE and CRAC channel function [82].

5   Summary

Dendritic cells (DCs) are antigen-presenting cells that provide a link between innate and adaptive immunity. Ca^{2+}-mediated signal transduction pathways play a central regulatory role in DC responses to diverse antigens, including Toll-like receptor (TLR) ligands, intact bacteria, and microbial toxins. However, the mechanisms leading to increased $[Ca^{2+}]_i$ upon DC activation are poorly understood. In the present study, treatment of mouse DCs with either lipopolysaccharide (LPS, 100 ng/ml) or peptidoglycan (PGN, 25 µg/ml) resulted in a rapid increase in $[Ca^{2+}]_i$ which was due to Ca^{2+} release from intracellular stores and influx of extracellular Ca^{2+} across the cell membrane. In DCs isolated from $tlr2^{-/-}$ mice the effect of PGN on $[Ca^{2+}]_i$ was dramatically impaired. In whole-cell voltage-clamp experiments, LPS-induced currents exhibited properties similar to I_{CRAC}. These currents were highly selective for Ca^{2+}, exhibited a prominent inward rectification of the current-voltage relationship, an anomalous mole fraction and a fast Ca^{2+}-dependent inactivation. Furthermore, the LPS- and PGN-induced incrase in $[Ca^{2+}]_i$ was dependent on voltage-gated K^+ (Kv) channel activity. MHC class II expression, CCL21-dependent migration, and cytokine production decreased, whereas phagocytic activity increased in LPS- or PGN-stimulated DCs in the presence of both Kv and CRAC channel blockers. Activation of the transcription factor nuclear factor κB (NF-κB), assessed as phosphorylation of inhibitory molecule IκB, was not affected by CRAC or Kv channel blockers.

The activity of DCs is suppressed by glucocorticoids, which induce potent immunosuppressive effects. Furthermore, DCs are primary targets of 1,25-dihydroxyvitamin D_3 (1,25$(OH)_2D_3$), a secosteroid hormone, that, in addition to its well-established action on Ca^{2+} homeostasis, possesses immunomodulatory properties. Nothing is known about the effects of 1,25$(OH)_2D_3$ and glucocorticoids on Ca^{2+} channels and transporters in DCs. The LPS-induced increase in $[Ca^{2+}]_i$ in mouse DCs was significantly blunted by prior incubation of the cells with either 1,25$(OH)_2D_3$ (100 nM, 24 h) or dexamethasone (10 nM, overnight). It could be further shown that DCs express both, K^+-independent (NCX1-3) and K^+-dependent (NCKX1, 3-5), Na^+/Ca^{2+} exchangers. The activity of Na^+/Ca^{2+} exchangers was assessed by removal of extracellular Na^+ in the presence of external Ca^{2+}, a maneuver that triggers the entry of extracellular Ca^{2+} and resulted in a measurable, rapid transient increase in $[Ca^{2+}]_i$ and an outwardly rectifying current measured in whole cell patch-clamp experiments. Both 1,25$(OH)_2D_3$ and dexamethasone enhanced the increase in $[Ca^{2+}]_i$ and the outward current following removal of external Na^+. While the effect of 1,25$(OH)_2D_3$ affected K^+-dependent Na^+/Ca^{2+} exchangers, the action of dexamethasone was directed against K^+-independent Na^+/Ca^{2+} exchangers. Furthermore, dexamethasone increased the transcript levels of NCX2

and NCX3. Thus, $1,25(OH)_2D_3$ and dexamethasone blunt the LPS-induced increase in $[Ca^{2+}]_i$ by stimulation of Na^+/Ca^{2+} exchanger-dependent Ca^{2+} extrusion. In addition, $1,25(OH)_2D_3$ further modulated $[Ca^{2+}]_i$ by upregulating the Ca^{2+}-binding protein calbindin-D28K and thereby the Ca^{2+} buffer capacity of the cells. The NCKX blocker 3',4'-dichlorobenzamyl reversed the inhibitory effect of $1,25(OH)_2D_3$ on LPS-induced increase of $[Ca^{2+}]_i$. Expression of the costimulatory molecule CD86 was down-regulated by $1,25(OH)_2D_3$ and dexamethasone, an effect reversed by 3',4'-dichlorobenzamyl and KB-R7943, blockers of NCKX and NCX, respectively.

6   Zusammenfassung

Dendritische Zellen (DZ) sind Antigen-präsentierende Zellen und stellen ein Bindeglied zwischen angeborener und erworbener Immunität dar. Ca^{2+}-vermittelte Signaltransduktionswege spielen eine zentrale Rolle bei der Regulation der Immunantwort von DZ auf verschiedene Antigene, einschließlich Toll-ähnlichen Rezeptor-Liganden, intakten Bakterien und mikrobiellen Toxinen. Die zugrundeliegenden Mechanismen die bei Aktivierung von DZ zu einem Anstieg der intrazellulären Calciumkonzentration $[Ca^{2+}]_i$ führen, sind jedoch noch nicht vollständig aufgeklärt. Behandlung von DZ der Maus mit Lipopolisaccharid (LPS, 100 ng/ml) oder Peptidoglykan (PGN, 25 µg/ml) führte zu einem raschen Anstieg der $[Ca^{2+}]_i$, welcher sich aus der Freisetzung von Ca^{2+} aus intrazellulären Speichern sowie dem Einstrom von extrazellulärem Ca^{2+} durch die Plasmamembran zusammensetzte. Der Effekt von PGN auf $[Ca^{2+}]_i$ war deutlich beeinträchtigt, wenn die DZ von TLR2-defizienten Mäusen isoliert wurden. *Patch-Clamp*-Experimente in der *Whole-Cell*-Konfiguration zeigten, dass die durch LPS induzierten Ströme Übereinstimmungen mit I_{CRAC} aufweisen. Die Ströme waren hoch selektiv für Ca^{2+} und wiesen eine deutliche Einwärtsausrichtung der Strom-Spannungs-Beziehung, eine anormale Molfraktion sowie eine schnelle Ca^{2+}-abhängige Inaktivierung auf. Weiterhin war der LPS- und PGN-induzierte Anstieg der $[Ca^{2+}]_i$ von der Aktivität spannungsregulierter K^+ (Kv) Kanäle abhängig. Die Expression von MHC Klasse II-Molekülen, CCL21-abhängige Migration sowie die Produktion von Zytokinen durch DZ waren in der Gegenwart von Blockern für Kv- und CRAC-Kanäle reduziert, während die phagozytische Aktivität der Zellen erhöht war. Die Aktivierung des Transkriptionsfaktors *nuclear factor κB* (NF-κB), erfasst als Phosphorylierung des inhibitorischen Moleküls IκB, war in der Gegenwart von Kv- und CRAC-Blockern nicht verändert.

Glucocorticoide haben eine starke immunosuppressive Wirkung und hemmen die Aktivität von DZ. Weiterhin sind DZ primäre Angriffspunkte für das Secosteroidhormon 1,25-Dihydroxyvitamin D_3 (1,25(OH)$_2$D$_3$), welches zusätzlich zu seiner gut etablierten Wirkung auf den Ca^{2+}-Haushalt immunomodulatorische Eigenschaften besitzt. Über die Effekte von 1,25(OH)$_2$D$_3$ und Dexamethason auf Ca^{2+}-Kanäle und -Transporter in DZ ist bisher nichts bekannt. Der LPS-induzierte Anstieg der $[Ca^{2+}]_i$ in DZ der Maus wurde durch vorausgegangene Inkubation der Zellen mit 1,25(OH)$_2$D$_3$ (100 nM, 24 h) oder Dexamethason (10 nM, über Nacht) signifikant gehemmt. Weiterhin konnte gezeigt werden, dass DZ sowohl K^+-unabhängige (NCX1-3) als auch K^+-abhängige (NCKX 1, 3-5) Na^+/Ca^{2+}-Austauscher exprimieren. Die Aktivität dieser Na^+/Ca^{2+}-Austauscher konnte unter Entfernung der extrazellulären Na^+-Ionen bei gleichzeitiger Anwesenheit von Ca^{2+}-Ionen erfasst werden. Der

Vorgang hatte einen Ca^{2+}-Einstrom zufolge, der zu einem messbaren, vorübergehenden raschen Anstieg der $[Ca^{2+}]_i$ sowie einem auswärtsgerichteten Strom führte, welcher mittels *Patch Clamp* in der *Whole-Cell*-Konfiguration erfasst werden konnte. Der durch Entfernung des extrazellulären Na^+ hervorgerufene Anstieg der $[Ca^{2+}]_i$ sowie der resultierende Auswärtsstrom wurden sowohl durch $1,25(OH)_2D_3$ als auch durch Dexamethason verstärkt. Während $1,25(OH)_2D_3$ einen Effekt auf K^+-abhängige Na^+/Ca^{2+}-Austauscher hatte, wirkte Dexamethason auf K^+-unabhängige Na^+/Ca^{2+}-Austauscher. Dexamethason führte weiterhin zu einer Erhöhung der Transkriptionsrate von NCX2 und NCX3. Folglich hemmen $1,25(OH)_2D_3$ und Dexamethason den LPS-induzierten Anstieg der $[Ca^{2+}]_i$ mittels Stimulation des Transports von Ca^{2+} aus der Zelle durch Na^+/Ca^{2+}-Austauscher. $1,25(OH)_2D_3$ beeinflusste die $[Ca^{2+}]_i$ weiterhin zusätzlich durch die Hochregulation des Ca^{2+}-Bindungsproteins Calbindin-D28K und bewirkte somit eine Erhöhung der Pufferkapazität der Zellen für Ca^{2+}. 3',4'-Dichlorobenzamyl, ein Blocker für NCKX, hob den hemmenden Effekt von $1,25(OH)_2D_3$ auf den LPS-induzierten Anstieg der $[Ca^{2+}]_i$ wieder auf. Der hemmende Effekt von $1,25(OH)_2D_3$ und Dexamethason auf die Expression des co-stimulatorischen Moleküls CD86 konnte mithilfe von 3',4'-dichlorobenzamyl bzw. KB-R7943, Blocker für NCKX bzw. NCX, wieder aufgehoben werden.

7   References

1.   Hoffmann, J. A., F. C. Kafatos, C. A. Janeway, and R. A. Ezekowitz. 1999. Phylogenetic perspectives in innate immunity. *Science* 284:1313-1318.

2.   Takeda, K., T. Kaisho, and S. Akira. 2003. Toll-like receptors. *Annu.Rev Immunol.* 21:335-376.

3.   Corthay, A. 2006. A three-cell model for activation of naive T helper cells. *Scand.J Immunol.* 64:93-96.

4.   Fukata, M., A. S. Vamadevan, and M. T. Abreu. 2009. Toll-like receptors (TLRs) and Nod-like receptors (NLRs) in inflammatory disorders. *Semin.Immunol.* 21:242-253.

5.   Diebold, S. S. 2009. Activation of dendritic cells by toll-like receptors and C-type lectins. *Handb.Exp Pharmacol.*3-30.

6.   Banchereau, J., F. Briere, C. Caux, J. Davoust, S. Lebecque, Y. J. Liu, B. Pulendran, and K. Palucka. 2000. Immunobiology of dendritic cells. *Annu.Rev.Immunol.* 18:767-811.

7.   Dubsky, P., H. Ueno, B. Piqueras, J. Connolly, J. Banchereau, and A. K. Palucka. 2005. Human dendritic cell subsets for vaccination. *J.Clin.Immunol.* 25:551-572.

8.   Szatmari, I. and L. Nagy. 2008. Nuclear receptor signalling in dendritic cells connects lipids, the genome and immune function. *EMBO J* 27:2353-2362.

9.   Austyn, J. M. 1992. Antigen uptake and presentation by dendritic leukocytes. *Semin.Immunol.* 4:227-236.

10.   Dougan, S. K., A. Kaser, and R. S. Blumberg. 2007. CD1 expression on antigen-presenting cells. *Curr.Top.Microbiol Immunol.* 314:113-141.

11.   Barral, D. C. and M. B. Brenner. 2007. CD1 antigen presentation: how it works. *Nat Rev Immunol.* 7:929-941.

12.   Fietta, P. and G. Delsante. 2009. The effector T helper cell triade. *Riv.Biol* 102:61-74.

13.   Harrington, L. E., R. D. Hatton, P. R. Mangan, H. Turner, T. L. Murphy, K. M. Murphy, and C. T. Weaver. 2005. Interleukin 17-producing CD4+ effector T cells develop via a lineage distinct from the T helper type 1 and 2 lineages. *Nat Immunol.* 6:1123-1132.

14.   Stockinger, B., M. Veldhoen, and B. Martin. 2007. Th17 T cells: linking innate and adaptive immunity. *Semin.Immunol.* 19:353-361.

15.   Nyirenda, M. H., K. O'Brien, L. Sanvito, C. S. Constantinescu, and B. Gran. 2009. Modulation of regulatory T cells in health and disease: role of toll-like receptors. *Inflamm.Allergy Drug Targets.* 8:124-129.

16.   Sakaguchi, S., K. Wing, Y. Onishi, P. Prieto-Martin, and T. Yamaguchi. 2009. Regulatory T cells: how do they suppress immune responses? *Int Immunol.* 21:1105-1111.

17.   Carpenter, S. and L. A. O'Neill. 2009. Recent insights into the structure of Toll-like receptors and post-translational modifications of their associated signalling proteins. *Biochem J* 422:1-10.

18. Flacher, V., M. Bouschbacher, E. Verronese, C. Massacrier, V. Sisirak, O. Berthier-Vergnes, B. Saint-Vis, C. Caux, C. Dezutter-Dambuyant, S. Lebecque, and J. Valladeau. 2006. Human Langerhans cells express a specific TLR profile and differentially respond to viruses and Gram-positive bacteria. *J Immunol.* 177:7959-7967.

19. Hashimoto, C., K. L. Hudson, and K. V. Anderson. 1988. The Toll gene of Drosophila, required for dorsal-ventral embryonic polarity, appears to encode a transmembrane protein. *Cell* 52:269-279.

20. Medzhitov, R., P. Preston-Hurlburt, and C. A. Janeway, Jr. 1997. A human homologue of the Drosophila Toll protein signals activation of adaptive immunity. *Nature* 388:394-397.

21. Re, F. and J. L. Strominger. 2004. IL-10 released by concomitant TLR2 stimulation blocks the induction of a subset of Th1 cytokines that are specifically induced by TLR4 or TLR3 in human dendritic cells. *J Immunol.* 173:7548-7555.

22. Takeda, K. and S. Akira. 2005. Toll-like receptors in innate immunity. *Int Immunol.* 17:1-14.

23. Kadowaki, N., S. Ho, S. Antonenko, R. W. Malefyt, R. A. Kastelein, F. Bazan, and Y. J. Liu. 2001. Subsets of human dendritic cell precursors express different toll-like receptors and respond to different microbial antigens. *J Exp Med* 194:863-869.

24. Seki, E. and D. A. Brenner. 2008. Toll-like receptors and adaptor molecules in liver disease: update. *Hepatology* 48:322-335.

25. Kirschning, C. J. and R. R. Schumann. 2002. TLR2: cellular sensor for microbial and endogenous molecular patterns. *Curr.Top.Microbiol Immunol.* 270:121-144.

26. Jin, Y., D. Gupta, and R. Dziarski. 1998. Endothelial and epithelial cells do not respond to complexes of peptidoglycan with soluble CD14 but are activated indirectly by peptidoglycan-induced tumor necrosis factor-alpha and interleukin-1 from monocytes. *J.Infect.Dis.* 177:1629-1638.

27. Dmitriev, B. A., S. Ehlers, E. T. Rietschel, and P. J. Brennan. 2000. Molecular mechanics of the mycobacterial cell wall: from horizontal layers to vertical scaffolds. *Int J Med.Microbiol.* 290:251-258.

28. Stewart-Tull, D. E. 1980. The immunological activities of bacterial peptidoglycans. *Annu.Rev Microbiol* 34:311-340.

29. Myhre, A. E., A. O. Aasen, C. Thiemermann, and J. E. Wang. 2006. Peptidoglycan--an endotoxin in its own right? *Shock* 25:227-235.

30. Girardin, S. E., I. G. Boneca, J. Viala, M. Chamaillard, A. Labigne, G. Thomas, D. J. Philpott, and P. J. Sansonetti. 2003. Nod2 is a general sensor of peptidoglycan through muramyl dipeptide (MDP) detection. *J Biol Chem.* 278:8869-8872.

31. Travassos, L. H., S. E. Girardin, D. J. Philpott, D. Blanot, M. A. Nahori, C. Werts, and I. G. Boneca. 2004. Toll-like receptor 2-dependent bacterial sensing does not occur via peptidoglycan recognition. *EMBO Rep.* 5:1000-1006.

32. Dziarski, R., Y. P. Jin, and D. Gupta. 1996. Differential activation of extracellular signal-regulated kinase (ERK) 1, ERK2, p38, and c-Jun NH2-terminal kinase mitogen-activated protein kinases by bacterial peptidoglycan. *J.Infect.Dis.* 174:777-785.

33. Wang, L., A. N. Weber, M. L. Atilano, S. R. Filipe, N. J. Gay, and P. Ligoxygakis. 2006. Sensing of Gram-positive bacteria in Drosophila: GNBP1 is needed to process and present peptidoglycan to PGRP-SA. *EMBO J* 25:5005-5014.

34. Wang, L., R. J. Gilbert, M. L. Atilano, S. R. Filipe, N. J. Gay, and P. Ligoxygakis. 2008. Peptidoglycan recognition protein-SD provides versatility of receptor formation in Drosophila immunity. *Proc Natl.Acad.Sci U.S.A* 105:11881-11886.

35. Carneiro, L. A., L. H. Travassos, and D. J. Philpott. 2004. Innate immune recognition of microbes through Nod1 and Nod2: implications for disease. *Microbes.Infect.* 6:609-616.

36. Chamaillard, M., S. E. Girardin, J. Viala, and D. J. Philpott. 2003. Nods, Nalps and Naip: intracellular regulators of bacterial-induced inflammation. *Cell Microbiol* 5:581-592.

37. Medzhitov, R., P. Preston-Hurlburt, E. Kopp, A. Stadlen, C. Chen, S. Ghosh, and C. A. Janeway, Jr. 1998. MyD88 is an adaptor protein in the hToll/IL-1 receptor family signaling pathways. *Mol Cell* 2:253-258.

38. Kawai, T., O. Adachi, T. Ogawa, K. Takeda, and S. Akira. 1999. Unresponsiveness of MyD88-deficient mice to endotoxin. *Immunity.* 11:115-122.

39. Seixas, E., J. F. Moura Nunes, I. Matos, and A. Coutinho. 2009. The interaction between DC and Plasmodium berghei/chabaudi-infected erythrocytes in mice involves direct cell-to-cell contact, internalization and TLR. *Eur.J Immunol.* 39:1850-1863.

40. Alvarez, J. I. 2005. Inhibition of Toll Like Receptor immune responses by microbial pathogens. *Front Biosci.* 10:582-587.

41. Kaisho, T., O. Takeuchi, T. Kawai, K. Hoshino, and S. Akira. 2001. Endotoxin-induced maturation of MyD88-deficient dendritic cells. *J Immunol.* 166:5688-5694.

42. Kaisho, T. and S. Akira. 2001. Dendritic-cell function in Toll-like receptor- and MyD88-knockout mice. *Trends Immunol.* 22:78-83.

43. Hoebe, K., E. M. Janssen, S. O. Kim, L. Alexopoulou, R. A. Flavell, J. Han, and B. Beutler. 2003. Upregulation of costimulatory molecules induced by lipopolysaccharide and double-stranded RNA occurs by Trif-dependent and Trif-independent pathways. *Nat Immunol.* 4:1223-1229.

44. Zhou, Z., K. Hoebe, X. Du, Z. Jiang, L. Shamel, and B. Beutler. 2005. Antagonism between MyD88- and TRIF-dependent signals in B7RP-1 up-regulation. *Eur.J Immunol.* 35:1918-1927.

45. Inohara, N., Y. Ogura, F. F. Chen, A. Muto, and G. Nunez. 2001. Human Nod1 confers responsiveness to bacterial lipopolysaccharides. *J Biol Chem.* 276:2551-2554.

46. Colino, J. and C. M. Snapper. 2003. Two distinct mechanisms for induction of dendritic cell apoptosis in response to intact Streptococcus pneumoniae. *J Immunol.* 171:2354-2365.

47. Michelsen, K. S., A. Aicher, M. Mohaupt, T. Hartung, S. Dimmeler, C. J. Kirschning, and R. R. Schumann. 2001. The role of toll-like receptors (TLRs) in bacteria-induced

maturation of murine dendritic cells (DCS). Peptidoglycan and lipoteichoic acid are inducers of DC maturation and require TLR2. *J Biol Chem.* 276:25680-25686.

48. Wischke, C., J. Zimmermann, B. Wessinger, A. Schendler, H. H. Borchert, J. H. Peters, T. Nesselhut, and D. R. Lorenzen. 2009. Poly(I:C) coated PLGA microparticles induce dendritic cell maturation. *Int J Pharm.* 365:61-68.

49. Reis e Sousa, P. D. Stahl, and J. M. Austyn. 1993. Phagocytosis of antigens by Langerhans cells in vitro. *J Exp Med* 178:509-519.

50. Nagl, M., L. Kacani, B. Mullauer, E. M. Lemberger, H. Stoiber, G. M. Sprinzl, H. Schennach, and M. P. Dierich. 2002. Phagocytosis and killing of bacteria by professional phagocytes and dendritic cells. *Clin Diagn.Lab Immunol.* 9:1165-1168.

51. Palucka, K. and J. Banchereau. 2002. How dendritic cells and microbes interact to elicit or subvert protective immune responses. *Curr.Opin.Immunol.* 14:420-431.

52. Guo, R. W. and L. Huang. 2008. New insights into the activation mechanism of store-operated calcium channels: roles of STIM and Orai. *J Zhejiang.Univ Sci B* 9:591-601.

53. Schwaller, B. 2009. The continuing disappearance of "pure" Ca2+ buffers. *Cell Mol Life Sci* 66:275-300.

54. Bronner, F. 2001. Extracellular and intracellular regulation of calcium homeostasis. *ScientificWorldJournal.* 1:919-925.

55. Clapham, D. E. 2007. Calcium signaling. *Cell* 131:1047-1058.

56. Clapham, D. E. 2003. TRP channels as cellular sensors. *Nature* 426:517-524.

57. Guerini, D., L. Coletto, and E. Carafoli. 2005. Exporting calcium from cells. *Cell Calcium* 38:281-289.

58. Herchuelz, A., A. Kamagate, H. Ximenes, and F. Van Eylen. 2007. Role of Na/Ca exchange and the plasma membrane Ca2+-ATPase in beta cell function and death. *Ann.N.Y.Acad.Sci* 1099:456-467.

59. Lytton, J. 2007. Na+/Ca2+ exchangers: three mammalian gene families control Ca2+ transport. *Biochem J* 406:365-382.

60. Visser, F. and J. Lytton. 2007. K+ -dependent Na+/Ca2+ exchangers: key contributors to Ca2+ signaling. *Physiology.(Bethesda.)* 22:185-192.

61. Aneiros, E., S. Philipp, A. Lis, M. Freichel, and A. Cavalie. 2005. Modulation of Ca2+ signaling by Na+/Ca2+ exchangers in mast cells. *J Immunol.* 174:119-130.

62. Blaustein, M. P. and W. J. Lederer. 1999. Sodium/calcium exchange: its physiological implications. *Physiol Rev.* 79:763-854.

63. Staiano, R. I., F. Granata, A. Secondo, A. Petraroli, S. Loffredo, A. Frattini, L. Annunziato, G. Marone, and M. Triggiani. 2009. Expression and function of Na+/Ca2+ exchangers 1 and 3 in human macrophages and monocytes. *Eur.J.Immunol.* 39:1405-1418.

64. Herrmann, T. L., C. T. Morita, K. Lee, and D. J. Kusner. 2005. Calmodulin kinase II regulates the maturation and antigen presentation of human dendritic cells. *J Leukoc.Biol* 78:1397-1407.

65. Means, A. R. 2008. The Year in Basic Science: calmodulin kinase cascades. *Mol Endocrinol.* 22:2759-2765.

66. Illario, M., M. L. Giardino-Torchia, U. Sankar, T. J. Ribar, M. Galgani, L. Vitiello, A. M. Masci, F. R. Bertani, E. Ciaglia, D. Astone, G. Maulucci, A. Cavallo, M. Vitale, V. Cimini, L. Pastore, A. R. Means, G. Rossi, and L. Racioppi. 2008. Calmodulin-dependent kinase IV links Toll-like receptor 4 signaling with survival pathway of activated dendritic cells. *Blood* 111:723-731.

67. Lambers, T. T., R. J. Bindels, and J. G. Hoenderop. 2006. Coordinated control of renal Ca2+ handling. *Kidney Int.* 69:650-654.

68. Oh-hora, M. and A. Rao. 2009. The calcium/NFAT pathway: role in development and function of regulatory T cells. *Microbes.Infect.* 11:612-619.

69. Jennings, C., B. Kusler, and P. P. Jones. 2009. Calcineurin inactivation leads to decreased responsiveness to LPS in macrophages and dendritic cells and protects against LPS-induced toxicity in vivo. *Innate.Immun.* 15:109-120.

70. Zanoni, I., R. Ostuni, G. Capuano, M. Collini, M. Caccia, A. E. Ronchi, M. Rocchetti, F. Mingozzi, M. Foti, G. Chirico, B. Costa, A. Zaza, P. Ricciardi-Castagnoli, and F. Granucci. 2009. CD14 regulates the dendritic cell life cycle after LPS exposure through NFAT activation. *Nature* 460:264-268.

71. Kallfelz, F. A., A. N. Taylor, and R. H. Wasserman. 1967. Vitamin D-induced calcium binding factor in rat intestinal mucosa. *Proc Soc Exp Biol Med* 125:54-58.

72. Taylor, A. N. and R. H. Wasserman. 1967. Vitamin D3-induced calcium-binding protein: partial purification, electrophoretic visualization, and tissue distribution. *Arch Biochem Biophys* 119:536-540.

73. Hemmingsen, C. 2000. Regulation of renal calbindin-D28K. *Pharmacol.Toxicol.* 87 Suppl 3:5-30.

74. Parekh, A. B. and J. W. Putney, Jr. 2005. Store-operated calcium channels. *Physiol Rev.* 85:757-810.

75. Parekh, A. B. 2003. Store-operated Ca2+ entry: dynamic interplay between endoplasmic reticulum, mitochondria and plasma membrane. *J Physiol* 547:333-348.

76. Putney, J. W., Jr. 2005. Capacitative calcium entry: sensing the calcium stores. *J Cell Biol* 169:381-382.

77. Koski, G. K., G. N. Schwartz, D. E. Weng, B. J. Czerniecki, C. Carter, R. E. Gress, and P. A. Cohen. 1999. Calcium mobilization in human myeloid cells results in acquisition of individual dendritic cell-like characteristics through discrete signaling pathways. *J Immunol.* 163:82-92.

78. Hsu, S., P. J. O'Connell, V. A. Klyachko, M. N. Badminton, A. W. Thomson, M. B. Jackson, D. E. Clapham, and G. P. Ahern. 2001. Fundamental Ca2+ signaling mechanisms in mouse dendritic cells: CRAC is the major Ca2+ entry pathway. *J Immunol.* 166:6126-6133.

79. Liou, J., M. L. Kim, W. D. Heo, J. T. Jones, J. W. Myers, J. E. Ferrell, Jr., and T. Meyer. 2005. STIM is a Ca2+ sensor essential for Ca2+-store-depletion-triggered Ca2+ influx. *Curr.Biol* 15:1235-1241.

80. Roos, J., P. J. DiGregorio, A. V. Yeromin, K. Ohlsen, M. Lioudyno, S. Zhang, O. Safrina, J. A. Kozak, S. L. Wagner, M. D. Cahalan, G. Velicelebi, and K. A. Stauderman. 2005. STIM1, an essential and conserved component of store-operated Ca2+ channel function. *J Cell Biol* 169:435-445.

81. Zhang, S. L., Y. Yu, J. Roos, J. A. Kozak, T. J. Deerinck, M. H. Ellisman, K. A. Stauderman, and M. D. Cahalan. 2005. STIM1 is a Ca2+ sensor that activates CRAC channels and migrates from the Ca2+ store to the plasma membrane. *Nature* 437:902-905.

82. Feske, S., Y. Gwack, M. Prakriya, S. Srikanth, S. H. Puppel, B. Tanasa, P. G. Hogan, R. S. Lewis, M. Daly, and A. Rao. 2006. A mutation in Orai1 causes immune deficiency by abrogating CRAC channel function. *Nature* 441:179-185.

83. Gwack, Y., S. Srikanth, S. Feske, F. Cruz-Guilloty, M. Oh-hora, D. S. Neems, P. G. Hogan, and A. Rao. 2007. Biochemical and functional characterization of Orai proteins. *J Biol Chem.* 282:16232-16243.

84. Vig, M., C. Peinelt, A. Beck, D. L. Koomoa, D. Rabah, M. Koblan-Huberson, S. Kraft, H. Turner, A. Fleig, R. Penner, and J. P. Kinet. 2006. CRACM1 is a plasma membrane protein essential for store-operated Ca2+ entry. *Science* 312:1220-1223.

85. Lewis, R. S. 2007. The molecular choreography of a store-operated calcium channel. *Nature* 446:284-287.

86. Barr, V. A., K. M. Bernot, S. Srikanth, Y. Gwack, L. Balagopalan, C. K. Regan, D. J. Helman, C. L. Sommers, M. Oh-hora, A. Rao, and L. E. Samelson. 2008. Dynamic movement of the calcium sensor STIM1 and the calcium channel Orai1 in activated T-cells: puncta and distal caps. *Mol Biol Cell* 19:2802-2817.

87. Feske, S. 2007. Calcium signalling in lymphocyte activation and disease. *Nat Rev Immunol.* 7:690-702.

88. Venkatachalam, K. and C. Montell. 2007. TRP channels. *Annu.Rev Biochem* 76:387-417.

89. Barbet, G., M. Demion, I. C. Moura, N. Serafini, T. Leger, F. Vrtovsnik, R. C. Monteiro, R. Guinamard, J. P. Kinet, and P. Launay. 2008. The calcium-activated nonselective cation channel TRPM4 is essential for the migration but not the maturation of dendritic cells. *Nat.Immunol.* 9:1148-1156.

90. Hijioka, T., R. L. Rosenberg, J. J. Lemasters, and R. G. Thurman. 1992. Kupffer cells contain voltage-dependent calcium channels. *Mol.Pharmacol.* 41:435-440.

91. Vukcevic, M., G. C. Spagnoli, G. Iezzi, F. Zorzato, and S. Treves. 2008. Ryanodine receptor activation by Ca v 1.2 is involved in dendritic cell major histocompatibility complex class II surface expression. *J.Biol.Chem.* 283:34913-34922.

92. Mullen, K. M., M. Rozycka, H. Rus, L. Hu, C. Cudrici, E. Zafranskaia, M. W. Pennington, D. C. Johns, S. I. Judge, and P. A. Calabresi. 2006. Potassium channels Kv1.3 and Kv1.5 are expressed on blood-derived dendritic cells in the central nervous system. *Ann.Neurol.* 60:118-127.

93. Shumilina, E., N. Zahir, N. T. Xuan, and F. Lang. 2007. Phosphoinositide 3-kinase dependent regulation of Kv channels in dendritic cells. *Cell Physiol Biochem.* 20:801-808.

94.   Ehring, G. R., H. H. Kerschbaum, C. Eder, A. L. Neben, C. M. Fanger, R. M. Khoury, P. A. Negulescu, and M. D. Cahalan. 1998. A nongenomic mechanism for progesterone-mediated immunosuppression: inhibition of K+ channels, Ca2+ signaling, and gene expression in T lymphocytes. *J Exp Med* 188:1593-1602.

95.   Connolly, S. F. and D. J. Kusner. 2007. The regulation of dendritic cell function by calcium-signaling and its inhibition by microbial pathogens. *Immunol.Res.* 39:115-127.

96.   Bagley, K. C., S. F. Abdelwahab, R. G. Tuskan, and G. K. Lewis. 2004. Calcium signaling through phospholipase C activates dendritic cells to mature and is necessary for the activation and maturation of dendritic cells induced by diverse agonists. *Clin.Diagn.Lab Immunol.* 11:77-82.

97.   Czerniecki, B. J., C. Carter, L. Rivoltini, G. K. Koski, H. I. Kim, D. E. Weng, J. G. Roros, Y. M. Hijazi, S. Xu, S. A. Rosenberg, and P. A. Cohen. 1997. Calcium ionophore-treated peripheral blood monocytes and dendritic cells rapidly display characteristics of activated dendritic cells. *J.Immunol.* 159:3823-3837.

98.   Panther, E., M. Idzko, S. Corinti, D. Ferrari, Y. Herouy, M. Mockenhaupt, S. Dichmann, P. Gebicke-Haerter, F. Di Virgilio, G. Girolomoni, and J. Norgauer. 2002. The influence of lysophosphatidic acid on the functions of human dendritic cells. *J.Immunol.* 169:4129-4135.

99.   Caparros, E., P. Munoz, E. Sierra-Filardi, D. Serrano-Gomez, A. Puig-Kroger, J. L. Rodriguez-Fernandez, M. Mellado, J. Sancho, M. Zubiaur, and A. L. Corbi. 2006. DC-SIGN ligation on dendritic cells results in ERK and PI3K activation and modulates cytokine production. *Blood* 107:3950-3958.

100. Seabra, V., R. F. Stachlewitz, and R. G. Thurman. 1998. Taurine blunts LPS-induced increases in intracellular calcium and TNF-alpha production by Kupffer cells. *J Leukoc.Biol* 64:615-621.

101. Zhou, X., W. Yang, and J. Li. 2006. Ca2+- and protein kinase C-dependent signaling pathway for nuclear factor-kappaB activation, inducible nitric-oxide synthase expression, and tumor necrosis factor-alpha production in lipopolysaccharide-stimulated rat peritoneal macrophages. *J Biol Chem.* 281:31337-31347.

102. Cantorna, M. T., Y. Zhu, M. Froicu, and A. Wittke. 2004. Vitamin D status, 1,25-dihydroxyvitamin D3, and the immune system. *Am.J.Clin.Nutr.* 80:1717S-1720S.

103. Deeb, K. K., D. L. Trump, and C. S. Johnson. 2007. Vitamin D signalling pathways in cancer: potential for anticancer therapeutics. *Nat Rev Cancer* 7:684-700.

104. Zehnder, D. and M. Hewison. 1999. The renal function of 25-hydroxyvitamin D3-1alpha-hydroxylase. *Mol.Cell Endocrinol.* 151:213-220.

105. Zehnder, D., R. Bland, E. A. Walker, A. R. Bradwell, A. J. Howie, M. Hewison, and P. M. Stewart. 1999. Expression of 25-hydroxyvitamin D3-1alpha-hydroxylase in the human kidney. *J Am Soc Nephrol* 10:2465-2473.

106. Heine, G., U. Niesner, H. D. Chang, A. Steinmeyer, U. Zugel, T. Zuberbier, A. Radbruch, and M. Worm. 2008. 1,25-dihydroxyvitamin D(3) promotes IL-10 production in human B cells. *Eur.J.Immunol.* 38:2210-2218.

107. Hewison, M., L. Freeman, S. V. Hughes, K. N. Evans, R. Bland, A. G. Eliopoulos, M. D. Kilby, P. A. Moss, and R. Chakraverty. 2003. Differential regulation of vitamin D

receptor and its ligand in human monocyte-derived dendritic cells. *J.Immunol.* 170:5382-5390.

108. Fritsche, J., K. Mondal, A. Ehrnsperger, R. Andreesen, and M. Kreutz. 2003. Regulation of 25-hydroxyvitamin D3-1 alpha-hydroxylase and production of 1 alpha,25-dihydroxyvitamin D3 by human dendritic cells. *Blood* 102:3314-3316.

109. Hewison, M., V. Kantorovich, H. R. Liker, A. J. Van Herle, P. Cohan, D. Zehnder, and J. S. Adams. 2003. Vitamin D-mediated hypercalcemia in lymphoma: evidence for hormone production by tumor-adjacent macrophages. *J.Bone Miner.Res.* 18:579-582.

110. van Etten, E. and C. Mathieu. 2005. Immunoregulation by 1,25-dihydroxyvitamin D3: basic concepts. *J.Steroid Biochem.Mol.Biol.* 97:93-101.

111. Gauzzi, M. C., C. Purificato, K. Donato, Y. Jin, L. Wang, K. C. Daniel, A. A. Maghazachi, F. Belardelli, L. Adorini, and S. Gessani. 2005. Suppressive effect of 1alpha,25-dihydroxyvitamin D3 on type I IFN-mediated monocyte differentiation into dendritic cells: impairment of functional activities and chemotaxis. *J.Immunol.* 174:270-276.

112. Penna, G., S. Amuchastegui, N. Giarratana, K. C. Daniel, M. Vulcano, S. Sozzani, and L. Adorini. 2007. 1,25-Dihydroxyvitamin D3 selectively modulates tolerogenic properties in myeloid but not plasmacytoid dendritic cells. *J.Immunol.* 178:145-153.

113. Adorini, L., G. Penna, N. Giarratana, A. Roncari, S. Amuchastegui, K. C. Daniel, and M. Uskokovic. 2004. Dendritic cells as key targets for immunomodulation by Vitamin D receptor ligands. *J.Steroid Biochem.Mol.Biol.* 89-90:437-441.

114. Yu, S. and M. T. Cantorna. 2008. The vitamin D receptor is required for iNKT cell development. *Proc.Natl Acad.Sci U.S.A* 105:5207-5212.

115. Griffin, M. D., X. Dong, and R. Kumar. 2007. Vitamin D receptor-mediated suppression of RelB in antigen presenting cells: a paradigm for ligand-augmented negative transcriptional regulation. *Arch.Biochem.Biophys.* 460:218-226.

116. Szeles, L., G. Keresztes, D. Torocsik, Z. Balajthy, L. Krenacs, S. Poliska, A. Steinmeyer, U. Zuegel, M. Pruenster, A. Rot, and L. Nagy. 2009. 1,25-dihydroxyvitamin D3 is an autonomous regulator of the transcriptional changes leading to a tolerogenic dendritic cell phenotype. *J.Immunol.* 182:2074-2083.

117. Ramasamy, I. 2006. Recent advances in physiological calcium homeostasis. *Clin.Chem.Lab Med.* 44:237-273.

118. Cantorna, M. T., C. E. Hayes, and H. F. DeLuca. 1996. 1,25-Dihydroxyvitamin D3 reversibly blocks the progression of relapsing encephalomyelitis, a model of multiple sclerosis. *Proc.Natl Acad.Sci U.S.A* 93:7861-7864.

119. Lemire, J. M. and D. C. Archer. 1991. 1,25-dihydroxyvitamin D3 prevents the in vivo induction of murine experimental autoimmune encephalomyelitis. *J.Clin.Invest* 87:1103-1107.

120. Cantorna, M. T., J. Humpal-Winter, and H. F. DeLuca. 1999. Dietary calcium is a major factor in 1,25-dihydroxycholecalciferol suppression of experimental autoimmune encephalomyelitis in mice. *J.Nutr.* 129:1966-1971.

121. Imazeki, I., J. Matsuzaki, K. Tsuji, and T. Nishimura. 2006. Immunomodulating effect of vitamin D3 derivatives on type-1 cellular immunity. *Biomed.Res.* 27:1-9.

122. Becklund, B. R., D. W. Hansen, Jr., and H. F. DeLuca. 2009. Enhancement of 1,25-dihydroxyvitamin D3-mediated suppression of experimental autoimmune encephalomyelitis by calcitonin. *Proc.Natl Acad.Sci U.S.A.*

123. Riccardi, C., S. Bruscoli, and G. Migliorati. 2002. Molecular mechanisms of immunomodulatory activity of glucocorticoids. *Pharmacol.Res.* 45:361-368.

124. Elenkov, I. J. 2004. Glucocorticoids and the Th1/Th2 balance. *Ann.N.Y.Acad.Sci.* 1024:138-146.

125. Franchimont, D. 2004. Overview of the actions of glucocorticoids on the immune response: a good model to characterize new pathways of immunosuppression for new treatment strategies. *Ann.N.Y.Acad.Sci.* 1024:124-137.

126. Kang, Y., L. Xu, B. Wang, A. Chen, and G. Zheng. 2008. Cutting edge: Immunosuppressant as adjuvant for tolerogenic immunization. *J Immunol.* 180:5172-5176.

127. Puccetti, P. and U. Grohmann. 2007. IDO and regulatory T cells: a role for reverse signalling and non-canonical NF-kappaB activation. *Nat.Rev.Immunol.* 7:817-823.

128. Elftman, M. D., C. C. Norbury, R. H. Bonneau, and M. E. Truckenmiller. 2007. Corticosterone impairs dendritic cell maturation and function. *Immunology* 122:279-290.

129. Hamdi, H., V. Godot, M. C. Maillot, M. V. Prejean, N. Cohen, R. Krzysiek, F. M. Lemoine, W. Zou, and D. Emilie. 2007. Induction of antigen-specific regulatory T lymphocytes by human dendritic cells expressing the glucocorticoid-induced leucine zipper. *Blood* 110:211-219.

130. Kitajima, T., K. Ariizumi, P. R. Bergstresser, and A. Takashima. 1996. A novel mechanism of glucocorticoid-induced immune suppression: the inhibiton of T cell-mediated terminal maturation of a murine dendritic cell line. *J.Clin.Invest* 98:142-147.

131. Roca, L., S. Di Paolo, V. Petruzzelli, G. Grandaliano, E. Ranieri, F. P. Schena, and L. Gesualdo. 2007. Dexamethasone modulates interleukin-12 production by inducing monocyte chemoattractant protein-1 in human dendritic cells. *Immunol.Cell Biol.* 85:610-616.

132. van Kooten, C., A. S. Stax, A. M. Woltman, and K. A. Gelderman. 2009. Handbook of experimental pharmacology "dendritic cells": the use of dexamethasone in the induction of tolerogenic DCs. *Handb.Exp.Pharmacol.* 233-249.

133. Piemonti, L., P. Monti, P. Allavena, M. Sironi, L. Soldini, B. E. Leone, C. Socci, and C. Di, V. 1999. Glucocorticoids affect human dendritic cell differentiation and maturation. *J Immunol.* 162:6473-6481.

134. Piemonti, L., P. Monti, P. Allavena, B. E. Leone, A. Caputo, and C. Di, V. 1999. Glucocorticoids increase the endocytic activity of human dendritic cells. *Int.Immunol.* 11:1519-1526.

135. Stahn, C. and F. Buttgereit. 2008. Genomic and nongenomic effects of glucocorticoids. *Nat Clin Pract.Rheumatol.* 4:525-533.

136. Auphan, N., J. A. DiDonato, C. Rosette, A. Helmberg, and M. Karin. 1995. Immunosuppression by glucocorticoids: inhibition of NF-kappa B activity through induction of I kappa B synthesis. *Science* 270:286-290.

137. Scheinman, R. I., P. C. Cogswell, A. K. Lofquist, and A. S. Baldwin, Jr. 1995. Role of transcriptional activation of I kappa B alpha in mediation of immunosuppression by glucocorticoids. *Science* 270:283-286.

138. D'Adamio, F., O. Zollo, R. Moraca, E. Ayroldi, S. Bruscoli, A. Bartoli, L. Cannarile, G. Migliorati, and C. Riccardi. 1997. A new dexamethasone-induced gene of the leucine zipper family protects T lymphocytes from TCR/CD3-activated cell death. *Immunity.* 7:803-812.

139. Rutella, S., G. Bonanno, and R. De Cristofaro. 2009. Targeting indoleamine 2,3-dioxygenase (IDO) to counteract tumour-induced immune dysfunction: from biochemistry to clinical development. *Endocr.Metab Immune.Disord.Drug Targets.* 9:151-177.

140. Cahalan, M. D., H. Wulff, and K. G. Chandy. 2001. Molecular properties and physiological roles of ion channels in the immune system. *J Clin.Immunol.* 21:235-252.

141. Roderick, H. L. and S. J. Cook. 2008. Ca2+ signalling checkpoints in cancer: remodelling Ca2+ for cancer cell proliferation and survival. *Nat Rev Cancer* 8:361-375.

142. Inaba, K., M. Inaba, N. Romani, H. Aya, M. Deguchi, S. Ikehara, S. Muramatsu, and R. M. Steinman. 1992. Generation of large numbers of dendritic cells from mouse bone marrow cultures supplemented with granulocyte/macrophage colony-stimulating factor. *J.Exp.Med.* 176:1693-1702.

143. Grynkiewicz, G., M. Poenie, and R. Y. Tsien. 1985. A new generation of Ca2+ indicators with greatly improved fluorescence properties. *J Biol Chem.* 260:3440-3450.

144. Hamill, O. P., A. Marty, E. Neher, B. Sakmann, and F. J. Sigworth. 1981. Improved patch-clamp techniques for high-resolution current recording from cells and cell-free membrane patches. *Pflugers Arch.* 391:85-100.

145. Schwandner, R., R. Dziarski, H. Wesche, M. Rothe, and C. J. Kirschning. 1999. Peptidoglycan- and lipoteichoic acid-induced cell activation is mediated by toll-like receptor 2. *J.Biol.Chem.* 274:17406-17409.

146. Takeuchi, O., K. Hoshino, T. Kawai, H. Sanjo, H. Takada, T. Ogawa, K. Takeda, and S. Akira. 1999. Differential roles of TLR2 and TLR4 in recognition of gram-negative and gram-positive bacterial cell wall components. *Immunity.* 11:443-451.

147. Prakriya, M., S. Feske, Y. Gwack, S. Srikanth, A. Rao, and P. G. Hogan. 2006. Orai1 is an essential pore subunit of the CRAC channel. *Nature* 443:230-233.

148. Li, Q. and I. M. Verma. 2002. NF-kappaB regulation in the immune system. *Nat.Rev.Immunol.* 2:725-734.

149. Lambers, T. T., R. J. Bindels, and J. G. Hoenderop. 2006. Coordinated control of renal Ca2+ handling. *Kidney Int.* 69:650-654.

150. Rogister, F., D. Laeckmann, P. Plasman, F. Van Eylen, M. Ghyoot, C. Maggetto, J. Liegeois, J. Geczy, A. Herchuelz, J. Delarge, and B. Masereel. 2001. Novel inhibitors of the sodium-calcium exchanger: benzene ring analogues of N-guanidino substituted amiloride derivatives. *Eur.J.Med.Chem.* 36:597-614.

151. Christakos, S., P. Dhawan, B. Benn, A. Porta, M. Hediger, G. T. Oh, E. B. Jeung, Y. Zhong, D. Ajibade, K. Dhawan, and S. Joshi. 2007. Vitamin D: molecular mechanism of action. *Ann.N.Y.Acad.Sci* 1116:340-348.

152. Schlatter, E. 2006. Who Wins the Competition: TRPV5 or Calbindin-D28K? *J.Am.Soc.Nephrol.* 17:2954-2956.

153. Dauer, M., B. Obermaier, J. Herten, C. Haerle, K. Pohl, S. Rothenfusser, M. Schnurr, S. Endres, and A. Eigler. 2003. Mature dendritic cells derived from human monocytes within 48 hours: a novel strategy for dendritic cell differentiation from blood precursors. *J Immunol.* 170:4069-4076.

154. Korthals, M., N. Safaian, R. Kronenwett, D. Maihofer, M. Schott, C. Papewalis, B. E. Diaz, M. Winter, A. Czibere, R. Haas, G. Kobbe, and R. Fenk. 2007. Monocyte derived dendritic cells generated by IFN-alpha acquire mature dendritic and natural killer cell properties as shown by gene expression analysis. *J Transl.Med* 5:46.

155. Anguille, S., E. L. Smits, N. Cools, H. Goossens, Z. N. Berneman, and V. F. Van Tendeloo. 2009. Short-term cultured, interleukin-15 differentiated dendritic cells have potent immunostimulatory properties. *J Transl.Med* 7:109.

156. Tsiatas, M. L., A. D. Gritzapis, N. T. Cacoullos, S. I. Papadhimitriou, C. N. Baxevanis, and M. Papamichail. 2001. A novel culture environment for generating mature human dentritic cells from peripheral blood CD14+ cells. *Anticancer Res* 21:1199-1206.

157. Schanen, B. C. and D. R. Drake, III. 2008. A novel approach for the generation of human dendritic cells from blood monocytes in the absence of exogenous factors. *J Immunol.Methods* 335:53-64.

158. Son, Y. I., S. Egawa, T. Tatsumi, R. E. Redlinger, Jr., P. Kalinski, and T. Kanto. 2002. A novel bulk-culture method for generating mature dendritic cells from mouse bone marrow cells. *J Immunol.Methods* 262:145-157.

159. Lutz, M. B., N. Kukutsch, A. L. Ogilvie, S. Rossner, F. Koch, N. Romani, and G. Schuler. 1999. An advanced culture method for generating large quantities of highly pure dendritic cells from mouse bone marrow. *J Immunol.Methods* 223:77-92.

160. Abramowitz, J. and L. Birnbaumer. 2009. Physiology and pathophysiology of canonical transient receptor potential channels. *FASEB J* 23:297-328.

161. Lang, F., F. Friedrich, E. Kahn, E. Woll, M. Hammerer, S. Waldegger, K. Maly, and H. Grunicke. 1991. Bradykinin-induced oscillations of cell membrane potential in cells expressing the Ha-ras oncogene. *J Biol Chem.* 266:4938-4942.

162. Carroll, J. and K. Swann. 1992. Spontaneous cytosolic calcium oscillations driven by inositol trisphosphate occur during in vitro maturation of mouse oocytes. *J Biol Chem.* 267:11196-11201.

163. Liljelund, P., J. G. Netzeband, and D. L. Gruol. 2000. L-Type calcium channels mediate calcium oscillations in early postnatal Purkinje neurons. *J Neurosci.* 20:7394-7403.

164. Arendshorst, W. J. and T. L. Thai. 2009. Regulation of the renal microcirculation by ryanodine receptors and calcium-induced calcium release. *Curr.Opin.Nephrol Hypertens.* 18:40-49.

165. Koulen, P., C. Madry, R. S. Duncan, J. Y. Hwang, E. Nixon, N. McClung, E. V. Gregg, and M. Singh. 2008. Progesterone potentiates IP(3)-mediated calcium signaling through Akt/PKB. *Cell Physiol Biochem* 21:161-172.

166. Parekh, A. B. 2008. Ca2+ microdomains near plasma membrane Ca2+ channels: impact on cell function. *J Physiol* 586:3043-3054.

167. Aki, D., Y. Minoda, H. Yoshida, S. Watanabe, R. Yoshida, G. Takaesu, T. Chinen, T. Inaba, M. Hikida, T. Kurosaki, K. Saeki, and A. Yoshimura. 2008. Peptidoglycan and lipopolysaccharide activate PLCgamma2, leading to enhanced cytokine production in macrophages and dendritic cells. *Genes Cells* 13:199-208.

168. Vig, M. and J. P. Kinet. 2009. Calcium signaling in immune cells. *Nat.Immunol.* 10:21-27.

169. Beeton, C. and K. G. Chandy. 2005. Potassium channels, memory T cells, and multiple sclerosis. *Neuroscientist.* 11:550-562.

170. Lewis, R. S. and M. D. Cahalan. 1995. Potassium and calcium channels in lymphocytes. *Annu.Rev.Immunol.* 13:623-653.

171. Launay, P., H. Cheng, S. Srivatsan, R. Penner, A. Fleig, and J. P. Kinet. 2004. TRPM4 regulates calcium oscillations after T cell activation. *Science* 306:1374-1377.

172. Vennekens, R., J. Olausson, M. Meissner, W. Bloch, I. Mathar, S. E. Philipp, F. Schmitz, P. Weissgerber, B. Nilius, V. Flockerzi, and M. Freichel. 2007. Increased IgE-dependent mast cell activation and anaphylactic responses in mice lacking the calcium-activated nonselective cation channel TRPM4. *Nat.Immunol.* 8:312-320.

173. Chandy, K. G., H. Wulff, C. Beeton, M. Pennington, G. A. Gutman, and M. D. Cahalan. 2004. K+ channels as targets for specific immunomodulation. *Trends Pharmacol.Sci.* 25:280-289.

174. Vicente, R., A. Escalada, M. Coma, G. Fuster, E. Sanchez-Tillo, C. Lopez-Iglesias, C. Soler, C. Solsona, A. Celada, and A. Felipe. 2003. Differential voltage-dependent K+ channel responses during proliferation and activation in macrophages. *J.Biol.Chem.* 278:46307-46320.

175. Aoki, Y. and P. N. Kao. 1997. Cyclosporin A-sensitive calcium signaling represses NFkappaB activation in human bronchial epithelial cells and enhances NFkappaB activation in Jurkat T-cells. *Biochem Biophys Res Commun.* 234:424-431.

176. Chen, N. X., D. J. Geist, D. C. Genetos, F. M. Pavalko, and R. L. Duncan. 2003. Fluid shear-induced NFkappaB translocation in osteoblasts is mediated by intracellular calcium release. *Bone* 33:399-410.

177. Fan, W. and N. G. Cooper. 2009. Glutamate-induced NFkappaB activation in the retina. *Invest Ophthalmol.Vis.Sci* 50:917-925.

178. Hayashi, M., Y. Yamaji, Y. Nakazato, and T. Saruta. 2000. The effects of calcium channel blockers on nuclear factor kappa B activation in the mesangium cells. *Hypertens.Res* 23:521-525.

179. Sappington, R. M. and D. J. Calkins. 2008. Contribution of TRPV1 to microglia-derived IL-6 and NFkappaB translocation with elevated hydrostatic pressure. *Invest Ophthalmol.Vis.Sci* 49:3004-3017.

180. Goodridge, H. S., R. M. Simmons, and D. M. Underhill. 2007. Dectin-1 stimulation by Candida albicans yeast or zymosan triggers NFAT activation in macrophages and dendritic cells. *J.Immunol.* 178:3107-3115.

181. Berridge, M. J., P. Lipp, and M. D. Bootman. 2000. The versatility and universality of calcium signalling. *Nat.Rev.Mol Cell Biol* 1:11-21.

182. Orrenius, S., B. Zhivotovsky, and P. Nicotera. 2003. Regulation of cell death: the calcium-apoptosis link. *Nat.Rev.Mol Cell Biol* 4:552-565.

183. Balasubramanyam, M., C. Rohowsky-Kochan, J. P. Reeves, and J. P. Gardner. 1994. Na+/Ca2+ exchange-mediated calcium entry in human lymphocytes. *J.Clin.Invest* 94:2002-2008.

184. Rumpel, E., U. Pilatus, A. Mayer, and I. Pecht. 2000. Na(+)-dependent Ca(2+) transport modulates the secretory response to the Fcepsilon receptor stimulus of mast cells. *Biophys.J.* 79:2975-2986.

185. Tintinger, G. R. and R. Anderson. 2004. Counteracting effects of NADPH oxidase and the Na+/Ca2+ exchanger on membrane repolarisation and store-operated uptake of Ca2+ by chemoattractant-activated human neutrophils. *Biochem.Pharmacol.* 67:2263-2271.

186. Schmitt, R., D. H. Ellison, N. Farman, B. C. Rossier, R. F. Reilly, W. B. Reeves, I. Oberbaumer, R. Tapp, and S. Bachmann. 1999. Developmental expression of sodium entry pathways in rat nephron. *Am.J.Physiol* 276:F367-F381.

187. Kimura, M., E. M. Jeanclos, R. J. Donnelly, J. Lytton, J. P. Reeves, and A. Aviv. 1999. Physiological and molecular characterization of the Na+/Ca2+ exchanger in human platelets. *Am.J.Physiol* 277:H911-H917.

188. Canitano, A., M. Papa, F. Boscia, P. Castaldo, S. Sellitti, M. Taglialatela, and L. Annunziato. 2002. Brain distribution of the Na+/Ca2+ exchanger-encoding genes NCX1, NCX2, and NCX3 and their related proteins in the central nervous system. *Ann.N.Y.Acad.Sci* 976:394-404.

189. Ottolia, M., S. John, Y. Xie, X. Ren, and K. D. Philipson. 2007. Shedding light on the Na+/Ca2+ exchanger. *Ann.N.Y.Acad.Sci.* 1099:78-85.

190. Reppel, M., B. K. Fleischmann, H. Reuter, F. Pillekamp, H. Schunkert, and J. Hescheler. 2007. Regulation of Na+/Ca2+ exchange current in the normal and failing heart. *Ann.N.Y.Acad.Sci* 1099:361-372.

191. Sipido, K. R., V. Bito, G. Antoons, P. G. Volders, and M. A. Vos. 2007. Na/Ca exchange and cardiac ventricular arrhythmias. *Ann.N.Y.Acad.Sci* 1099:339-348.

192. Venetucci, L. A., A. W. Trafford, S. C. O'Neill, and D. A. Eisner. 2007. Na/Ca exchange: regulator of intracellular calcium and source of arrhythmias in the heart. *Ann.N.Y.Acad.Sci* 1099:315-325.

193. Kim, M. H., G. S. Lee, E. M. Jung, K. C. Choi, G. T. Oh, and E. B. Jeung. 2009. Dexamethasone differentially regulates renal and duodenal calcium-processing genes in calbindin-D9k and -D28k knockout mice. *Exp.Physiol* 94:138-151.

194. Kim, M. H., G. S. Lee, E. M. Jung, K. C. Choi, and E. B. Jeung. 2009. The negative effect of dexamethasone on calcium-processing gene expressions is associated with a glucocorticoid-induced calcium-absorbing disorder. *Life Sci* 85:146-152.

195. Harr, M. W., Y. Rong, M. D. Bootman, H. L. Roderick, and C. W. Distelhorst. 2009. Glucocorticoid-mediated inhibition of LCK modulates the pattern of TCR-induced calcium signals by downregulatig IP3 receptors. *J.Biol.Chem.*

196. Herrmann, T. L., R. S. Agrawal, S. F. Connolly, R. L. McCaffrey, J. Schlomann, and D. J. Kusner. 2007. MHC Class II levels and intracellular localization in human dendritic cells are regulated by calmodulin kinase II. *J.Leukoc.Biol.* 82:686-699.

197. Lyakh, L. A., M. Sanford, S. Chekol, H. A. Young, and A. B. Roberts. 2005. TGF-beta and vitamin D3 utilize distinct pathways to suppress IL-12 production and modulate rapid differentiation of human monocytes into CD83+ dendritic cells. *J.Immunol.* 174:2061-2070.

198. Penna, G., S. Amuchastegui, G. Laverny, and L. Adorini. 2007. Vitamin D receptor agonists in the treatment of autoimmune diseases: selective targeting of myeloid but not plasmacytoid dendritic cells. *J Bone Miner.Res* 22 Suppl 2:V69-V73.

199. Smith, J. B., H. W. Lee, and L. Smith. 1996. Regulation of expression of sodium-calcium exchanger and plasma membrane calcium ATPase by protein kinases, glucocorticoids, and growth factors. *Ann.N.Y.Acad.Sci* 779:258-271.

200. Smith, L. and J. B. Smith. 1994. Regulation of sodium-calcium exchanger by glucocorticoids and growth factors in vascular smooth muscle. *J.Biol.Chem.* 269:27527-27531.

201. Lee, S. L., A. S. Yu, and J. Lytton. 1994. Tissue-specific expression of Na(+)-Ca2+ exchanger isoforms. *J.Biol.Chem.* 269:14849-14852.

202. Vazquez, G., A. R. de Boland, and R. Boland. 1997. Stimulation of Ca2+ release-activated Ca2+ channels as a potential mechanism involved in non-genomic 1,25(OH)2-vitamin D3-induced Ca2+ entry in skeletal muscle cells. *Biochem Biophys Res Commun.* 239:562-565.

203. Forsell, P., M. Eberhardson, H. Lennernas, T. Knutson, and L. Knutson. 2006. Rapid modulation of Ca2+ uptake in human jejunal enterocytes. *Biochem Biophys Res Commun.* 340:961-966.

204. Adorini, L. and G. Penna. 2008. Control of autoimmune diseases by the vitamin D endocrine system. *Nat Clin Pract.Rheumatol.* 4:404-412.

205. VanAmerongen, B. M., C. D. Dijkstra, P. Lips, and C. H. Polman. 2004. Multiple sclerosis and vitamin D: an update. *Eur.J Clin Nutr.* 58:1095-1109.

206. Lampert, A., M. M. Muller, S. Berchtold, K. S. Lang, M. Palmada, O. Dobrovinskaya, and F. Lang. 2003. Effect of dexamethasone on voltage-gated K+ channels in Jurkat T-lymphocytes. *Pflugers Arch* 447:168-174.

207. Pedersen, A. E., E. G. Schmidt, M. Gad, S. S. Poulsen, and M. H. Claesson. 2009. Dexamethasone/1alpha-25-dihydroxyvitamin D3-treated dendritic cells suppress colitis in the SCID T-cell transfer model. *Immunology* 127:354-364.

8 Akademische Lehrer

Kernfach Grund-/ Hauptstudium	Dozent
Allgemeine Chemie	Prof. Dr. G. Lagaly
	Dr. U. Wille
Anatomie und Physiologie des Menschen	Prof. Dr. Haase
Biologie der Pflanzen	Prof. Dr. F. Kempken
	Prof. Dr. H. Uhlarz
Ernährungslehre	Prof. Dr. M.J. Müller
	Prof. Dr. R. Schindler
	Prof. Dr. E. Wisker
Ernährungsökonomik	Prof. Dr. B. Friedl
	Prof. Dr. M. Missong
Ernährungsphysiologie	Dr. K.-H. Südekum
	Prof. Dr. E. Wisker
Ernährungswirtschaft	Prof. Dr. C.-H. Hanf
	Prof. Dr. Leitner
	Prof. Dr. M. Missong
Erzeugung von Nahrungsmitteln	PD Dr. K. Sieling
	Prof. Dr. A. Susenbeth
Haushaltsökonomik	Prof. Dr. J. Roosen
Lebensmittellehre	Prof. Dr. med. vet. H. F. Erbersdobler
	Dr. Günther
	Dr. H. Meisel
	Prof. Dr. G. Rimbach
	Prof. Dr. Teufel
Lebensmitteltechnologie	Prof. Dr. K. Schwarz
	Dr. H. Stöckmann
Mikrobiologie und Hygiene	Dr. H. Neve
	Prof. Dr. E. Schallenberger
Physik	Prof. Dr. U. Stroth
	Prof. Dr. K. Wolschendorf
Statistik und Informationsverarbeitung	Prof. Dr. R.A.E. Müller
	Dr. Rave
Stoffwechselphysiologie	Prof. Dr. S. Wolffram
Volkswirtschaftslehre	Prof. Dr. J. Bröcker
	Prof. Dr. T. Lux

9 Curriculum Vitae

PERSÖNLICHE DATEN

Vor- und Zuname:	Nicole Heise geb. Matzner
Geburtsdatum:	16.07.1982
Geburtsort:	Hannover
Familienstand:	ledig
Staatsangehörigkeit:	deutsch

AUSBILDUNG

03/2009 – 09/2009	Forschungsaufenthalt im Rahmen der Promotion im Labor von Prof. Doreen Cantrell in Dundee, UK (Thema: *Charakterisierung der Serum- und Glucocorticoid-induzierbaren Kinase SGK1 in CD8$^+$ Effektor T-Zellen*)
01/2007 – 03/2010	Anfertigung der Doktorarbeit am Institut für Physiologie der Eberhard-Karls-Universität Tübingen als Stipendiatin des Internationalen Graduiertenkollegs „PI3 Kinase Pathway in Tumor and Diabetes" (Thema: *Role of ion channels and exchangers in the regulation of dendritic cells/ Bedeutung von Ionenkanälen und –austauschern bei der Regulation von Dendritischen Zellen*)
28.11.2006	Master der Ökotrophologie, Abschlussnote: 1,3
04/2006 – 11/2006	Anfertigung der Masterarbeit am Institut für Humanernährung und Lebensmittelkunde (Thema: *Untersuchungen zum Einfluss von Gingko biloba auf die Expression neuronaler β-Sekretase*)
25.11.2004	Bachelor der Ökotrophologie, Abschlussnote: 1,6

10/2001 – 11/2006	Studium der Ökotrophologie an der Christian-Albrechts-Universität Kiel
22.06.2001	Abitur, Abschlussnote: 2,0

PRAKTIKA UND STUDIENBEGLEITENDE TÄTIGKEITEN

10/2004 – 09/2006	Studentische Hilfskraft am Institut für Humanernährung und Lebensmittelkunde, Lehrstuhl für Lebensmittelwissenschaft, Christian-Albrechts-Universität Kiel
01.08.-30.09.2005	Deutsche Forschungsanstalt für Lebensmittelchemie Garching bei München (Thema: *Untersuchung der chemopräventiven Wirksamkeit von Kaffeeinhaltsstoffen in humanen Magenkarzinomzellen*)
06.09.-06.10.2004	Fachklinik Erbprinzentanne für Hämatologie, Onkologie, Herz-/Kreislauferkrankungen und Erkrankungen des Stütz- und Bewegungsapparates, Clausthal-Zellerfeld
18.-29.01.1999	Heilpädagogischer Kindergarten und Tagesbildungsstätte Hannover

SONSTIGE KENNTNISSE UND FÄHIGKEITEN

Sprachkenntnisse:	Englisch (fließend)
	Französisch (Grundkenntnisse)
IT-Kenntnisse:	MetaFluor Imaging Software
	Canvas Graphical Software

10 Publications

Matzner N, Shumilina E, Xuan N, Wang K, Zemtsova IM, Duszenko M, Lang F. Effect of dexamethasone on calcium signaling in dendritic cells. – *[in preparation]*

Zemtsova IM, **Matzner N**, Kucherenko Y, Boini KM, Pearce D, Shumilina E, Lang F. Blunted IgE-mediated activation of mast cells in mice lacking the Serum- and Glucocorticoid-inducible kinase SGK3. *AJP-Cell Physiology – [revision]*

Shumilina E, Xuan N, **Matzner N**, Bhandaru M, Zemtsova IM, Lang F. Regulation of calcium signaling in dendritic cells by 1,25-Dihydroxyvitamin D3. *FASEB J. 2010 Feb 2 – [Epub ahead of print]*

Sobiesiak M, Shumilina E, Lam RS, Woelbing F, **Matzner N**, Kaesler S, Zemtsova IM, Lupescu A, Zahir N, Kuhl D, Schaller M, Biedermann T, Lang F. Impaired mast cell activation in gene-targeted mice lacking the Serum- and glucocorticoid-inducible kinase SGK1. *J Immunol. 2009 183(7): 4395-402.*

Xuan N, Shumilina E, **Matzner N**, Zemtsova IM, Biedermann T, Goetz F, Lang F. Ca^{2+}-dependent functions in peptidoglycan-stimulated mouse dendritic cells. *Cell Physiol Biochem. 2009 24(3-4):167-76.*

Rudner J, Mueller AC, **Matzner N**, Huber SM, Handrick R, Belka C, Jendrossek V. The additional loss of Bak and not the lack of the protein tyrosine kinase p56/Lck in one JcaM1.6 subclone caused pronounced apoptosis resistance in response to stimuli of the intrinsic pathway. *Apoptosis. 2009 Apr 4 – [Epub ahead of print]*

Hundhausen C, Boesch-Saadatmandi C, **Matzner N**, Lang F, Blank R, Wolffram S, Blaschek W, Rimbach G. Ochratoxin A lowers mRNA levels of genes encoding for key proteins of liver cell metabolism. *Cancer Genomics Proteomics. 2008 5(6):319-32.*

Matzner N, Zemtsova IM, Nguyen TX, Duszenko M, Shumilina E, Lang F. Ion channels modulating mouse dendritic cell functions. *J Immunol. 2008 181(10): 6803-9.*

Lam RS, Shumilina E, **Matzner N**, Zemtsova IM, Sobiesiak M, Felder E, Dietl P, Huber SM, Lang F. Phosphatidylinositol-3-kinase regulates mast cell ion channel activity. *Cell Physiol Biochem. 2008 22(1-4):169-76.*

Shumilina E, Lam RS, Woelbing F, **Matzner N**, Zemtsova IM, Sobiesiak M, Mahmud H, Sausbier U, Biedermann T, Ruth P, Sausbier M, Lang F. Blunted IgE-mediated activation of mast cells in mice lacking the Ca^{2+}-activated K^+ channel $K_{Ca}3.1$. *J Immunol. 2008 180(12):8040-7.*

Augustin S, Huebbe P, **Matzner N**, Augustin K, Schliebs R, Cermak R, Wolffram S, Rimbach G. *Ginkgo biloba* extract and its flavonol and terpenelacton fractions do not affect β-secretase mRNA and enzyme activity levels in cultured neurons and in laboratory mice. *Planta Med. 2008 74(1):6-13.*

Erklärung

Hiermit erkläre ich, dass die vorliegende Dissertation im Rahmen eines Gemeinschaftsprojektes erstellt worden ist.

Dieses Projekt befasst sich mit der Identifizierung und Charakterisierung von Ionenkanälen und Ionentransportern, welche für die Funktion von Immunzellen von Bedeutung sind. Der wesentliche Anteil der in der vorliegenden Dissertation präsentierten Daten wurde von mir persönlich erhoben. Mittels der *Patch Clamp*-Technik erhobene Daten wurden von Dr. E. Shumilina erstellt. Weiterhin erhielt ich Hilfe bei der Erlernung der in der vorliegenden Arbeit gezeigten Methoden von Dr. I. Zemtsova und Dr. X. NguyenThi.